A DISTRIBUTIONALLY ROBUST OPTIMIZATION APPROACH FOR THE OPTIMAL WIND FARM ALLOCATION IN MULTI-AREA POWER SYSTEMS

A Dissertation

by

FAHAD SALEH M ALISMAIL

Submitted to the Office of Graduate and Professional Studies of
Texas A&M University
in partial fulfillment of the requirements for the degree of

DOCTOR OF PHILOSOPHY

Chair of Committee,	Chanan Singh
Committee Members,	Mehrdad Ehsani
	Laszlo Kish
	Lewis Ntaimo
Head of Department,	Miroslav Begovic

December 2016

Major Subject: Electrical Engineering

Copyright 2016 Fahad Saleh M Alismail

ABSTRACT

This dissertation presents a distributionally robust planning model to determine the optimal allocation of wind farms in a multi-area power system, so that the expected energy not served (EENS) is minimized under uncertain conditions of wind power and generator forced outages. Unlike conventional stochastic programming approaches that rely on detailed information of the exact probability distribution, this proposed method attempts to minimize the expectation term over a collection of distributions characterized by accessible statistical measures, so it is more practical in cases where the detailed distribution data is unavailable. This planning model is formulated as a two-stage problem, where the wind power capacity allocation decisions are determined in the first stage, before the observation of uncertainty outcomes, and operation decisions are made in the second stage under specific uncertainty realizations.

In this dissertation, the second-stage decisions are approximated by linear decision rule functions, so that the distributionally robust model can be reformulated into a tractable second-order cone programming problem. Case studies based on a five-area system are conducted to demonstrate the effectiveness of the proposed method. The model is extended to deal with the hybrid system by including the solar power as a third source of uncertainty besides the wind power and conventional generation forced outages. The correlation between the wind and solar power is investigated to capture the diversity and the availability of all included power resources.

Capacity credit is calculated to measure the effective load carrying capacity of the allocated renewable resources. The probabilistic method including Monte Carlo simulation is used to calculate the loss of load expectation (LOLE) at different peak

loads and analytically determined the capacity credit of wind and solar power generation for several installed wind capacities. The penetration factor and the availability of the renewable power generation are major factors influencing the capacity credit value, besides the overall power system reliability level.

The results reflect the usefulness of utilizing the distributionally robust optimization approach in the data-driven decision making. It positively responds with the amount of the information provided regarding the uncertain variables in the renewable power generation allocation problem and sequentially in the system reliability and the yielded capacity credit values of the allocated renewable generation units.

DEDICATION

To the loving memory of my beloved father, Saleh Mohammad Alismail, who Almighty Allah has chosen to be next to Him, who brought me up in the best ways. His wise teachings, warm feelings and continuous support were very influential on my personality and success. He encouraged me to seek knowledge, and I hope that in future I would be exactly as he dreamed.

My beloved mother, "Um-Fahad", for her love, and constant encouragement who always worried about my studies and my life conditions. Your prayers and moral support will always boot my progress.

My wife, Fatimah, without whose love, endurance, constant support, patience, care and understanding I could never have made it through these studies. Thanks for your strong emotional support which make my life pleasant and more meaningful even in the hardest times.

My beautiful children, Iqbal, Saleh and Tareq. You always inspire me and have made me stronger and more fulfilled than I could have ever thought.

My brother Mohammad and my sisters Munerah, Nourah, Dalal, Shimaa, Aseel, Seba and Hissah. I am always grateful to you for your kind care and your interest in my success. You deserve my warm thanks for your encouragements and love.

To my beloved family, I dedicate this dissertation.

ACKNOWLEDGEMENTS

I would like to convey my profound thanks and appreciation to my advisor, Professor Chanan Singh, whose experience, knowledge and persistence provide me a valuable assistance to accomplish my dissertation. I appreciate his patience and endurance. Professor Singh supported me throughout my coursework, built my confidence, encouraged me to a challenging dissertation topic, and guided me technically with his experience.

I would also like to thank my committee members Professor Mehrdad Ehsani, Professor Laszlo Kish and Professor Lewis Ntaimo for their guidance, constructive and positive feedback.

Very special thanks are due to Dr. Peng Xiong, for his eloquent, total support and invaluable advising.

NOMENCLATURE

System Indices

i Indices of areas

j Indices of areas

l Indices of generation capacity levels or wind power levels

s Indices of wind distribution types, e.g. seasons, day or night

t Indices of load segments

System Sets

$\mathcal{F}$ Set of all transmission lines

$\mathcal{I}$ Set of all areas for wind farms

$\mathcal{J}_i^f$ Set of areas receiving power from area i by tie lines

$\mathcal{J}_i^t$ Set of areas delivering power to area i by tie lines

$\mathcal{L}^\alpha$ Set of all wind power levels

$\mathcal{L}^\gamma$ Set of all levels of the generation in one area

$\mathcal{L}^\delta$ Set of all levels of the total generation

$\mathcal{S}$ Set of all wind distribution types

$\mathcal{T}$ Set of all load segments

Notations for Uncertain Wind Power Generation

$\tilde{w}_i^s$ Random wind power generation as a percentage of the installed capacity, in area i under distribution type s. The vector of all $\tilde{w}_i^s$ is denoted by $\tilde{\boldsymbol{w}}$, and a specific realization of $\tilde{\boldsymbol{w}}$ is denoted by $\boldsymbol{w}$

$\bar{w}_i^s$ The mean value of random wind power in area i under wind power distribution type s (p.u.)

$\mathcal{W}$ Uncertainty set of uncertain wind power $\tilde{\boldsymbol{w}}$

W_{il}^s The selected level l of random wind power output $\tilde{w}_i^s$ (p.u.)

α_{il}^s Absolute deviation of $\tilde{w}_i^s$ around the selected level W_{il}^s (p.u.)

β_{ij}^s Mean absolute deviation of the summation of $\tilde{w}_i^s$ and $\tilde{w}_j^s$ (p.u.)

λ_i^s The variance of random wind power $\tilde{w}_i^s$ (p.u.)

ζ_{ij}^s The covariance value between $\tilde{w}_i^s$ and $\tilde{w}_j^s$ (p.u.)

Notations for Uncertain Generation Capacity

$\tilde{p}_i$ Random generation capacity in area i. The vector of all $\tilde{p}_i$ is denoted by $\tilde{\boldsymbol{p}}$, and a specific realization of $\tilde{\boldsymbol{p}}$ is denoted by $\boldsymbol{p}$ (MW)

$\bar{p}_i$ The mean value of the uncertain generation capacity in area i (MW)

p_i^{max} Upper bound of $\tilde{p}_i$ (MW)

p_i^{min} Lower bound of $\tilde{p}_i$ (MW)

$\mathcal{P}$ Uncertainty set of random generation capacity $\tilde{\boldsymbol{p}}$

P_{il} The selected generation level l of random generation capacity $\tilde{p}_i$ (MW)

Q_l The selected generation level l of the total generation capacity $\sum_{i\in\mathcal{I}} \tilde{p}_i$ (MW)

γ_{il} The expected value of the positive part of $P_{il} - \tilde{p}_{it}$ (MW)

δ_l The expected value of the positive part of $Q_l - \sum_{i\in\mathcal{I}} \tilde{p}_i$ (MW)

System Constants

D_{it}^s The tth segment of load in area i under wind pattern type s (MW)

F_{ij} Capacity of tie line between areas i and j (MW)

T_t^s The duration of the tth segment of load under wind pattern type s (hours)

Π_i The maximum wind capacity that can be installed in area i (MW)

Ω Total wind capacity that should be installed (MW)

Decision Variables

f_{ijt}^{s} Power flow from area i to area j for demand segment t under wind distribution s (MW)

q_{it}^{s} Generation for demand segment t in area i under wind distribution s (MW)

l_{it}^{s} Load loss for demand segment t in area i under wind distribution s (MW)

x_i Wind power capacity installed in area i (MW)

Indices for the Mathematical Formulation

k Indices of all functions characterizing the distributions of random variables, it is equivalent to the indices of auxiliary variables $\tilde{\boldsymbol{u}}$

m Indices of all first-stage and second-stage constraints

n Indices of all first-stage and second-stage decision variables

r Indices of all constraints that define the extended support set $\bar{\mathcal{Z}}$

v Indices of all random variables $\tilde{\boldsymbol{z}}$

Sets for the Mathematical Formulation

$\mathbb{F}$	Ambiguity set defining the distributions of all random variables
$\bar{\mathbb{F}}$	Extended ambiguity set
$\mathcal{K}$	Set of all functions characterizing the distributions of random variables, equivalent to the sets of auxiliary variables $\tilde{\boldsymbol{u}}$
$\mathcal{M}_1$	Set of all first-stage constraints
$\mathcal{M}_2$	Set of all second-stage constraints
$\mathcal{N}_1$	Set of all first-stage decision variables
$\mathcal{N}_2$	Set of all second-stage decision variables
$\mathcal{R}$	Set of all constraints that define the extended support set $\bar{\mathcal{Z}}$
$\mathcal{V}$	Set of all random variables $\tilde{\boldsymbol{z}}$
$\mathcal{Z}$	Uncertainty set of random variables $\tilde{\boldsymbol{z}}$
$\bar{\mathcal{Z}}$	Extended support set of random variables $\tilde{\boldsymbol{z}}$

Matrices and Vectors of the Mathematical Formulation

$\boldsymbol{A}$	Matrix of the coefficients of $\boldsymbol{x}$ for first-stage constraints
$\boldsymbol{b}$	Right-hand-side vector of the first-stage constraints
$\boldsymbol{C}(\boldsymbol{z})$	Uncertain left-hand-side matrix of coefficient of $\boldsymbol{x}$ for the second-stage constraints
$\boldsymbol{D}$	Left-hand-side matrix of coefficient of $\boldsymbol{y}$ for the second-stage constraints
$\boldsymbol{d}(\boldsymbol{z})$	Uncertain right-hand-side vector of the second-stage constraints
$\boldsymbol{H}$	Matrix of the coefficients of $\boldsymbol{u}$ for the constraints defining the extended support set $\bar{\mathcal{Z}}$
$\boldsymbol{h}$	Right-hand-side vector of the constraints defining extended support set $\bar{\mathcal{Z}}$
$\boldsymbol{u}$	Auxiliary variables introduced into the extended ambiguity set $\bar{\mathbb{F}}$
$\boldsymbol{x}$	Vector of first-stage decision variables
$\boldsymbol{y}$	Vector of second-stage decision variables or decision rules
$\boldsymbol{z}$	Vector of random variables

Others

$\mathbb{E}_{\mathbb{P}}$	Expected value under distribution $\mathbb{P}$
$g_k(\cdot)$	Linear representable functions characterizing the distributions of random variables $\boldsymbol{z}$
$L(\cdot)$	Function indicating energy not served
$\mathbb{P}$	A distribution of all random variables $\boldsymbol{z}$
$\mathbb{Q}$	A distribution of all random variables $\boldsymbol{z}$ and auxiliary variables $\boldsymbol{u}$
$\mathcal{Q}_0(\cdot)$	Set of all distributions for random variables with the given dimension
$\lvert\cdot\rvert$	The cardinality of a set or the absolute value of a mathematical expression

TABLE OF CONTENTS

Page

LIST OF FIGURES

FIGURE Page

LIST OF TABLES

TABLE Page

1. INTRODUCTION

1.1 Wind Power Generation

Wind power generation (WPG) is the most widely used and the fastest expanding renewable resource for electric power generation worldwide [1–3]. It shows a remarkable increase in growth rate over the past two decades [4], and it has become a primary source for electric power generation in several countries [5]. Furthermore, besides the issue of the global warming and the depletion of fossil fuels needed to generate electricity, the trend in the sector of the electric power industry is towards the investment in renewable energy resources [6], to accomplish goals such as carbon dioxide emission reduction, energy self-sufficiency, increasing the system reliability, prevent load curtailment and improving the social welfare [7].

Consequently, the dramatic expansion of WPG poses several challenges in terms of power system operation, since WPG is intermittent, uncertain and not fully dispatchable, which requires extra attention to power system planning and operation studies with a particular emphasis on modeling the uncertainty of power system, to ideally perform economic dispatch, unit commitment and spinning reserve, as the generation should balance the load demand on a moment-by-moment basis keeping the operational constraints of both generation units and transmission lines networks with no violation [8–10]. So in long-term power system planning, an optimal decision to efficiently integrate a large-scale WPG into the power system besides the existing conventional generation has played a significant role in a reliable and economical operation for the entire power system [3, 11, 12], which indeed motivates to more development in planning procedures and techniques to examine a wide range of uncertainty representation methods [4, 13].

1.2 Probabilistic Modeling of Uncertainty

Unlike conventional power generation, many renewable energy resources such as the wind or solar have a maximum power output that varies with time which is described by random variability [14]. Such uncertain behavior of the renewable energy resources increases the difficulties of power system operation, in which the generation should balance the load demand on a moment-by-moment basis keeping the operational constraints of both generation units and transmission lines networks with no violation [10]. To accommodate high penetration of variable energy resources in the power systems generation, the system is required to be more flexible to follow the variable net demand and deal with the uncertainties to maintain the reliability and the security of the system within the desired levels [15].

To cope with the uncertain nature imposed by the renewable energy resources and the electric power components, the application of probabilistic tool is useful to investigate and represent the uncertain system. [16]. The uncertain arbitrary variable can be modeled and described by the probability distribution functions (PDF), which is an important step to deal with the variability issue. The intensive meteorological observation of the wind and solar pattern to represent it in proper statistical parameters reduces the problem of uncertainty, and it assures the highest possible flexibility and availability needed to keep the load-generation balance during the operation [15]. In the next section, the methods and system models which are used to deal with system uncertainty are introduced.

1.3 Optimization Model under Uncertainty

It is important to develop a non-deterministic optimal wind power allocation framework which includes the uncertain nature of both the wind power availability and other random power system components. The method should be computationally tractable and statistically consistent, for finding a flexible solution against different realizations of uncertainty representation. In power system operation and planning studies, several methodologies like scenario interpretation and probabilistic analysis have been developed to deal with the uncertainty of wind power.

Stochastic Programming (SP) [17], represents uncertain variables through scenarios based on the assumption that the exact probability distribution of wind power is available [11]. A high accuracy probability distribution function representation of the uncertain nature of variable generation has to be obtained in order to ideally apply SP, and that requires sufficient historical data which is not always available. The lack of sufficient data limits the ability of SP and deteriorates its performance [18].

Although this problem has been mitigated by introducing Robust Optimization (RO) [19,20], which can be used even with no availability of any distributions data parameters, except some data which can preserve the system against a pre-determined uncertainty set [21], such approach drives the solution to be conservative [10]. RO models uncertainty as a deterministic set without any probabilistic information. It affords a robust solution that is preserved to any possible scenario of the uncertainty set, which is an essential perspective in the security-constrained electric power systems planning, however, that would lead to a conservative and sometimes less effective solution [22]. Furthermore, RO uses bounded intervals to handle a broad range of uncertainty sources in modeling the uncertain random variables.

As a matter of fact, RO is generally more useful in terms of less frequent un-

certainty sources, since it only requires the relative variation intervals of uncertain variables rather than generating scenarios as applied in SP. Furthermore, RO is more conservative compared to SP. While the solution of RO is optimal for the worst case realization of uncertain variables, the solution of SP is optimal on average for a set of deterministic scenarios which capture the nature of uncertainty [12]. As an intermediate methodology, Distributionally Robust Optimization (DRO) [23], is introduced to mitigate the limitations of SP and RO by providing a tractable approach to probabilistically include the available characteristic information of the uncertain variables in an ambiguity set [24–26], and it is less conservative by avoiding the extreme decision of totally neglecting the probability distribution of the random variables as applied in RO. The detailed procedure of the proposed approached is demonstrated in the following section.

1.4 Distributionally Robust Optimization

DRO has been recently applied in several power system problems to represent the uncertainty of random variables [10, 27]. Its capability in probabilistic interpretation of the data-driven decision making is the bottom line behind its success [28]. DRO operates by including certain probabilistic information of the uncertain variables appropriately in the optimization modeling; it deals with the uncertain parameter as a random variable that tracks the stochastic nature by involving a family of probability distributions characteristics defined by an ambiguity set [29].

Compared to SP, which improve the optimal solution by minimizing the expectation of the energy not served under the scenarios representation of the system uncertainties following one distinct probability distribution, DRO overcomes the critical assumption in SP regarding the availability of the exact distribution information. Additionally, DRO resolves the computational difficulties addressed by the SP scenario

representation which requires decomposition and scenario selection algorithms [4,30].

On the other hand, the conventional RO achieves the objective under the worst-case energy not served over all possible realizations within a deterministic uncertainty set of the uncertain variables. It solves the issue of the scenarios interpretation proposed in SP, but it can not model indices in terms of the expected values and leads to more conservative solution by totally neglecting the probability distribution [20]. So, DRO is primarily the integrated robust practice of the stochastic programming. [22] which provides a moderate method to represent uncertainty in reliability based design optimization.

The objective of this research is to allocate a certain amount of renewable power genration in a multi-area power system to minimize the expected energy not served under the worst-case probability distribution that is characterized by the ambiguity set of the renewable power uncertainty and generator forced outages. The linear decision rule approximation [23, 31, 32] is used to restrict the second-stage recourse decisions to be affinely dependent on uncertain parameters as well as auxiliary random variables where the distributional statistical information of uncertain variables are represented, so that the overall problem can be solved in a tractable manner [33].

1.5 Monte Carlo Simulation for Generation Adequacy Evaluation

The sampling based Monte Carlo simulation (MCS) is utilized to perform the sensitivity analysis of the proposed renewable generation expansion design problem. This practice is widely used in the planning studies due to its simplicity in implementing and effectiveness in evaluating the proposed decisions. It is beneficial with calculating all required system operation information and reliability indices.

In general, this simulation approach offers more flexibility with handling the system's operational conditions, because it allows for the scenarios representation

based simulation which should reflect all possible operational system states with sufficient number of scenarios to secure the convergence and provide accurate results for a fair evaluation of any stage of reliability analysis. Reliability indices like loss of load expectation (LOLE) and expected energy not served (EENS) are estimated using MCS. However, to yield a converged and trusted solution the MCS may need a long computational time to process such large number of scenarios.

In the sampling technique, the main procedure is to generate random samples of the system states including the wind power, conventional generation, and all other random variables of the system components according to their particular probability distributions. The other fixed information like the system configuration, operational limits, and the constraints are fixed for every iteration. Then after simulating a sufficient number of samples which lead to an acceptable value of the coefficient of variance (COV) for that distinct set of samples or scenarios, the reliability indices are then analytically calculated from those samples.

The convergence of the simulation occurs when the coefficient of variation of the calculated index from a set of samples lies within a consistent range, such range is set to be generally less or equal to 5%. Such convergence is strongly associated with the loss of load probability (LOLP) since the COV calculation depends on the events occurring on the power system. In a reliable power system, where the loss of load events happen relatively rarely, observing the variation requires a long computational time since the change is small due to the estimation of relatively low value of the LOLP, which makes the MCS more computationally challenging with a reliable power system.

A combination of optimization schemes incorporating with reliability evaluation is practiced in many types of planning and design problems. In [34], adequacy determination of locational generation and transmission lines transfer capacities are eval-

uated. The optimization procedure is used for a planning investigation of any additional expansion of both power generation and transmission lines. References [35,36] discusse an optimization procedure for generation expansion determination based on a reliability evaluation in multi-area power systems. The global decomposition approach is utilized to get a proper tradeoff between the cost and the power system reliability. The stochastic programming based optimization to represent the uncertainties in conventional generation, transmission lines and the load demands to evaluate the power generation expansion problem in the multi-area power system is introduced in [37–40]. A stochastic programming using Bender's decomposition algorithm is used to optimize the transmission lines expansion problem with the high penetration of the wind power is investigated in [41]. All the above problems usually seek for the solution that maximizes the system reliability and minimizing the planning or operational cost. Because of the system uncertainties presence during the reliability evaluation the system is classified to be a stochastic problem which requires more attention to probabilistic modeling of their components and find the optimization approach which takes this particular feature into account.

To construct the probability distribution function or the density function of the conventional generation availability using MCS, the historical information like failure rates and repair rates of all generation components have to be available.

1.6 Multi-Area Power System

When realizing a multi-area power system as a wide geographically connected regions with separated wind farms, the second and minute variations in a single area can be relieved by the smoothing effect of the other areas wind generation diversity which is accounted as an advantage in stabilizing the system operation while the wind power generation is appropriately distributed [15].

Multi-area power systems can be modeled as a network flow structure of multiple areas connected by tie lines where each area represents an electrical power system consisting of generators, transformers, transmission lines and load buses. Each area has its particular configuration with different component ratings and reliability based information like forced outages rate (FOR), mean up time and mean down time which allows finding the failure and repair rates to conduct the Monte Carlo simulation.

The generation system is modeled based on its discrete probability distribution function which can be constructed using Monte Carlo simulation or analytically using Markov chain by knowing its generation units capacities and their forced outage rates (FOR). In this research the Monte Carlo based simulation to construct the generation model is used for each area of the system. The load model is formed as load duration curve (LDC), such model is sufficient in the planning problem studies using non-sequential Monte Carlo based simulation, whereas the hourly model or chronological model is preferred in the operational type studies where the analysis at a small time scale is critical. However, in the planning problem which considers a large set of historical data to be analyzed, considering the chronological model will make the study of different realization for multiple case studies in a single year difficult and not practical due to the high computational time required to do the simulation.

Considerable attention therefore has been given to multi-area system reliability assessment while allocating wind power generation and which area should be reinforced with wind power generation among other areas in the overall system [42]. The adoption of reliability evaluation and optimization schemes is utilized in many kinds of system planning and operation problems [43]. These problems usually search for the optimal solution that maximizes system reliability subjected to the operational constraints [8].

In this research, the model considers the wind power correlations between the

areas. Since each area generally follows a different probability distribution comparing to other far distance areas, such difference would fulfill the shortage of certain areas by the excess of others, which would enhance the generation adequacy and the overall power system reliability [9,44]. Moreover, the association of transmission constraints in the model would impose additional security obligations to ensure system reliability, since transmission constraints heavily influence the optimal precept for allocating the wind power generation in each area of the network [13]. The planning problem determines the percentage of investment committed to each area according to an overall specific budget that would minimize the expected energy not served in the entire system, which could mitigate the influence of outages, encourage affordable and stable market prices, and promote investments in sustain and more efficient manner [45].

1.7 Organization of the Dissertation

The dissertation is organized as follows. Chapter 2 describes the mathematical model of DRO based approach for wind farm allocation using the linear representation of statistical wind power data; the proposed method is validated with a case study on a five-area power system. Chapter 3 improves the method introduced in Chapter 2 by applying further effective procedure in representing wind power data using second-order cone programming. Chapter 4 introduces the DRO based planning scheme in allocating hybrid (the wind and solar) power generation system and how the diversity in utilizing the renewable power generation improves the power system reliability. Chapter 5 address the capacity credit evaluation using the analytical approach to estimate the effective load carrying of the installed renewable power generation units. The conclusion of the results in this dissertation is given in Chapter 6. The References and the appendixes are attached at the end.

2. WIND FARM ALLOCATION PLANNING PROBLEM

2.1 Linear Representation Formulation of Wind Power Statistical Parameters

2.1.1 A Two-Stage Wind Farm Allocation Model

The wind farm allocation model is formulated as a two-stage problem, where the wind power allocation decisions are made in the first stage, and the operation decisions are determined as the random wind power $\tilde{\boldsymbol{w}}$ and the uncertain generator capacity $\tilde{\boldsymbol{p}}$ are realized.

The first-stage wind power planning problem is expressed as follows.

$$\min \ \sup_{\mathbb{P}\in\mathbb{F}} \mathbb{E}_{\mathbb{P}} \left\{ L(\boldsymbol{x}, \tilde{\boldsymbol{w}}, \tilde{\boldsymbol{p}}) \right\} \tag{2.1}$$

$$\text{s.t. } 0 \leq x_i \leq \Pi_i \tag{2.2}$$

$$\sum_{i\in\mathcal{I}} x_i = \Omega \tag{2.3}$$

where $\boldsymbol{x}$ is the vector of first-stage decision variables, where x_i represents the wind power capacity placed in area i. The constraints (2.2) indicates that the wind capacity x_i in each area is subject to an upper limitation Π_i, due to geographic conditions, environmental or social concerns. The total capacity of installed wind power for all areas in $\mathcal{I}$ is denoted by Ω in (2.3).

The objective function (2.1) minimizes the expected energy not served (EENS) under the worst-case distribution of $\tilde{\boldsymbol{w}}$ and $\tilde{\boldsymbol{p}}$, which is denoted by $\mathbb{P}$ over an *ambiguity set* $\mathbb{F}$. The detailed discussion on the ambiguity set $\mathbb{F}$ is given in the next subsection. The expression $L(\boldsymbol{x}, \boldsymbol{w}, \boldsymbol{p})$ in (2.1) indicates the amount of energy not served for the wind farm allocation decision $\boldsymbol{x}$ under the wind power outcome $\boldsymbol{w}$ and the generation capacity realization $\boldsymbol{p}$. It is expressed as the second-stage optimization problem

shown below.

$$L(\boldsymbol{x},\boldsymbol{w},\boldsymbol{p}) = \min \sum_{s\in\mathcal{S}}\sum_{t\in\mathcal{T}}\sum_{i\in\mathcal{I}} T_t^s l_{it}^s \tag{2.4}$$

$$\text{s.t.} \quad x_i w_i^s + q_{it}^s - \sum_{j\in\mathcal{J}_i^f} f_{jit}^s + \sum_{j\in\mathcal{J}_i^t} f_{ijt}^s = D_{it}^s - l_{it}^s,$$

$$\forall i \in \mathcal{I}, \forall t \in \mathcal{T}, \forall s \in \mathcal{S} \tag{2.5}$$

$$-F_{ij} \le f_{ijt}^s \le F_{ij},$$

$$\forall j \in \mathcal{J}_i^f, \forall i \in \mathcal{I}, \forall t \in \mathcal{T}, \forall s \in \mathcal{S} \tag{2.6}$$

$$0 \le q_{it}^s \le p_i, \quad \forall i \in \mathcal{I}, \forall t \in \mathcal{T}, \forall s \in \mathcal{S} \tag{2.7}$$

$$l_{it}^s \ge 0 \quad \forall i \in \mathcal{I}, \forall t \in \mathcal{T}, \forall s \in \mathcal{S} \tag{2.8}$$

This formulation considers a set of wind power distributions, denoted by $\mathcal{S}$, in order to capture the seasonal or day-night differences of wind power patterns [13]. The load duration curve under each wind power distribution type s is approximated by a segment expression, illustrated by an example in Fig. 2.1. The index of each load segment is denoted by t, and the set $\mathcal{T}$ is the set of all load segments [46–49].

For each time segment t under wind power distribution s, the constant T_t^s denotes the duration of load segment t under wind power distribution type s, and D_{it}^s is the corresponding load in area i. The variables q_{it}^s and l_{it}^s are the conventional generation and load loss in area i, respectively, and the power transmitted from area j to area i is denoted by f_{ijt}^s. The objective function (2.4) indicates the amount of energy not served over a year. The power balance in each area is enforced by equation (2.5). Constraint (2.6) suggests that the power flow from area i to area j should be within the capacity of transmission lines. The conventional generation q_{it}^s should also be constrained below the available capacity p_i, as expressed by (2.7). The last inequality

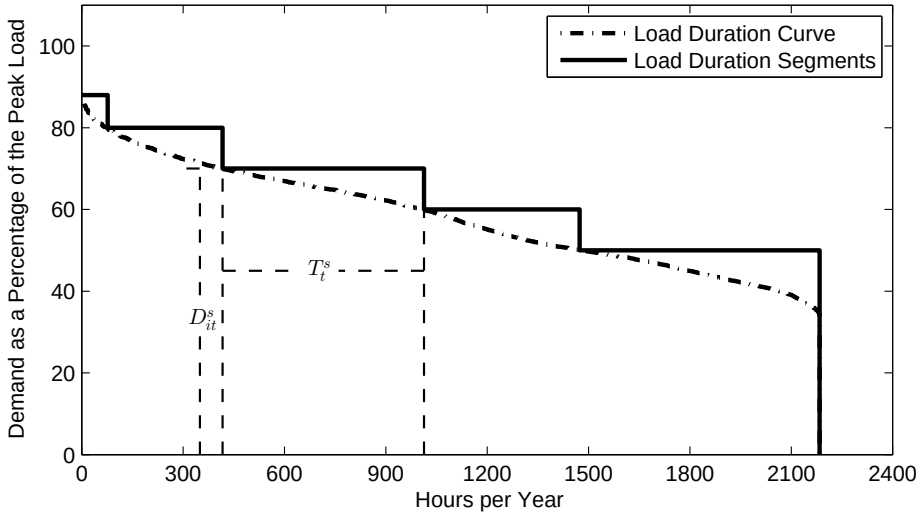

Figure 2.1: Illustration of the segment approximation of load duration, as an example of the RTS-1996 load data in Spring

(2.8) indicates that the loss of load l_{it}^s should be nonnegative.

2.1.2 Ambiguity Set

The proposed wind power planning formulation in this research addresses two types of uncertainties: the random wind power generation and the forced outages of generators. Unlike the stochastic programming approaches that optimize the expectation based on one underlying distribution, this distributionally robust optimization model manages system uncertainties by considering a family of distributions, defined by an ambiguity set [8, 50]. against the incomplete or the lack of accuracy of distribution information.

The following expressions (2.9)-(2.12) are applied in the ambiguity set to define

a family of wind power distributions.

$$\Pr\{\tilde{\boldsymbol{w}} \in \mathcal{W}\} = 1 \tag{2.9}$$

$$\mathbb{E}_{\mathbb{P}}\{\tilde{w}_i^s\} = \bar{w}_i^s, \forall i \in \mathcal{I}, \forall s \in \mathcal{S} \tag{2.10}$$

$$\mathbb{E}_{\mathbb{P}}\{\max\{\tilde{w}_i^s - W_{il}^s, 0\}\} \leq \alpha_{il}^s,$$
$$\forall i \in \mathcal{I}, \forall l \in \mathcal{L}^{\alpha}, \forall s \in \mathcal{S} \tag{2.11}$$

$$\mathbb{E}_{\mathbb{P}}\left\{\max\{\tilde{w}_i^s + \tilde{w}_j^s - \bar{w}_i^s - \bar{w}_j^s, 0\}\right\} \leq \beta_{ij}^s,$$
$$\forall j < i \in \mathcal{I}, \forall s \in \mathcal{S} \tag{2.12}$$

The equation (2.9) suggests that the vector of random wind power generation is constrained within an uncertainty set $\mathcal{W}$, which is designed similarly to that in the conventional robust optimization problems. In this research, the uncertainty set $\mathcal{W}$ is defined as (2.13).

$$\mathcal{W} = \left\{\boldsymbol{w} \in \mathbb{R}^{|\mathcal{I}|\times|\mathcal{S}|} : \ 0 \leq w_i^s \leq 1, \ \forall i \in \mathcal{I}, \forall s \in \mathcal{S}\right\} \tag{2.13}$$

The equation (2.10) implies that the expected value of each $\tilde{w}_i^s$ is $\bar{w}_i^s$, and the next inequality (2.11) incorporates distribution information α_{il}^s in terms the absolute deviation of $\tilde{w}_i^s$ around a selected wind power level W_{il}^s into the ambiguity set. Because the distribution of wind power is typically skewed and long-tailed [51, 52], or even bimodal [53,54], the expression (2.11) is used for multiple wind power levels W_{il}^s in order to capture the variability and skewness of wind power distributions, illustrated by the upper plot in Fig. 2.2. As more wind power levels are considered, the distributions of wind power generation can be represented in a more precise manner and the worst-case distribution should be less adverse, leading to less conservative solutions [55, 56]. The last expression (2.12) is used to limit the mean absolute de-

viation of the generation summation from two wind farms below a constant β_{ij}^s, as illustrated by the lower plot in Fig. 2.2. This inequality implicitly incorporates the information on the correlation between wind farms into the ambiguity set. If the power output from two wind farms are negatively correlated, the constant β_{ij}^s is likely to be smaller, and positive correlation commonly lead to larger β_{ij}^s. Notice that unlike the stochastic programming approaches that consider one wind power distribution by the scenario-representation, the proposed uncertainty model addresses a family of distributions characterized by the parameters $\bar{w}_i^s$, α_{il}^s and β_{ij}^s, which can be calculated straightforwardly based on the historical data, thus more practical than identifying the exact distribution of wind power generation.

The uncertain conventional generation capacities $\tilde{\boldsymbol{p}}$ can be modeled in a similar way, as expressed by (2.14)-(2.17).

$$\Pr\left\{\tilde{\boldsymbol{p}} \in \mathcal{P}\right\} = 1 \tag{2.14}$$

$$\mathbb{E}_{\mathbb{P}}\left\{\tilde{p}_i\right\} = \bar{p}_i, \qquad \forall i \in \mathcal{I} \tag{2.15}$$

$$\mathbb{E}_{\mathbb{P}}\left\{\max\{P_{il} - \tilde{p}_i, 0\}\right\} \leq \gamma_{il}, \quad \forall i \in \mathcal{I}, \forall l \in \mathcal{L}^{\gamma} \tag{2.16}$$

$$\mathbb{E}_{\mathbb{P}}\left\{\max\left\{Q_l - \sum_{i\in\mathcal{I}} \tilde{p}_i, 0\right\}\right\} \leq \delta_l, \qquad \forall l \in \mathcal{L}^{\delta} \tag{2.17}$$

The first expression (2.14) implies that the vector of uncertain generation capacity is constrained within an uncertainty set $\mathcal{P}$, which is defined as follows:

$$\mathcal{P} = \left\{\boldsymbol{p} \in \mathbb{R}^{|\mathcal{I}|} : \ p_i^{min} \leq p_i \leq p_i^{max}, \ \forall i \in \mathcal{I} \right\} \tag{2.18}$$

Similar to (2.10), the second equation (2.15) defines the expected value of the uncertain generation capacity $\tilde{p}_i$. The third expression (2.16) selects a set of generation levels P_{il}, denoted by $\mathcal{L}^{\gamma}$, and enforces the expected value of the positive

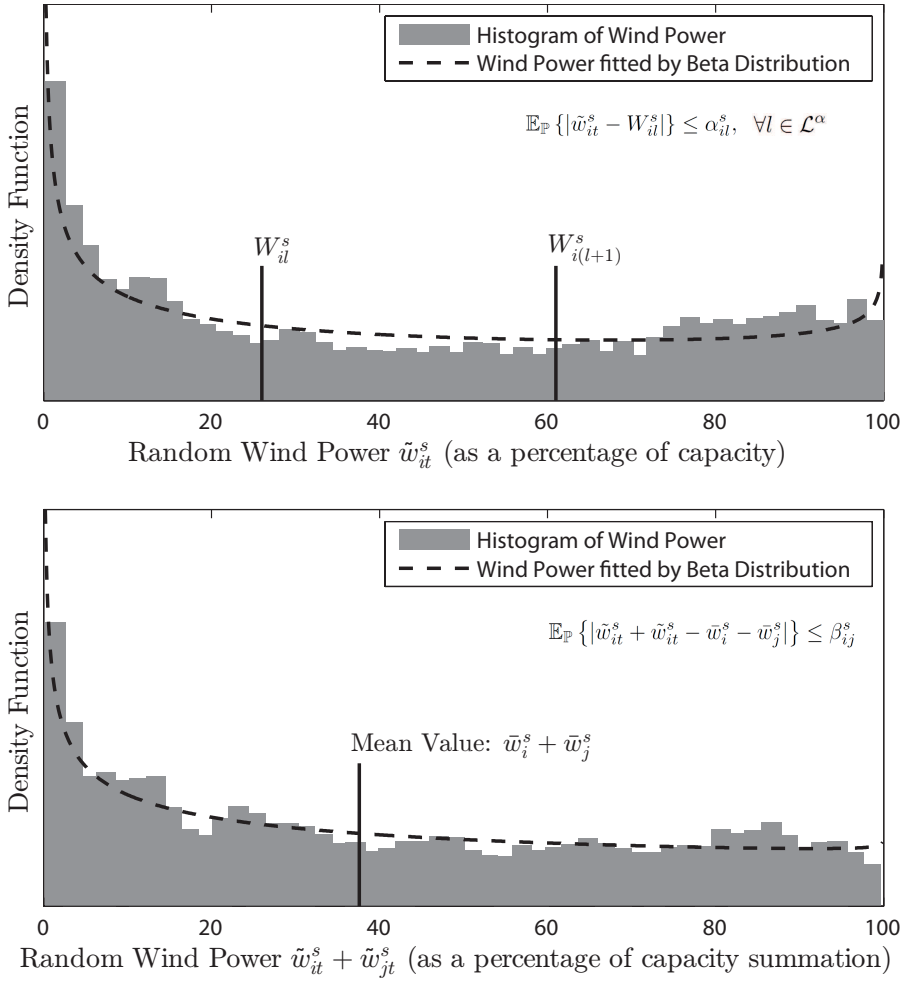

Figure 2.2: Illustration of the expressions that characterize the wind power distributions, based on an example of California wind farms in Spring

part of $P_{il} - \tilde{p}_i$ below a constant γ_{il}, as illustrated by the upper plot in Fig. 2.3. The last expression characterizes the distribution of the total generation capacity in the same fashion, i.e., the expected value of the positive part of $Q_l - \sum_{i \in \mathcal{I}} p_i$ is constrained below a constant δ_l, where Q_l is the selected generation level, and $\mathcal{L}^\delta$ is the set of all selected levels, as shown in the lower plot of Fig. 2.3. Note that both the expressions (2.16) and (2.17) are utilized to incorporate the information on distribution patterns of generation capacities into the ambiguity set, and this uncer-

tainty model is more practical than conventional stochastic programming methods because there is no need to attain the detailed data on the exact generation capacity distribution, which is usually inaccessible or too complex to represent. Instead, we only need to calculate the constants γ_{il} and δ_l based on the historical data and the selected generation levels. Including more generation levels into the sets $\mathcal{L}^\gamma$ and $\mathcal{L}^\delta$ will improve the precision of characterizing the distribution of generation capacities in the ambiguity set.

By combining the wind power uncertainty model (2.9)-(2.12) and the generation capacity expressions (2.14)-(2.17), the overall ambiguity set, denoted by $\mathbb{F}$, can be formulated as (2.19).

Based on the ambiguity set presented above, the proposed wind power allocation model minimizes the expected energy not serve under the worst-case distribution. In the next section, this two-stage formulation is reformulated into a tractable linear programming problem using the linear decision rule approximation.

$$\mathbb{F} = \left\{ \mathbb{P} \in \mathcal{Q}_0 \left(\mathbb{R}^{|\mathcal{I}|\times|\mathcal{S}|} \times \mathbb{R}^{|\mathcal{I}|} \right) : \begin{array}{l} \tilde{\boldsymbol{w}} \in \mathbb{R}^{|\mathcal{I}|\times|\mathcal{S}|} \\ \Pr\{\tilde{\boldsymbol{w}} \in \mathcal{W}\} = 1 \\ \mathbb{E}_{\mathbb{P}}\{\tilde{w}_i^s\} = \bar{w}_i^s \\ \mathbb{E}_{\mathbb{P}}\{\max\{\tilde{w}_i^s - W_{il}^s, 0\}\} \le \alpha_{il}^s, \forall i \in \mathcal{I} \\ \mathbb{E}_{\mathbb{P}}\left\{\max\{\tilde{w}_i^s + \tilde{w}_j^s - \bar{w}_i^s - \bar{w}_j^s, 0\}\right\} \le \beta_{ij}^s \\ \tilde{\boldsymbol{p}} \in \mathbb{R}^{|\mathcal{I}|} \\ \Pr\{\tilde{\boldsymbol{p}} \in \mathcal{P}\} = 1 \\ \mathbb{E}_{\mathbb{P}}\{\tilde{p}_i\} = \bar{p}_i \\ \mathbb{E}_{\mathbb{P}}\{\max\{P_{il} - \tilde{p}_i, 0\}\} \le \gamma_{il} \\ \mathbb{E}_{\mathbb{P}}\left\{\max\left\{Q_l - \sum\limits_{i\in\mathcal{I}} \tilde{p}_i, 0\right\}\right\} \le \delta_l \end{array} \right\} \quad (2.19)$$

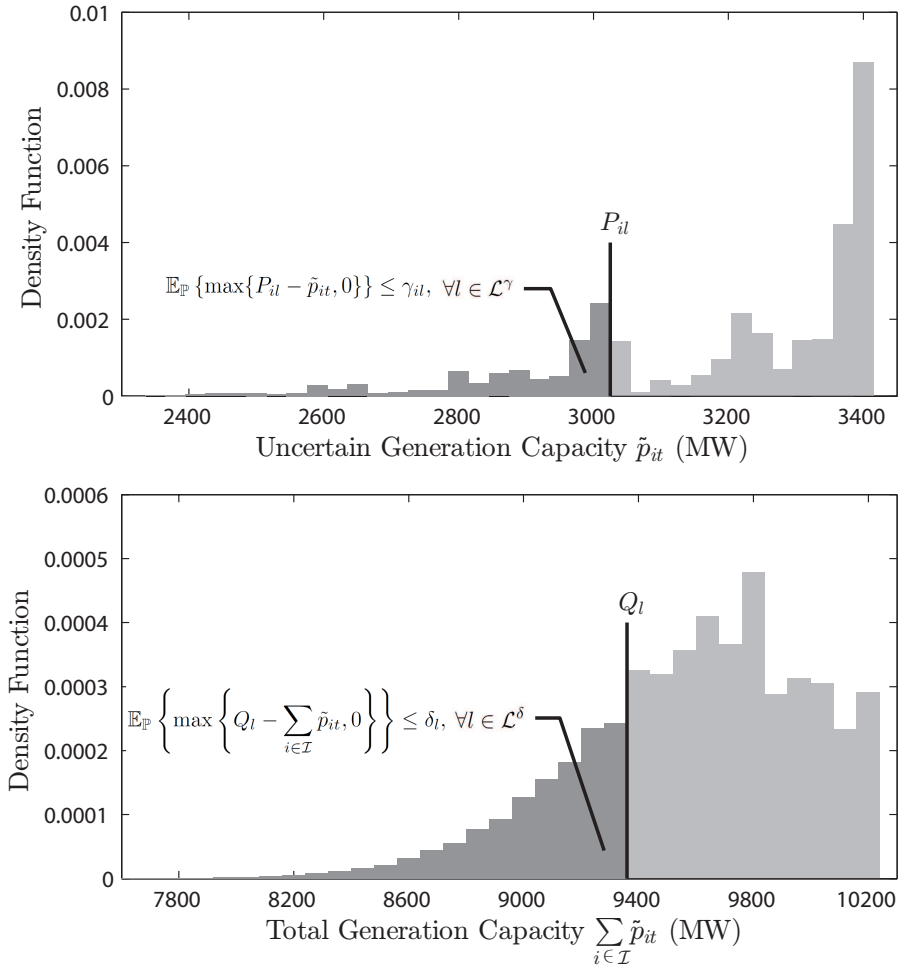

Figure 2.3: Illustration of the expressions that characterize the generation capacity distributions, based on an example of the Reliability Test System 1996

2.2 Problem Solving Procedure

2.2.1 Compact Matrix Formulation

The formulation presented in the previous section is expressed in more general compact matrix forms, in order to facilitate the discussion of the reformulation procedure. In this section, vectors are represented by bold lower case letters, and matrices are represented by bold capital letters. Elements of vectors or matrices are denoted

by regular letters with subscripts indicating the indices. The first-stage decisions are still denoted by $\boldsymbol{x}$, and the set of all first-stage decisions is named as $\mathcal{N}_1$. All second-stage decisions, including q_{it}^s, f_{ijt}^s, and l_{it}^s, are represented by a vector $\boldsymbol{y}$, and the set of all second-stage decision variables is denoted by $\mathcal{N}_2$. The random variables $\boldsymbol{w}$ and $\boldsymbol{p}$ are combined as a vector $\boldsymbol{z} \in \mathbb{R}^{|\mathcal{V}|}$, where $\mathcal{V}$ is the set of all random variables.

The first-stage problem (2.1)-(2.3) is then expressed as the matrix form (2.20)-(2.21).

$$\min \ \sup_{\mathbb{P}\in\mathbb{F}} \mathbb{E}_{\mathbb{P}} \left\{ L(\boldsymbol{x}, \tilde{\boldsymbol{z}}) \right\} \tag{2.20}$$

$$\text{s.t. } \boldsymbol{A}\boldsymbol{x} \leq \boldsymbol{b} \tag{2.21}$$

with $\boldsymbol{x} \in \mathbb{R}^{|\mathcal{N}_1|}$, $\boldsymbol{A} \in \mathbb{R}^{|\mathcal{M}_1|\times|\mathcal{N}_1|}$ and $\boldsymbol{b} \in \mathbb{R}^{|\mathcal{M}_1|}$, where $\mathcal{M}_1$ is the set of all first-stage constraints.

The second-stage problem (2.4)-(2.8) used for calculating function $L(\boldsymbol{x}, \boldsymbol{z})$ is given as (2.22)-(2.23).

$$L(\boldsymbol{x}, \boldsymbol{z}) = \min \ \boldsymbol{q}^T \boldsymbol{y} \tag{2.22}$$

$$\text{s.t. } \boldsymbol{C}(\boldsymbol{z}) + \boldsymbol{D}\boldsymbol{y} \leq \boldsymbol{d}(\boldsymbol{z}) \tag{2.23}$$

with $\boldsymbol{q} \in \mathbb{R}^{|\mathcal{N}_2|}$, $\boldsymbol{C}(\boldsymbol{z}) \in \mathbb{R}^{|\mathcal{M}_2|\times|\mathcal{N}_1|}$, $\boldsymbol{D} \in \mathbb{R}^{|\mathcal{M}_2|\times|\mathcal{N}_2|}$, and $\boldsymbol{d}(\boldsymbol{z}) \in \mathbb{R}^{|\mathcal{M}_2|}$, where $\mathcal{M}_2$ represents the set of all second-stage constraints. Notice that both the left-hand-side constraints matrix $\boldsymbol{C}(\boldsymbol{z})$ and the right-hand-side coefficient vector $\boldsymbol{d}(\boldsymbol{z})$ are affected by the random variables $\boldsymbol{z}$. They are commonly assumed to be the following linear

affine form [33].

$$\boldsymbol{C}(\boldsymbol{z}) = \boldsymbol{C}^0 + \sum_{v \in \mathcal{V}} \boldsymbol{C}^v z_v \tag{2.24}$$

$$\boldsymbol{d}(\boldsymbol{z}) = \boldsymbol{d}^0 + \sum_{v \in \mathcal{V}} \boldsymbol{d}^v z_v \tag{2.25}$$

with constants $\boldsymbol{C}^0, \boldsymbol{C}^v \in \mathbb{R}^{|\mathcal{M}_2| \times |\mathcal{N}_1|}$, and $\boldsymbol{d}^0, \boldsymbol{d}^v \in \mathbb{R}^{|\mathcal{M}_2|}$. The other parameters in matrix $\boldsymbol{D}$ are independent from the random variables, hence is the case of fixed recourse [17].

The ambiguity set (2.19) is expressed as the compact matrix form below.

$$\mathbb{F} = \left\{ \mathbb{P} \in \mathcal{Q}_0 \left(\mathbb{R}^{|\mathcal{V}|} \right) : \begin{array}{l} \tilde{\boldsymbol{z}} \in \mathbb{R}^{|\mathcal{V}|} \\ \Pr\{\tilde{\boldsymbol{z}} \in \mathcal{Z}\} = 1 \\ \mathbb{E}_{\mathbb{P}}\{\tilde{z}_v\} = \bar{z}_v, \quad \forall v \in \mathcal{V} \\ \mathbb{E}_{\mathbb{P}}\{g_k(\tilde{\boldsymbol{z}})\} \leq \sigma_k, \forall k \in \mathcal{K} \end{array} \right\} \tag{2.26}$$

The second line of (2.26) suggests that the vector of random variables is constrained within an uncertainty set $\mathcal{Z}$, which is the combination of set $\mathcal{W}$ in (2.9) and $\mathcal{P}$ in (2.14). The third line of (2.26) is the generalized form of expressions (2.10) and (2.15), used to define the expected value of random variables. The last line in (2.26) is the compact matrix form of the remaining inequalities in (2.19). The function $g_k(\tilde{\boldsymbol{z}})$ in (2.26) generalizes the absolute deviation and the positive part expression in (2.11)-(2.12) and (2.16)-(2.17), and all constants α_{il}^s, β_{ij}^s, γ_{il}, and δ_l are represented by σ_k.

2.2.2 Extended Ambiguity Set

In this subsection, the ambiguity set $\mathbb{F}$ in (2.26) is extended in (2.27) by by introducing auxiliary variables $\tilde{u}_k$ that express the upper bound of each function $g_k(\tilde{\boldsymbol{z}})$ into the formulation.

$$\bar{\mathbb{F}} = \left\{ \mathbb{Q} \in \mathcal{Q}_0 \left(\mathbb{R}^{|\mathcal{V}|} \times \mathbb{R}^{|\mathcal{K}|} \right) : \begin{array}{l} (\tilde{\boldsymbol{z}}, \tilde{\boldsymbol{u}}) \in \mathbb{R}^{|\mathcal{V}|} \times \mathbb{R}^{|\mathcal{K}|} \\ \Pr\left\{ (\tilde{\boldsymbol{z}}, \tilde{\boldsymbol{u}}) \in \bar{\mathcal{Z}} \right\} = 1 \\ \mathbb{E}_{\mathbb{P}} \left\{ \tilde{z}_v \right\} = \bar{z}_v, \forall v \in \mathcal{V} \\ \mathbb{E}_{\mathbb{P}} \left\{ \tilde{u}_k \right\} \leq \sigma_k, \forall k \in \mathcal{K} \end{array} \right\} \tag{2.27}$$

where $\bar{\mathcal{Z}}$ is the extended form of the uncertainty set $\mathcal{Z}$, expressed as (2.28).

$$\bar{\mathcal{Z}} = \left\{ (\boldsymbol{z}, \boldsymbol{u}) \in \mathbb{R}^{|\mathcal{V}|} \times \mathbb{R}^{|\mathcal{K}|} : \begin{array}{ll} \boldsymbol{z} \in \mathcal{Z} & \\ g_k(\boldsymbol{z}) \leq u_k, & \forall k \in \mathcal{K} \\ u_k \leq \max\limits_{\boldsymbol{z} \in \mathcal{Z}} g_k(\boldsymbol{z}), & \forall k \in \mathcal{K} \end{array} \right\} \tag{2.28}$$

Note that the uncertainty set $\mathcal{Z}$ are defined by linear constraints (2.9) and (2.14), and the function $g_k(\boldsymbol{z})$ is also linear representable because it is expressed as the absolute deviation in (2.11)-(2.12) and the positive part in (2.16)-(2.17). As a result, the extended support set $\bar{\mathcal{Z}}$ in (2.28) can be written as the following linear matrix form.

$$\bar{\mathcal{Z}} = \left\{ (\boldsymbol{z}, \boldsymbol{u}) \in \mathbb{R}^{|\mathcal{V}|} \times \mathbb{R}^{|\mathcal{K}|} : \ \boldsymbol{F}\boldsymbol{z} + \boldsymbol{H}\boldsymbol{u} \leq \boldsymbol{h} \right\} \tag{2.29}$$

with $\boldsymbol{F} \in \mathbb{R}^{|\mathcal{R}| \times |\mathcal{V}|}$, $\boldsymbol{H} \in \mathbb{R}^{|\mathcal{R}| \times |\mathcal{K}|}$, and $\boldsymbol{h} \in \mathbb{R}^{|\mathcal{R}|}$, where $\mathcal{R}$ denotes the set of all linear constraints defining the extended support set $\bar{\mathcal{Z}}$.

The extended ambiguity set $\bar{\mathbb{F}}$ and the uncertainty set $\bar{\mathcal{Z}}$ are utilized in the next subsection to transform the two-stage wind power planning problem into a computationally tractable formulation.

2.2.3 Reformulation with the Generalized Linear Decision Rule

The exact solution for this two-stage optimization problem is generally intractable, because the expectation of $L(\boldsymbol{x}, \tilde{\boldsymbol{z}})$ must be calculated by solving the second-stage recourse problem (2.22)-(2.23) under all realizations of random variables $\tilde{\boldsymbol{z}}$. This difficulty is normally addressed by linear decision rule techniques [32, 33, 57]. In this approach, we utilize the generalized linear decision rule [32] to approximate the recourse decision $\boldsymbol{y}$ by a linear affine function of some system uncertainties $\boldsymbol{z}$ and auxiliary variables $\boldsymbol{u}$, expressed as equation (2.30).

$$y_n(\boldsymbol{z}, \boldsymbol{u}) = y_n^0 + \sum_{v \in \mathcal{V}_n} y_{nv}^z z_v + \sum_{k \in \mathcal{K}_n} y_{nk}^u u_k \tag{2.30}$$

with $(\boldsymbol{z}, \boldsymbol{u}) \in \bar{\mathcal{Z}}$, recalling that $\bar{\mathcal{Z}}$ is the extended support set defined in (2.28). that affect the recourse decision y_n, and similarly, the set $\mathcal{K}_n$ is a subset of $\mathcal{K}$, involving all auxiliary variables that influence decision y_n. It is pointed out by [32] that the problem size can be reduced if fewer random and auxiliary variables are included in each decision rule, the recourse decision rule thus assumes that decision y_n is a function of the random and auxiliary variables for the same load segment and wind power distribution type as y_n. The sets of all random variables $\boldsymbol{z}$ and auxiliary variables $\boldsymbol{u}$ that are incorporated into the decision rule function y_n are respectively denoted by $\mathcal{V}_n$ and $\mathcal{K}_n$ in (2.30). This assumption should be valid because the occurrence of load loss under every load segment and wind power distribution type is independent, e.g., the energy not served at wind nights are unlikely to be affected

by wind power outcomes during the day time in summer. y_n is denoted by $\mathcal{K}_n$.

It has also been shown in reference [32] that the ambiguity set $\mathbb{F}$ is equivalent to the set of marginal distributions of uncertain variables $\tilde{\boldsymbol{z}}$ under $\mathbb{Q}$, for all $\mathbb{Q} \in \bar{\mathbb{F}}$, where $\bar{\mathbb{F}}$ is the extended ambiguity set (2.27) discussed in the previous subsection. We can hence derive the following equation.

$$\max_{\mathbb{P}\in\mathbb{F}} \mathbb{E}_{\mathbb{P}} \left\{ \boldsymbol{q}^T \boldsymbol{y}(\tilde{\boldsymbol{z}}, \tilde{\boldsymbol{u}}) \right\} = \max_{\mathbb{Q}\in\bar{\mathbb{F}}} \mathbb{E}_{\mathbb{Q}} \left\{ \boldsymbol{q}^T \boldsymbol{y}(\tilde{\boldsymbol{z}}, \tilde{\boldsymbol{u}}) \right\} \tag{2.31}$$

for some decision rules $\boldsymbol{y}(\boldsymbol{z}, \boldsymbol{u})$ that are feasible under all realizations of system uncertainties $\tilde{\boldsymbol{z}}$. The original two-stage problem can be therefore transformed into the following formulation by replacing the recourse decision $\boldsymbol{y}$ by the linear decision rule approximation $\boldsymbol{y}(\boldsymbol{z}, \boldsymbol{u})$.

$$\min \quad \max_{\mathbb{Q}\in\bar{\mathbb{F}}} \boldsymbol{q}^T \boldsymbol{y}(\tilde{\boldsymbol{z}}, \tilde{\boldsymbol{u}}) \tag{2.32}$$

$$\text{s.t } \boldsymbol{A}\boldsymbol{x} \leq \boldsymbol{b} \tag{2.33}$$

$$\boldsymbol{C}(\boldsymbol{z})\boldsymbol{x} + \boldsymbol{D}\boldsymbol{y}(\boldsymbol{z}, \boldsymbol{u}) \leq \boldsymbol{d}(\boldsymbol{z}), \quad \forall (\boldsymbol{z}, \boldsymbol{u}) \in \bar{\mathcal{Z}} \tag{2.34}$$

The optimization problem (2.32)-(2.34) is then reformulated into the following robust optimization problem by taking the dual of the inner maximization of the objective

(2.32).

$$\min \ \rho + \bar{\boldsymbol{z}}^T \boldsymbol{\eta} + \boldsymbol{\sigma}^T \boldsymbol{\lambda} \tag{2.35}$$

$$\text{s.t. } \boldsymbol{A}\boldsymbol{x} \leq \boldsymbol{b} \tag{2.36}$$

$$\rho + \boldsymbol{z}^T \boldsymbol{\eta} + \boldsymbol{u}^T \boldsymbol{\lambda} \geq \boldsymbol{q}^T \boldsymbol{y}(\boldsymbol{z}, \boldsymbol{u}), \quad \forall (\boldsymbol{z}, \boldsymbol{u}) \in \bar{\mathcal{Z}} \tag{2.37}$$

$$\boldsymbol{C}(\boldsymbol{z})\boldsymbol{x} + \boldsymbol{D}\boldsymbol{y}(\boldsymbol{z}, \boldsymbol{u}) \leq \boldsymbol{d}(\boldsymbol{z}), \qquad \forall (\boldsymbol{z}, \boldsymbol{u}) \in \bar{\mathcal{Z}} \tag{2.38}$$

$$\boldsymbol{\lambda} \leq 0, \rho \in \mathbb{R}, \boldsymbol{\eta} \in \mathbb{R}^{|\mathcal{S}|}, \boldsymbol{\lambda} \in \mathbb{R}^{|\mathcal{K}|} \tag{2.39}$$

where ρ is the dual variable associated with the underlying implication that the probability summation is one, and the other dual variables $\boldsymbol{\eta}$ and $\boldsymbol{\lambda}$ are respectively associated with the third and fourth line of the ambiguity set $\bar{\mathbb{F}}$ in (2.27).

It can be seen that the problem (2.35)-(2.39) is a typical robust counterpart, which leads to an equivalent linear programming formulation. Let $\mathcal{N}_v^z$ denote the set of recourse decisions that are affected by random variable $\tilde{z}_v$, and $\mathcal{N}_k^u$ be the set of recourse decisions affected by the auxiliary variable $\tilde{u}_k$. Both sets can be derived from the set $\mathcal{V}_n$ and set $\mathcal{K}_n$ in the decision rule equation (2.30). The equivalent linear

program can be thus expressed as (2.40)-(2.49).

$$\min\ \rho + \bar{\boldsymbol{z}}^T\boldsymbol{\eta} + \boldsymbol{\sigma}^T\boldsymbol{\lambda} \tag{2.40}$$

$$\text{s.t. } \boldsymbol{A}\boldsymbol{x} \leq \boldsymbol{b} \tag{2.41}$$

$$\rho - \boldsymbol{q}^T\boldsymbol{y}^0 \geq \boldsymbol{h}^T\boldsymbol{\pi}^0 \tag{2.42}$$

$$\sum_{r\in\mathcal{R}} F_{rv}\pi_r^0 = \sum_{n\in\mathcal{N}_v^z} q_n y_{nv}^z - \eta_v, \forall v \in \mathcal{V},\ \forall m \in \mathcal{M}_2 \tag{2.43}$$

$$\sum_{r\in\mathcal{R}} H_{rk}\pi_r^0 = \sum_{n\in\mathcal{N}_k^u} q_n y_{nk}^u - \lambda_k, \forall k \in \mathcal{K}, \forall m \in \mathcal{M}_2 \tag{2.44}$$

$$\sum_{r\in\mathcal{R}} h_r\pi_r^m \leq d_m^0 - \sum_{n\in\mathcal{N}_1} C_{mn}^0 x_n - \sum_{n\in\mathcal{N}_2} D_{mn} y_n, \quad \forall m \in \mathcal{M}_2 \tag{2.45}$$

$$\sum_{r\in\mathcal{R}} F_{rv}\pi_r^m = \sum_{n\in\mathcal{N}_1} C_{mn}^v x_n - d_m^v + \sum_{n\in\mathcal{N}_v^z} D_{mn} y_{nk}^z, \quad \forall v \in \mathcal{V}, \forall m \in \mathcal{M}_2 \tag{2.46}$$

$$\sum_{r\in\mathcal{R}} H_{rk}\pi_r^m = \sum_{n\in\mathcal{N}_k^u} D_{mn} y_{kn}^u,\ \forall k \in \mathcal{K}, \forall m \in \mathcal{M}_2 \tag{2.47}$$

$$\boldsymbol{\lambda} \leq 0, \boldsymbol{\pi}^0 \leq 0, \boldsymbol{\pi}^m \leq 0, \quad \forall m \in \mathcal{M}_2 \tag{2.48}$$

$$\rho \in \mathbb{R}, \boldsymbol{\eta} \in \mathbb{R}^{|\mathcal{S}|}, \boldsymbol{\lambda} \in \mathbb{R}^{|\mathcal{K}|}, \boldsymbol{\pi}^0, \boldsymbol{\pi}^m \in \mathbb{R}^{|\mathcal{R}|}, \quad \forall m \in \mathcal{M}_2 \tag{2.49}$$

The uncertain constraints (2.38) and (2.39) are reformulated into (2.42)-(2.44) and (2.45)-(2.47), respectively, by considering the dual variable $\boldsymbol{\pi}^0$ and $\boldsymbol{\pi}^m$ associated with constraints in the extended support $\bar{\mathcal{Z}}$ in (2.28).

It can be seen that the two-stage wind power planning model is reformulated into a tractable linear programming problem (2.40)-(2.49). By applying the linear decision rule approximation, the resultant linear optimization formulation might be more conservative, but it is much easier to be solved than the original two-stage model. Case studies are presented in the next section to demonstrate the effectiveness and tractability of the proposed method.

2.3 Five-Area System Case Study

To validate the proposed DRO technique on the wind farm allocation planning problem, a five-area power system (Fig. 2.4) is used to allocate a certain amount of megawatts, which is formerly determined by the power generation entity according to their budget. In this case study, 1500 MW of WPG as an example is optimally

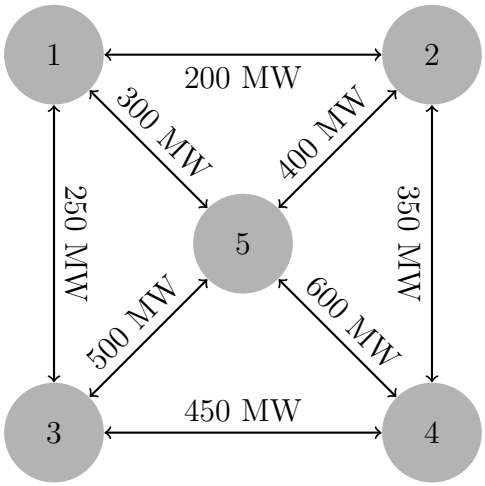

Figure 2.4: Five areas power system configuration and transmission lines transfer capacities

distributed within the system using the DRO framework to utilize the maximum obtainable wind power resources so that the minimum EENS is attained. The power system configuration of each area follows the IEEE RTS system [58] with different generation and load levels that distinguish the areas from each other. The power system data and the case study results are shown in the first part of TABLE 2.1. After assigning the optimal WPG in the system, random sampling Monte Carlo simulation [46] is performed to validate the results and to calculate the reliability indices for each area such as loss of load expectation ($LOEEi$), loss of energy expectation ($LOEE_i$)

and the entire system reliability index EENS to evaluate the system after WPG integration.

Table 2.1: Power system data and the results

Power System Data and Reliability Assessment for Distributing 1500 (MW) of Wind Power							
Area (i)	System Data			Reliability Indices Without Wind Power		Reliability Indices With Wind Power	
	Peak Load (MW)	Conventional Generation (MW)	Wind Generation (MW)	$LOLE_i$ (hrs/yr)	$LOEE_i$ (GWh/yr)	$LOLE_i$ (hrs/yr)	$LOEE_i$ (GWh/yr)
1	3,536	3,990	0	219.40	57.78	185.76	45.04
2	4,158	4,655	250	223.49	63.98	192.43	56.93
3	4,851	5,985	500	134.33	30.51	126.70	27.99
4	5,544	5,320	500	380.62	142.80	308.73	117.64
5	5,418	5,652	250	145.36	49.40	122.63	45.65

The Results of Optimal Wind Power Allocation for Different Probability Distribution Data Used in DRO						
Wind Power Probability Distribution Data	Wind Generation (MW)					Reliability Indices
	x_1	x_2	x_3	x_4	x_5	EENS (GWh/year)
α^s_{il}	0	119	500	500	381	803.57
α^s_{il}, β^s_{ij}	0	250	500	500	250	139.36

The second part of TABLE 2.1 demonstrates how the robustness of the decisions improves when more probability distribution information about the system variables is provided. This enhances the results and gives better intuition about the main data needed to accomplish such planning studies. According to this specific example, the proposed approach based on the information provided excludes area 1 from any investment in WPG ($x_1 = 0$) for the given limited budget. Several factors control the optimization process, like the relative adequacy in conventional generation of

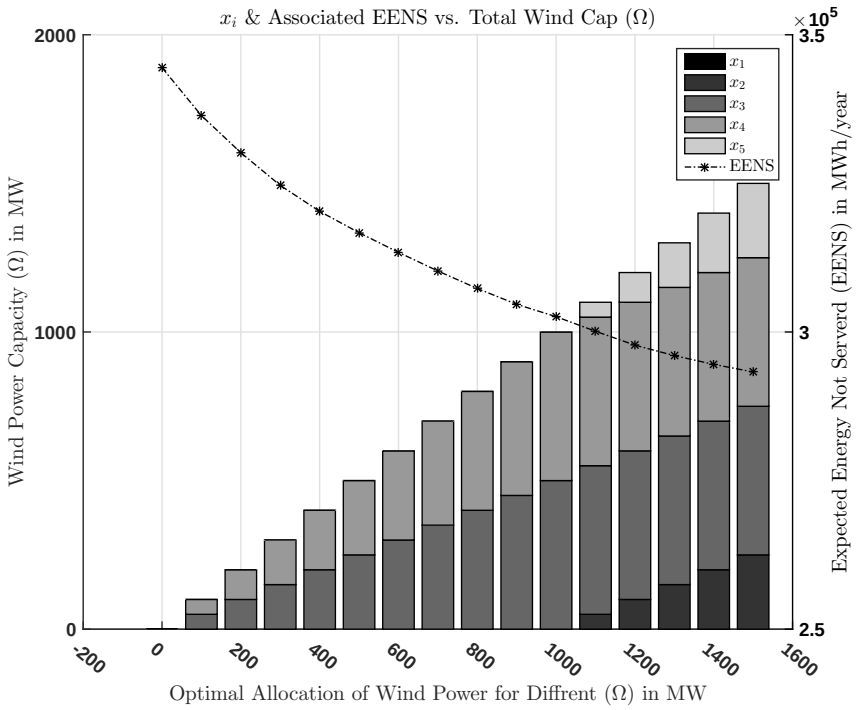

Figure 2.5: The optimal allocation of WPG when the total wind capacity (Ω) varies from 0-1500 MW

area 1, which is reflected in better reliability indices compared to other areas with no wind power. Furthermore, it has the lowest wind power availability among other areas represented in the wind resources statistical parameters such as $\bar{w}_1^s$, α_{1l}^s and β_{1j}^s. Moreover, area 1 has 750 MW of transmission transfer capacity from other neighboring areas, which allows their excess power to be delivered to it in case of generation shortages. Referring to Fig. 2.5, which illustrates that area 1 is not assigned with any WPG in all the cases of Ω from 0 MW to 1500 MW, except in a limited manner when there is no interconnection with other areas Fig. 2.6.

The transmission lines transfer capacities between areas apparently affect the optimal planning decisions. Fig. 2.6 explains the relationship between the transmission transfer capacity and the allocation of the WPG in each area. It shows that with

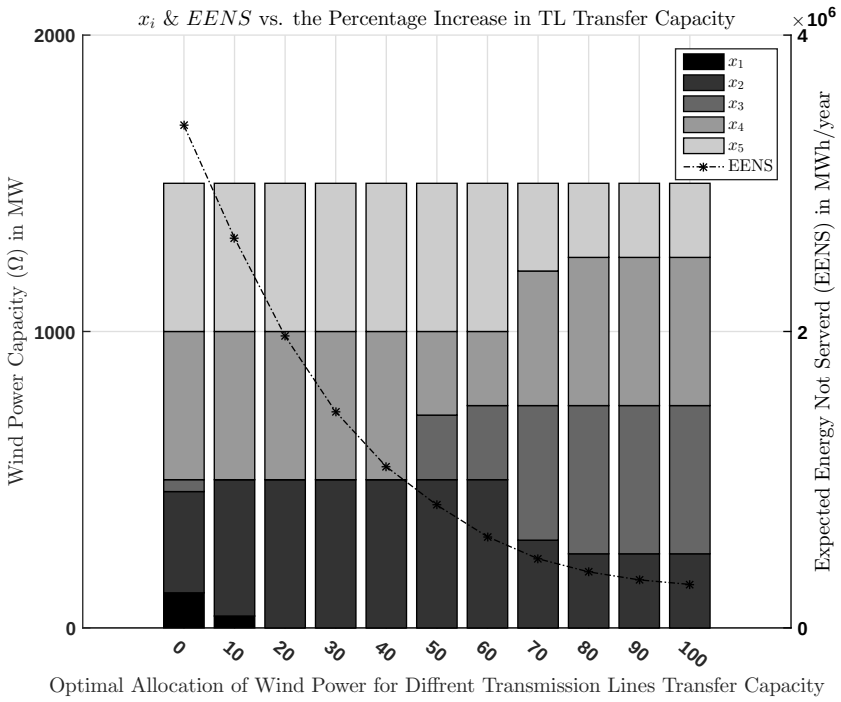

Figure 2.6: The optimal allocation of WPG when the transmission lines transfer capacity varies from 0% - 100%

a fixed amount of WPG, the EENS decreases as the transfer capacity increases and the WPG is uniquely distributed with different power transfer capability. Eventually, the results reveal an extraordinary reliability improvement with the interconnected power system, and the utilization of the renewable resources is improved, especially with a negatively correlated wind power availability between areas. Eventually, the results show an extraordinary reliability improvement in area 1 after installing just 5.85% of the total system's generation capacity as a WPG to its interconnected areas by 15.13%, 15.33% and 22.05% decrees in $LOLP_1$, $LOLE_1$ and $LOEE_1$ respectively. in a nutshell, the multi-area power system gets benefit from the investment in WPG by decreasing in EENS by around 14.94%, and with the interconnecting system the utilization of the renewable resources is increased. The wind power statistical param-

eters α_{il}^{s} and β_{ij}^{s} which are used in the problem formulation are linear in order to gain the advantages of the linear programming optimization which is convex and can be easily solved using simplex method. However, this technique represents wind data in an approximate linear formatting which requires a lot of piece-wise data segments to construct the wind power probability distribution function. As a result, additional standard wind power parameters such as wind power mean absolute deviation, variance and covariance are introduced, since the variance and covariance are nonlinear parameters which convert the problem to a second order cone programming which is quadratically constrained linear program, it is convex and it can be solved using interior point method. This approach will be discussed in the next chapter.

3. NONLINEAR FORMULATION OF WIND FARM ALLOCATION PLANNING PROBLEM

3.1 Nonlinear Representation of Wind Power Statistical Parameters

3.1.1 A Two-Stage Wind Farm Allocation Model

Similar to the previous chapter, two types of uncertainties are addressed in the proposed wind power planning formulation: the random wind power generation $\tilde{\boldsymbol{w}}$ and the available thermal generation capacity $\tilde{\boldsymbol{p}}$. The model is formulated as a two-stage problem where the wind power allocation decisions are made in the first stage and the operation decisions are determined as the $\tilde{\boldsymbol{w}}$ and $\tilde{\boldsymbol{p}}$ are realized.The first-stage wind power planning problem is expressed as follows:

$$\min \ \sup_{\mathbb{P}\in\mathbb{F}} \mathbb{E}_{\mathbb{P}} \left\{ L(\boldsymbol{x}, \tilde{\boldsymbol{w}}, \tilde{\boldsymbol{p}}) \right\} \tag{3.1}$$

$$\text{s.t. } 0 \leq x_i \leq \Pi_i \tag{3.2}$$

$$\sum_{i\in\mathcal{I}} x_i = \Omega \tag{3.3}$$

where $\boldsymbol{x}$ is the vector of first-stage decision variables and each x_i represents the wind power capacity in area i. The constraints (3.2) indicate that the wind capacity x_i in each area is subject to an upper limitation Π_i due to geographic conditions and environmental or social concerns. The total capacity of installed wind power for all areas in $\mathcal{I}$ is denoted by Ω in (3.3). The objective function (3.1) minimizes the expected energy not served (EENS) under the worst-case distribution of $\tilde{\boldsymbol{w}}$ and $\tilde{\boldsymbol{p}}$, which is denoted by $\mathbb{P}$, over an *ambiguity set* $\mathbb{F}$. The expression $L(\boldsymbol{x}, \boldsymbol{w}, \boldsymbol{p})$ in (3.1) indicates the amount of energy not served for the wind farm allocation decision $\boldsymbol{x}$

under the wind power outcome $\boldsymbol{w}$ and the available generation capacity realization $\boldsymbol{p}$. It is expressed as the second-stage optimization problem shown in Section 2.1.1.

3.1.2 Ambiguity Set

The DRO model address system uncertainties by considering a family of distributions, defined by an ambiguity set $\mathbb{F}$ [8, 50]. In this section, the power distributions are represented using some standard statistical data representation. The expressions (3.4)-(3.8) are applied in the ambiguity set to define a family of wind power distributions.

$$\mathbb{P}\left\{\tilde{\boldsymbol{w}} \in \mathcal{W}\right\} = 1 \tag{3.4}$$

$$\mathbb{E}_{\mathbb{P}}\left\{\tilde{w}_i^s\right\} = \bar{w}_i^s, \forall i \in \mathcal{I}, \forall s \in \mathcal{S} \tag{3.5}$$

$$\mathbb{E}_{\mathbb{P}}\left\{|\tilde{w}_i^s - \bar{w}_i^s|\right\} \leq \phi_i^s, \forall i \in \mathcal{I}, \forall s \in \mathcal{S} \tag{3.6}$$

$$\mathbb{E}_{\mathbb{P}}\left\{(\tilde{w}_i^s - \bar{w}_i^s)^2\right\} \leq \lambda_i^s, \forall i \in \mathcal{I}, \forall s \in \mathcal{S} \tag{3.7}$$

$$\mathbb{E}_{\mathbb{P}}\left\{(\tilde{w}_i^s + \tilde{w}_j^s - \bar{w}_i^s - \bar{w}_j^s)^2\right\} \leq \lambda_i^s + \lambda_j^s + 2\zeta_{ij}^s,$$
$$\forall j < i \in \mathcal{I}, \forall s \in \mathcal{S} \tag{3.8}$$

Equation (3.4) suggests that the vector of random wind power generation is constrained within a support set $\mathcal{W}$, which is designed similarly to that in the conventional RO problems. In this research, the support set $\mathcal{W}$ is defined by equation (3.9):

$$\mathcal{W} = \left\{\boldsymbol{w} \in \mathbb{R}^{|\mathcal{I}|\times|\mathcal{S}|} : \ 0 \leq w_i^s \leq 1, \ \forall i \in \mathcal{I}, \forall s \in \mathcal{S}\right\} \tag{3.9}$$

Equation (3.5) implies that the expected value of each $\tilde{w}_i^s$ is $\bar{w}_i^s$, and the next inequality (3.6) suggests that the mean absolute deviation of $\tilde{w}_i^s$ is less than or equal

to ϕi^s. Similarly, constraints (3.7) suggest that the variance of $\tilde{w}_i^s$ is no higher than the constant λ_i^s. The last expression (3.8) implies that the covariance between $\tilde{w}_i^s$ and $\tilde{w}_j^s$ is limited below ζ_{ij}^s. It can be seen that constraints (3.4)-(3.8) in the ambiguity set attempts to capture the location, spread, and dependence of random wind power generation in terms of basic statistical measures, such as expectations, mean absolute deviations, variances and covariances. Such parameters should be much easier to estimate than the exact probability distribution.

The available conventional generation capacity $\tilde{\boldsymbol{p}}$ is modeled exactly as applied in the previous chapter, by the equations (3.10)-(3.13):

$$\mathbb{P}\left\{\tilde{\boldsymbol{p}} \in \mathcal{P}\right\} = 1 \tag{3.10}$$

$$\mathbb{E}_{\mathbb{P}}\left\{\tilde{p}_i\right\} = \bar{p}_i, \qquad \forall i \in \mathcal{I} \tag{3.11}$$

$$\mathbb{E}_{\mathbb{P}}\left\{\max\{P_{il} - \tilde{p}_i, 0\}\right\} \leq \gamma_{il}, \quad \forall i \in \mathcal{I}, \forall l \in \mathcal{L}^{\gamma} \tag{3.12}$$

$$\mathbb{E}_{\mathbb{P}}\left\{\max\left\{Q_l - \sum_{i \in \mathcal{I}} \tilde{p}_i, 0\right\}\right\} \leq \delta_l, \qquad \forall l \in \mathcal{L}^{\delta} \tag{3.13}$$

The first expression (3.10) implies that the vector of uncertain generation capacity is constrained within a support set $\mathcal{P}$, which is defined as follows:

$$\mathcal{P} = \left\{\boldsymbol{p} \in \mathbb{R}^{|\mathcal{I}|} : \ p_i^{min} \leq p_i \leq p_i^{max}, \ \forall i \in \mathcal{I} \right\} \tag{3.14}$$

By combining the wind power uncertainty model (3.4)-(3.8) and the generation capacity expressions (3.10)-(3.13), the overall $\mathbb{F}$ can be formulated as (3.15). In the next section, this two-stage formulation is reformulated into a tractable second-order cone programming problem using linear decision rule approximations.

$$\mathbb{F} = \left\{ \mathbb{P} \in \mathcal{Q}_0 \left(\mathbb{R}^{|\mathcal{I}|\times|\mathcal{S}|} \times \mathbb{R}^{|\mathcal{I}|} \right) : \begin{array}{l} \tilde{\boldsymbol{w}} \in \mathbb{R}^{|\mathcal{I}|\times|\mathcal{S}|} \\ \mathbb{P}\left\{\tilde{\boldsymbol{w}} \in \mathcal{W}\right\} = 1 \\ \mathbb{E}_{\mathbb{P}}\left\{\tilde{w}_i^s\right\} = \bar{w}_i^s \\ \mathbb{E}_{\mathbb{P}}\left\{|\tilde{w}_i^s - \bar{w}_i^s|\right\} \leq \phi_i^s \\ \mathbb{E}_{\mathbb{P}}\left\{(\tilde{w}_i^s - \bar{w}_i^s)^2\right\} \leq \lambda_i^s \\ \mathbb{E}_{\mathbb{P}}\left\{(\tilde{w}_i^s + \tilde{w}_j^s - \bar{w}_i^s - \bar{w}_j^s)^2\right\} \leq \lambda_i^s + \lambda_j^s + 2\zeta_{ij}^s \\ \tilde{\boldsymbol{p}} \in \mathbb{R}^{|\mathcal{I}|} \\ \mathbb{P}\left\{\tilde{\boldsymbol{p}} \in \mathcal{P}\right\} = 1 \\ \mathbb{E}_{\mathbb{P}}\left\{\tilde{p}_i\right\} = \bar{p}_i \\ \mathbb{E}_{\mathbb{P}}\left\{\max\{P_{il} - \tilde{p}_i, 0\}\right\} \leq \gamma_{il} \\ \mathbb{E}_{\mathbb{P}}\left\{\max\left\{Q_l - \sum\limits_{i\in\mathcal{I}} \tilde{p}_i, 0\right\}\right\} \leq \delta_l \end{array} \right\} \tag{3.15}$$

3.2 Problem Reformulation

3.2.1 Compact Matrix Formulation

The formulation presented in the previous section is expressed in more general compact matrix forms in order to facilitate the discussion of the reformulation procedure. In this section, vectors and matrices are represented by bold lowercase letters. Entries of vectors or matrices are denoted by regular letters with subscripts indicating the indices. The first-stage decisions are still denoted by $\boldsymbol{x} \in \mathbb{R}^{|\mathcal{N}_1|}$, where $\mathcal{N}_1$ is the set of all first-stage decisions. All second-stage decisions, including q_{it}^s, f_{ijt}^s, and l_{it}^s, are represented by a vector $\boldsymbol{y} \in \mathbb{R}^{|\mathcal{N}_2|}$, where $\mathcal{N}_2$ is the set of all second-stage decisions. Random variables $\boldsymbol{w}$ and $\boldsymbol{p}$ are combined as a vector $\boldsymbol{z} \in \mathbb{R}^{|\mathcal{V}|}$, where $\mathcal{V}$ is the set of all random variables. The first-stage problem (3.1)-(3.3) is then expressed

in the matrix form (3.16)-(3.17).

$$\min \ \sup_{\mathbb{P}\in\mathbb{F}} \mathbb{E}_{\mathbb{P}}\left\{L(\boldsymbol{x},\tilde{\boldsymbol{z}})\right\} \tag{3.16}$$

$$\text{s.t. } \boldsymbol{A}\boldsymbol{x} \leq \boldsymbol{b} \tag{3.17}$$

with $\boldsymbol{A} \in \mathbb{R}^{|\mathcal{M}_1|\times|\mathcal{N}_1|}$ and $\boldsymbol{b} \in \mathbb{R}^{|\mathcal{M}_1|}$; where $\mathcal{M}_1$ is the set of all first-stage constraints. The second-stage problem used for calculating function $L(\boldsymbol{x},\boldsymbol{z})$ is given as (3.18)-(3.19):

$$L(\boldsymbol{x},\boldsymbol{z}) = \min \ \boldsymbol{q}^T\boldsymbol{y} \tag{3.18}$$

$$\text{s.t. } \boldsymbol{C}(\boldsymbol{z}) + \boldsymbol{D}\boldsymbol{y} \leq \boldsymbol{d}(\boldsymbol{z}) \tag{3.19}$$

with $\boldsymbol{q} \in \mathbb{R}^{|\mathcal{N}_2|}$, $\boldsymbol{C}(\boldsymbol{z}) \in \mathbb{R}^{|\mathcal{M}_2|\times|\mathcal{N}_1|}$, $\boldsymbol{D} \in \mathbb{R}^{|\mathcal{M}_2|\times|\mathcal{N}_2|}$, and $\boldsymbol{d}(\boldsymbol{z}) \in \mathbb{R}^{|\mathcal{M}_2|}$; where $\mathcal{M}_2$ represents the set of all second-stage constraints. Notice that both the left-hand-side constraints matrix $\boldsymbol{C}(\boldsymbol{z})$ and the right-hand-side coefficient vector $\boldsymbol{d}(\boldsymbol{z})$ are affected by the random variables $\boldsymbol{z}$. They are commonly assumed to be the following linear affine form:

$$\boldsymbol{C}(\boldsymbol{z}) = \boldsymbol{C}^0 + \sum_{v\in\mathcal{V}} \boldsymbol{C}^v z_v \tag{3.20}$$

$$\boldsymbol{d}(\boldsymbol{z}) = \boldsymbol{d}^0 + \sum_{v\in\mathcal{V}} \boldsymbol{d}^v z_v \tag{3.21}$$

with constants $\boldsymbol{C}^0, \boldsymbol{C}^v \in \mathbb{R}^{|\mathcal{M}_2|\times|\mathcal{N}_1|}$, and $\boldsymbol{d}^0, \boldsymbol{d}^v \in \mathbb{R}^{|\mathcal{M}_2|}$. The other parameters in matrix $\boldsymbol{D}$ are independent from the random variables; hence, this is the case of fixed recourse. [17]. The ambiguity set (3.15) is expressed as the compact matrix form

below:

$$\mathbb{F} = \left\{ \mathbb{P} \in \mathcal{Q}_0 \left(\mathbb{R}^{|\mathcal{V}|} \right) : \begin{array}{ll} \tilde{\boldsymbol{z}} \in \mathbb{R}^{|\mathcal{V}|} & \\ \mathbb{P}\left\{ \tilde{\boldsymbol{z}} \in \mathcal{Z} \right\} = 1 & \\ \mathbb{E}_{\mathbb{P}}\left\{ \tilde{z}_v \right\} = \bar{z}_v, & \forall v \in \mathcal{V} \\ \mathbb{E}_{\mathbb{P}}\left\{ g_k(\tilde{\boldsymbol{z}}) \right\} \leq \sigma_k, & \forall k \in \mathcal{K} \end{array} \right\} \tag{3.22}$$

The second line of (3.22) suggests that the vector of random variables is constrained within a support set $\mathcal{Z}$, which is the combination of set $\mathcal{W}$ in (3.4) and $\mathcal{P}$ in (3.10). The set of all random variables is denoted by $\mathcal{V}$. The third line of (3.22) is the generalized form of expressions (3.5) and (3.11), used to define the expected value of random variables. The last line in (3.22) is the compact matrix form of the remaining inequalities in (3.15). The function $g_k(\tilde{\boldsymbol{z}})$ in (3.22) generalizes the absolute deviation, variance, covariance and the positive part expression in (3.6)-(3.8) and (3.12)-(3.13), and $\mathcal{K}$ is the set of all constraints involving the expected value of function $g_k(\tilde{\boldsymbol{z}})$. All constants ϕ_i^s, λ_i^s, ζ_{ij}^s, γ_{il}, and δ_l in the ambiguity set are represented by σ_k.

3.2.2 Extended Ambiguity Set

The proposed two-stage problem is challenging to solve due to the complex form of function $g_k(\tilde{\boldsymbol{z}})$ and recourse decisions $\boldsymbol{y}$ that are determined after the realization of system uncertainties. In order to derive a tractable formulation, we follow previous studies [23,31,32] to extend the ambiguity set into a lifted form $\bar{\mathbb{F}}$ in equation (3.23) by introducing a set of auxiliary variables $\boldsymbol{u}$ to express the upper bound of each

function $g_k(\tilde{\boldsymbol{z}})$.

$$\bar{\mathbb{F}} = \left\{ \mathbb{Q} \in \mathcal{Q}_0 \left(\mathbb{R}^{|\mathcal{V}|} \times \mathbb{R}^{|\mathcal{K}|} \right) : \begin{array}{l} (\tilde{\boldsymbol{z}}, \tilde{\boldsymbol{u}}) \in \mathbb{R}^{|\mathcal{V}|} \times \mathbb{R}^{|\mathcal{K}|} \\ \mathbb{Q}\left\{ (\tilde{\boldsymbol{z}}, \tilde{\boldsymbol{u}}) \in \bar{\mathcal{Z}} \right\} = 1 \\ \mathbb{E}_{\mathbb{Q}} \left\{ \tilde{z}_v \right\} = \bar{z}_v, \forall v \in \mathcal{V} \\ \mathbb{E}_{\mathbb{Q}} \left\{ \tilde{u}_k \right\} \leq \sigma_k, \forall k \in \mathcal{K} \end{array} \right\} \tag{3.23}$$

where $\bar{\mathcal{Z}}$ is the extended form of the support set $\mathcal{Z}$, expressed as (3.24).

$$\bar{\mathcal{Z}} = \left\{ (\boldsymbol{z}, \boldsymbol{u}) \in \mathbb{R}^{|\mathcal{V}|} \times \mathbb{R}^{|\mathcal{K}|} : \begin{array}{ll} \boldsymbol{z} \in \mathcal{Z} & \\ g_k(\boldsymbol{z}) \leq u_k, & \forall k \in \mathcal{K} \\ u_k \leq \sup\limits_{\boldsymbol{z} \in \mathcal{Z}} g_k(\boldsymbol{z}), & \forall k \in \mathcal{K} \end{array} \right\} \tag{3.24}$$

Besides enforcing the support set of random variables $\tilde{\boldsymbol{z}}$, the extended set also suggest that the upper limits of function $g_k(\boldsymbol{z})$ are bounded by vector $\boldsymbol{u}$. Note that the support set $\mathcal{Z}$ is defined by linear constraints (3.4) and (3.10), and the function $g_k(\boldsymbol{z})$ is quadratic or linear for expressing various distribution information in equation (3.15). According to reference [59], all inequalities involving function $g_k(\boldsymbol{z})$ are transformed into the following second-order cone constraints, so that we can derive the dual formulation easily in the subsequent subsection.

$$\bar{\mathcal{Z}} = \left\{ (\boldsymbol{z}, \boldsymbol{u}) \in \mathbb{R}^{|\mathcal{V}|} \times \mathbb{R}^{|\mathcal{K}|} : \begin{array}{l} \|\boldsymbol{F}_r \boldsymbol{z} + \boldsymbol{H}_r \boldsymbol{u} \leq \boldsymbol{h}_r\| \\ \leq \boldsymbol{a}_r^T \boldsymbol{z} + \boldsymbol{c}_r^T \boldsymbol{u} + e_r, \ r \in \mathcal{R} \end{array} \right\} \tag{3.25}$$

with $\boldsymbol{F}_r \in \mathbb{R}^{M_r \times |\mathcal{V}|}$, $\boldsymbol{H}_r \in \mathbb{R}^{M_r \times |\mathcal{K}|}$, and $\boldsymbol{h}_r \in \mathbb{R}^{M_r}$, where M_r is the row number for the rth constraint, and $\mathcal{R}$ denotes the set of all constraints defining the extended

support set $\bar{\mathcal{Z}}$. The extended ambiguity set $\bar{\mathbb{F}}$ and the support set $\bar{\mathcal{Z}}$ are utilized in the next subsection to transform the two-stage wind power planning problem into a computationally tractable formulation.

3.2.3 Reformulation with the Generalized Linear Decision Rule

The exact solution for this two-stage optimization problem is generally intractable because the expectation of $L(\boldsymbol{x}, \tilde{\boldsymbol{z}})$ must be calculated by solving the second-stage recourse problem (3.18)-(3.19) under all realizations of uncertaitny $\tilde{\boldsymbol{z}}$. This difficulty is normally addressed by linear decision rule approximations [32, 33, 57]. In this method, the decision rule function is defined to be dependent on some random variables $\boldsymbol{z}$ as well as some auxiliary variables $\boldsymbol{u}$, expressed as function $\bar{y}_n$ in equation (3.26)

$$\bar{y}_n(\boldsymbol{z}, \boldsymbol{u}) = y_n^0 + \sum_{v \in \mathcal{V}_n} y_{nv}^z z_v + \sum_{k \in \mathcal{K}_n} y_{nk}^u u_k, \ \forall n \in \mathcal{N}_2 \tag{3.26}$$

with $(\boldsymbol{z}, \boldsymbol{u}) \in \bar{\mathcal{Z}}$, recalling that $\bar{\mathcal{Z}}$ is the extended support set defined in (3.24). In the equation (3.26), the set $\mathcal{V}_n$, as a subset of $\mathcal{V}$, consists of all random variables affects the recourse decision $\bar{y}_n$. Similarly, the set $\mathcal{K}_n$ is a subset of $\mathcal{K}$, involving all auxiliary variables that influence decision $\bar{y}_n$. In this approach, it is assumed that the decision rule $\bar{y}_n$ depends on random variables and auxiliary variables for the same load segment and wind power distribution type as $\bar{y}_n$. The linear decision rule function is further generalized into the following matrix form.

$$\bar{\boldsymbol{y}} = \boldsymbol{y}^0 + \boldsymbol{Y}^z \boldsymbol{z} + \boldsymbol{Y}^u \boldsymbol{u} \tag{3.27}$$

where $\boldsymbol{y}^0 \in \mathbb{R}^{|N|_2}$ indicates the constant term coefficients, and entries of matrices $\boldsymbol{Y}^z \in \mathbb{R}^{|\mathcal{N}_2| \times |\mathcal{V}|}$ and $\boldsymbol{Y}^u \in \mathbb{R}^{|\mathcal{N}_2| \times |\mathcal{K}|}$, specified by (3.28) and (3.29), are the linear term

coefficients associated with $\boldsymbol{z}$ and $\boldsymbol{u}$, respectively.

$$Y^z_{nv} = \begin{cases} y^z_{nv}, & \text{if } v \in \mathcal{V}_n \\ 0, & \text{if } v \in \mathcal{V} \setminus \mathcal{V}_n \end{cases} \qquad \forall n \in \mathcal{N}_2 \tag{3.28}$$

$$Y^u_{nk} = \begin{cases} y^u_{nk}, & \text{if } k \in \mathcal{K}_n \\ 0, & \text{if } k \in \mathcal{K} \setminus \mathcal{K}_n \end{cases} \qquad \forall n \in \mathcal{N}_2 \tag{3.29}$$

By replacing the actual recourse decision $\boldsymbol{y}$ for each uncertainty realization by the decision rule function, an approximated formulation can be derived as follows.

$$\min \ \sup_{\mathbb{Q} \in \bar{\mathbb{F}}} \mathbb{E}_{\mathbb{Q}} \left\{ \boldsymbol{q}^T \boldsymbol{y}(\tilde{\boldsymbol{z}}, \tilde{\boldsymbol{u}}) \right\} \tag{3.30}$$

$$\text{s.t. } \boldsymbol{A}\boldsymbol{x} \leq \boldsymbol{b} \tag{3.31}$$

$$\boldsymbol{C}(\boldsymbol{z}) + \boldsymbol{D}\bar{\boldsymbol{y}}(\boldsymbol{z}, \boldsymbol{u}) \leq \boldsymbol{d}(\boldsymbol{z}), \qquad \forall (\boldsymbol{z}, \boldsymbol{u}) \in \bar{\mathcal{Z}} \tag{3.32}$$

Apparently, the decision rule may not be the optimal case under all uncertainty realizations, so the problem above is a conservative approximation which gives an upper bound of the expected energy not served. Note that the inner supremum expression can be written as the semi-infinite problem below.

$$\sup \ \int_{\bar{\mathcal{Z}}} \boldsymbol{q}^T \bar{y}(\boldsymbol{z}, \boldsymbol{u}) df(\boldsymbol{z}, \boldsymbol{u}) \tag{3.33}$$

$$\text{s.t. } \int_{\bar{\mathcal{Z}}} z_v df(\boldsymbol{z}, \boldsymbol{u}) = \bar{z}_v, \qquad \forall v \in \mathcal{V} \tag{3.34}$$

$$\int_{\bar{\mathcal{Z}}} u_k df(\boldsymbol{z}, \boldsymbol{u}) \leq \sigma_k, \qquad \forall k \in \mathcal{K} \tag{3.35}$$

$$\int_{\bar{\mathcal{Z}}} f(\boldsymbol{z}, \boldsymbol{u}) = 1 \tag{3.36}$$

$$f(\boldsymbol{z}, \boldsymbol{u}) \geq 0, \qquad \forall (\boldsymbol{z}, \boldsymbol{u}) \in \bar{\mathcal{Z}} \tag{3.37}$$

By taking the dual of the semi-infinite formulation (3.33)-(3.37), the problem (3.30)-(3.32) is then reformulated into the following robust optimization problem.

$$\min \ \rho + \bar{\boldsymbol{z}}^T \boldsymbol{\eta} + \boldsymbol{\sigma}^T \boldsymbol{\beta} \tag{3.38}$$

$$\text{s.t. } \boldsymbol{A}\boldsymbol{x} \leq \boldsymbol{b} \tag{3.39}$$

$$\rho + \boldsymbol{z}^T \boldsymbol{\eta} + \boldsymbol{u}^T \boldsymbol{\beta} \geq \boldsymbol{q}^T \bar{\boldsymbol{y}}(\boldsymbol{z}, \boldsymbol{u}), \quad \forall (\boldsymbol{z}, \boldsymbol{u}) \in \bar{\mathcal{Z}} \tag{3.40}$$

$$\boldsymbol{C}(\boldsymbol{z})\boldsymbol{x} + \boldsymbol{D}\bar{\boldsymbol{y}}(\boldsymbol{z}, \boldsymbol{u}) \leq \boldsymbol{d}(\boldsymbol{z}), \qquad \forall (\boldsymbol{z}, \boldsymbol{u}) \in \bar{\mathcal{Z}} \tag{3.41}$$

$$\rho \in \mathbb{R}, \boldsymbol{\eta} \in \mathbb{R}^{|\mathcal{V}|}, \boldsymbol{\beta} \in \mathbb{R}_{-}^{|\mathcal{K}|} \tag{3.42}$$

where $\boldsymbol{\eta}$ and $\boldsymbol{\beta}$ are dual variables associated with constraints (3.34) and (3.35), respectively, and ρ is the dual variable associated with (3.36). The problem (3.38)-(3.42) is a typical robust optimization problem with a tractable uncertainty set $\bar{\mathcal{Z}}$, which leads to the robust counterpart (3.43)-(3.55).

$$\min \ \rho + \bar{\boldsymbol{z}}^T \boldsymbol{\eta} + \boldsymbol{\sigma}^T \boldsymbol{\beta} \tag{3.43}$$

$$\text{s.t. } \boldsymbol{A}\boldsymbol{x} \leq \boldsymbol{b} \tag{3.44}$$

$$\rho - \boldsymbol{q}^T \boldsymbol{y}^0 + \sum_{r \in \mathcal{R}} \left(\boldsymbol{h}_r^T \boldsymbol{\pi}_r^0 + e_r \mu_r^0 \right) \geq 0 \tag{3.45}$$

$$\sum_{r \in \mathcal{R}} \left(\boldsymbol{F}_r^T \boldsymbol{\pi}_r^0 - \mu_r^0 \boldsymbol{a}_r \right) = \boldsymbol{\eta} - \boldsymbol{Y}^z \boldsymbol{q} \tag{3.46}$$

$$\sum_{r\in\mathcal{R}}\left(\boldsymbol{H}_r^T\boldsymbol{\pi}_r^0-\mu_r^0\boldsymbol{c}_r\right)=\boldsymbol{\beta}-\boldsymbol{Y}^u\boldsymbol{q} \tag{3.47}$$

$$\|\boldsymbol{\pi}_r^0\|\le\mu_r^0, \qquad \forall r\in\mathcal{R} \tag{3.48}$$

$$\boldsymbol{\pi}_r^0\in\mathbb{R}^{M_r},\ \mu_r^0\in\mathbb{R}_+, \qquad \forall r\in\mathcal{R} \tag{3.49}$$

$$\left(\boldsymbol{C}^0\boldsymbol{x}+\boldsymbol{D}\boldsymbol{y}^0\right)_m\le d_m^0+\sum_{r\in\mathcal{R}}\left(\boldsymbol{h}_r^T\boldsymbol{\pi}_r^m+e_r\mu_r^m\right), \quad \forall m\in\mathcal{M}_2 \tag{3.50}$$

$$\sum_{r\in\mathcal{R}}\left(\boldsymbol{F}_r^T\boldsymbol{\pi}_r^m-\mu_r^m\boldsymbol{a}_r\right)_v=(\boldsymbol{d}^v-\boldsymbol{C}^v\boldsymbol{x})_m-(\boldsymbol{D}\boldsymbol{Y}^z)_{mv}, \quad \forall v\in\mathcal{V},\forall m\in\mathcal{M}_2 \tag{3.51}$$

$$\sum_{r\in\mathcal{R}}\left(\boldsymbol{H}_r^T\boldsymbol{\pi}_r^m-\mu_r^m\boldsymbol{c}_r\right)_v=-(\boldsymbol{D}\boldsymbol{Y}^z)_{mv}, \quad \forall v\in\mathcal{V},\forall m\in\mathcal{M}_2 \tag{3.52}$$

$$\|\boldsymbol{\pi}_r^0\|\le\mu_r^0, \qquad \forall r\in\mathcal{R} \tag{3.53}$$

$$\boldsymbol{\pi}_r^m\in\mathbb{R}^{M_r},\ \mu_r^m\in\mathbb{R}_+, \qquad \forall r\in\mathcal{R},\forall m\in\mathcal{M}_2 \tag{3.54}$$

$$\rho\in\mathbb{R},\boldsymbol{\eta}\in\mathbb{R}^{|\mathcal{V}|},\boldsymbol{\beta}\in\mathbb{R}_-^{|\mathcal{K}|} \tag{3.55}$$

The uncertain constraints (3.40) are reformulated into constraints (3.45)-(3.49) by taking the dual of the extended uncertainty set $\bar{\mathcal{Z}}$. The dual variables are denoted by $\boldsymbol{\pi}_r^0$ and μ_r^0. Similarly, the mth constraint of (3.41) are transformed into expression (3.50)-(3.54) by considering dual variables $\boldsymbol{\pi}_r^m$ and μ_r^m. It can be seen that the robust counterpart of the proposed two-stage wind power planning model is a tractable second-order cone programming problem (3.43)-(3.54). By applying the linear decision rule approximation, the resultant linear optimization formulation might be more conservative, but it is much easier to be solved than the original two-stage model. Case studies are presented in the next section to demonstrate the effectiveness and tractability of the proposed method.

3.3 Case Studies on DRO Based Wind Power Generation

To examine the proposed DRO technique on the wind farm allocation problem, the factors which primarily influence the performance of the DRO model on the objective and the WPG decisions are investigated. These factors are mainly associated with the power system configuration and the system uncertainties which exist in the wind power and conventional generation forced outages. A five-area power

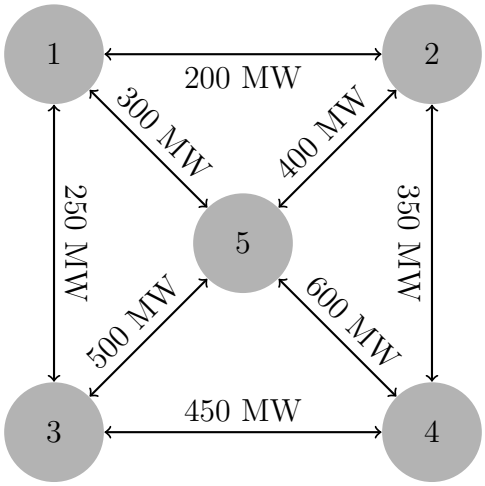

Figure 3.1: Five areas power system configuration

system with its areas interconnected by tie-lines of different transfer capacities as shown in Fig. 3.1 is used to allocate certain megawatts of WPG. The power system configuration of each area follows the IEEE-RTS system with various generation and load levels that distinguish the areas from each other. The conventional generation installed capacities and the peak loads of each area in the system are listed in TABLE 3.1. The historical wind power data used in this study are available in NREL/3TIER website as explained in [60]. The wind power profiles of five distinct locations are used to represent the wind power pattern of the five-area power sys-

tem. The statistical parameters $\bar{w}_i^s$, ϕ_i^s, λ_i^s and ζ_{ij}^s, for each area i and for the eight wind power distributions s which represent the seasonal and day-night wind pattern, are determined and provided to the DRO by incorporating them into the ambiguity sets. Similarly, the statistical information of conventional power generation γ_{il} and δ_l are calculated from its probability distribution of the five-area system to include them into the ambiguity set for the forced outages uncertainties representation. The IBM ILOG CPLEX solver is used to solve the second-order cone programming of the DRO problem. The computer used for this numerical experiment has a 3.10GHz Intel Core processor and 32GB memory, and the average solution time is approximately 3 minutes. In this example, the proposed method optimally allocates 5000 MW of WPG within the five-area system, so that the EENS over the ambiguity set is minimized. Detailed system data and the solution are provided in TABLE 3.1. More tests are conducted to explore the influence of the statistical data of wind power and generator outages.

Table 3.1: Power system data and the DRO results

Five-Area Power System Data & DRO Results						
Area (i)	System Data		Wind Data		DRO Results	
	Peak Load (MW)	Installed Capacity (MW)	Mean (%)	Variance (%)	WPG (MW)	EENS (GWh/yr)
1	3,465	3,485	28.23	11.70	985	664.54
2	4,158	4,306	29.85	9.25	435	
3	4,851	5,578	32.74	9.92	1295	
4	5,544	4,972	29.46	9.27	1025	
5	5,418	5,322	31.92	10.40	1260	

3.3.1 The Influence of Wind Power Statistical Data

The proposed method is capable of incorporating statistical data of wind power, in terms of the mean absolute deviation, the variance, and the covariance between two wind sources into the formulation, so that the EENS is minimized with consideration of such ambiguous distribution information. The influence of the wind power uncertainty represented by the statistical parameters ϕ_i^s, λ_i^s and ζ_{ij}^s, which are incorporated in the ambiguity set is illustrated. The assessment has two perspectives; the first perspective examines the performance of the DRO as more distribution information about the wind power is provided. The second perspective measures the sensitivity of a specific governing parameter comparing to the others by changing its magnitude back and forth from its original value by 50% on the EENS and on the Decisions. Case studies in this subsection are therefore conducted to examine how the wind allocation decisions are affected by considering different types of statistical data and by varying the values of specific statistical parameters. Table 3.2 shows the results of the proposed DRO model as different types of statistical data are considered in the ambiguity set to capture the distribution of wind power. It can be seen that the EENS decreases as more statistical data is taken into consideration, and the lowest EENS is achieved when all types of parameters ϕ_i^s, λ_i^s, and ζ_{ij}^s are taken into consideration. This is because the distribution of wind power can be captured with higher accuracy with more information. If some of these parameters are unavailable, the solution tends to be more conservative in order to protect the system against more adverse wind power distributions. It is also observed that area 1 is excluded from any WPG if only mean absolute deviation ϕ_i^s is provided. Whereas it is considered with 171 MW when the variance λ_i^s is included, and it is heavily integrated by 985 MW when the information about the correlation ζ_{ij}^s is incorporated.

So the decision-making procedure is affected by the information of distributions in an efficient manner as more useful information about the uncertainty is provided.

Table 3.2: DRO results of different wind statistical data

The Results of Optimal Wind Power Allocation for Different Probability Distribution Data Used in DRO						
Wind Power Data	Wind Power Generation (MW)					Objective Value
	x_1	x_2	x_3	x_4	x_5	EENS (GWh/year)
ϕ_i^s	0	1030	1410	1115	1445	696.90
λ_i^s	171	462	1746	1040	1581	754.06
ϕ_i^s, λ_i^s	261	624	1446	1204	1465	695.96
λ_i^s, ζ_{ij}^s	994	471	1080	1103	1352	671.52
ϕ_i^s, λ_i^s, ζ_{ij}^s	985	435	1295	1025	1260	664.54

Fig. 3.2 shows how the reliability of the system with wind power generation is enhanced when the global variance of the system is minimized. The figure also indicates as more statistical data are exercised in DRO the more confident and less conservative solution are proposed with optimal worse case expected objective is introduced.

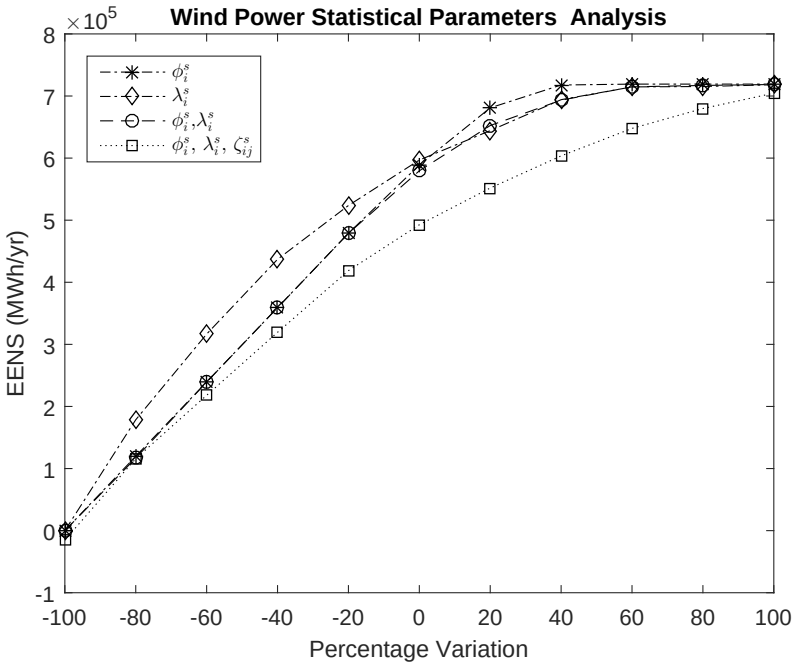

Figure 3.2: The effect of incorporating the wind power statistical data in DRO

The following numerical studies are utilized to demonstrate the impact of changing parameter values on DRO solutions. Fig. 3.3 displays the wind allocation decisions as well as the resultant EENS under various values of ϕ_1^s, which indicates the mean absolute deviation of wind power at area 1. It is observed that as ϕ_1^s decreases, more wind capacity is deployed from other areas to area 1, so that the total fluctuation of wind power is reduced, leading to lower EENS.

Similar pattern can be observed in Fig. 3.4, which shows the wind allocation decisions and EENS under different values of λ_1^s, which implies the variance of wind power. It is noted that more wind power is committed to area 1 due to the reduction of its wind power variance. Such improvement in λ_1^s results in less wind uncertainty and consequently the lower value of EENS is achieved.

The results above suggest that the proposed method is capable of incorporating

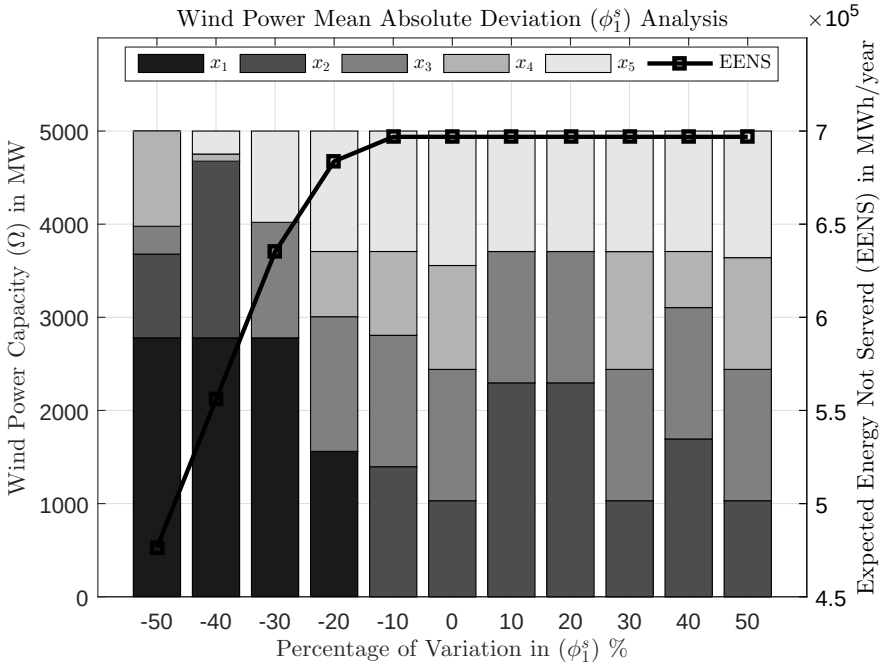

Figure 3.3: The effect of ϕ_1^s variation on WPG

statistical data, such as mean absolute deviations and variances, into the optimal planning model. The wind allocation decisions, therefore, can well adapt to the change of wind power variations.

The proposed method is also able to capture the correlation between two areas implicitly by the parameter ζ_{ij}^s, which denotes the covariance of wind power between area i and j. In the subsequent tests, the covariance between two areas is expressed by equation (3.56).

$$\zeta_{ij}^s = \xi_{ij}\sqrt{\lambda_i^s \lambda_j^s}, \qquad \forall j < i \in \mathcal{I}, s \in \mathcal{S} \tag{3.56}$$

where ξ_{ij} is a varying constant indicating the correlation coefficient. The wind power covariance ζ_{ij}^s provides information about the wind power diversification in means of the correlation between the areas. Fig. 3.5 shows the ζ_{ij}^s, changing effects on the

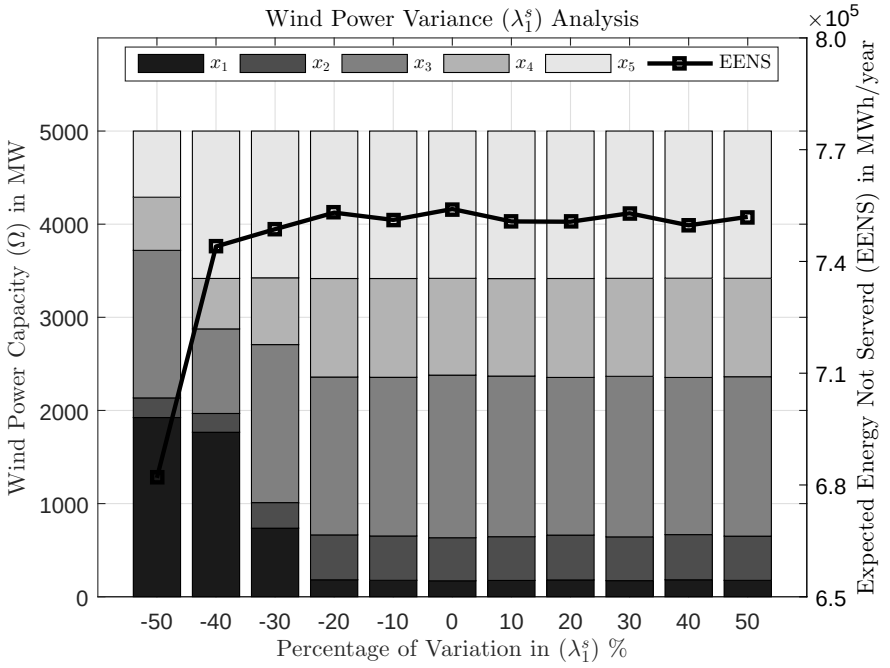

Figure 3.4: The effect of λ_1 variation on WPG

EENS and the decisions when the ϕ_i^s and λ_i^s are used but fixed as their original values. It is clear that the EENS improves when the correlation is more likely to be negatively correlated which provides more diversification in the wind power availability.

Fig. 3.6, shows the wind capacity allocation, in terms of the total wind power capacities in area 2 and 4, and the overall EENS as the correlation factor between area 2 and 4 changes. The results suggest that as the coefficient ξ_{24}^s goes to -1, implying that wind power generation in these two areas are negatively correlated, the total wind capacity in these two areas steadily increases, as a measure to reduce the overall wind power uncertainty for the system, and apparently a lower level of wind uncertainty can greatly reduce the EENS.

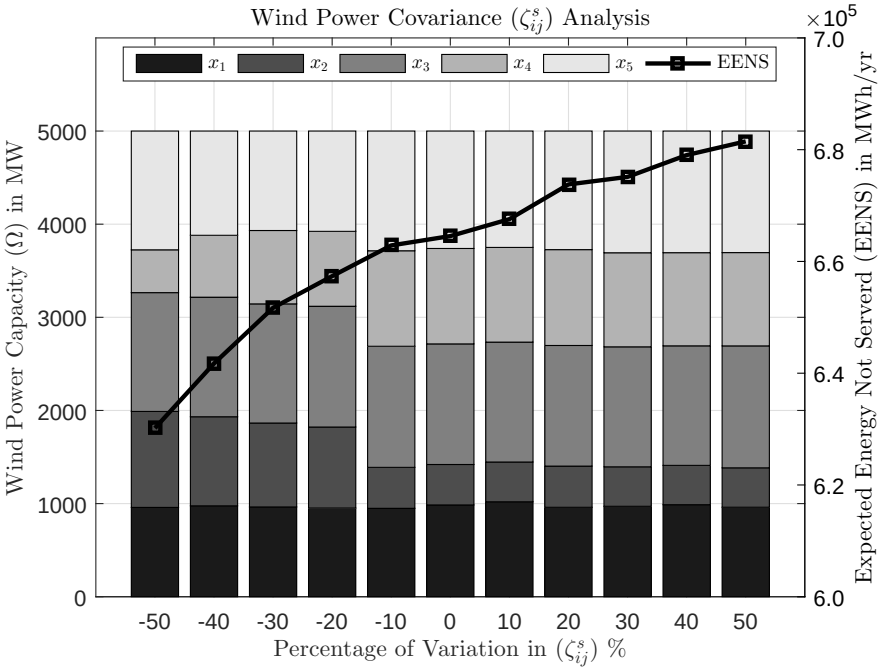

Figure 3.5: The response of ζ_{ij}^s change on WPG

3.3.2 The Effect of Power System Configuration

Many Indicators assist the system planner in evaluating the decisions and explain which areas are more likely preferred to be installed with wind power generation, like looking at the mean wind power $\bar{w}_i^s$ of each area i to inspect the availability and checking the wind power's mean absolute deviation, variance and covariance to evaluate the variability and uncertainty. Nevertheless, these useful data alone are not sufficient to decide the decisions, the optimal WPG distribution changes in each case due to several factors that govern it besides the wind power statistical analysis, there are also the system's configuration and the system's reliability status which are taken in the account during the DRO optimization process.

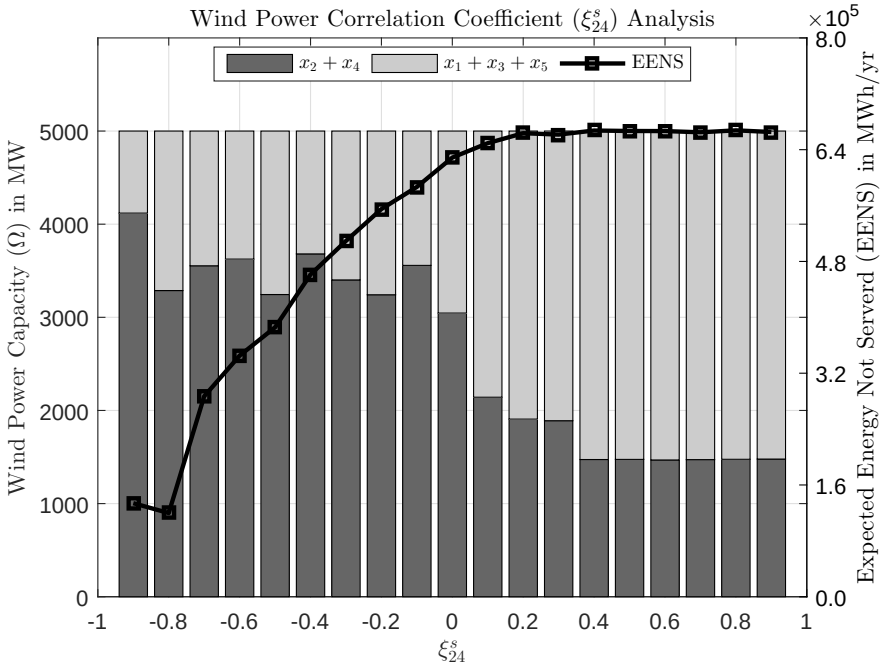

Figure 3.6: The effect of ξ^s_{24} variation on WPG

3.3.2.1 The Impact of the Total Wind Power Capacity Ω

In Fig. 3.7, a range of total wind power capacity Ω varies from 0-5000 MW in step of 500 MW are allocated in the five-area system, the results show the improvement in the $EENS$ as the total wind power capacity is increased.

3.3.2.2 The Assessment of the Transmission Lines Effect on the WPG allocation

In this subsection, the effectiveness of the tie-lines interconnection between the areas, on the WPG allocation is evaluated in the five-area power system example. Fig. 3.8 indicates the decisions and their associated EENS for different transmission lines levels from 0% to 120% of the installed transfer capacities. At the isolated scenario, x_4 is assigned to have 2744 MW of WPG which is 54.88% of the total budget, the worst case EENS for this particular realization is 2029 GWh/yr. On

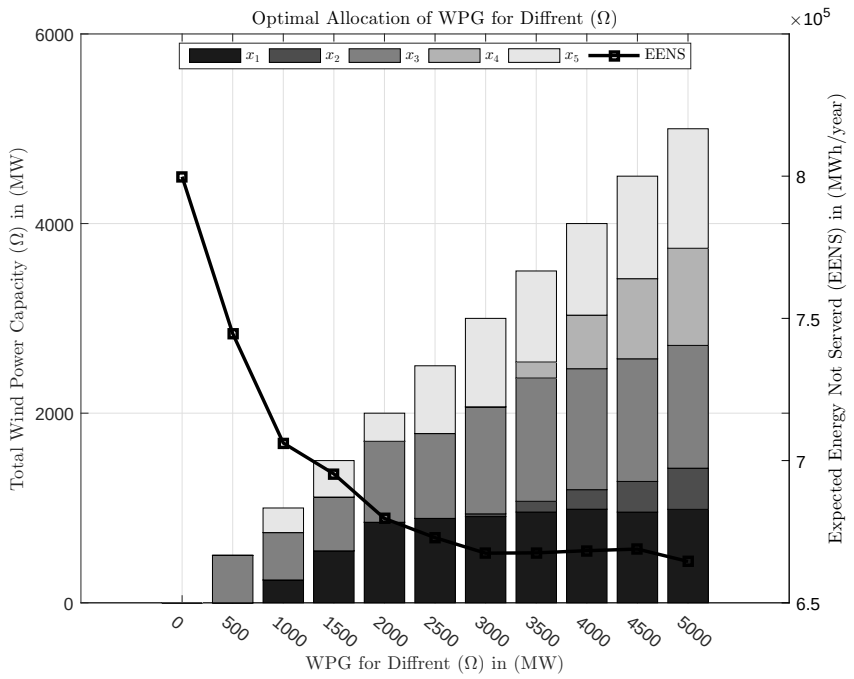

Figure 3.7: The optimal allocation of WPG

the other hand, the EENS reduces gradually if the areas are allowed to deliver some of their electric power to the neighboring areas, whether it is from conventional generation or Wind. This privilege assists in rearranging the decisions in such a way that EENS is improved. x_4, for instance, is not dominating the wind power allocation anymore when the tie-lines are at 60% or more of their capacities, at this realization, the EENS is 672 GWh/yr which is reduced by 33% comparing to the isolated case. It is also remarked, that the EENS saturated 666 GWh/yr and the expansion of the tie-lines transfer capacities beyond 60% is unbeneficial for the WPG budget used in this example.

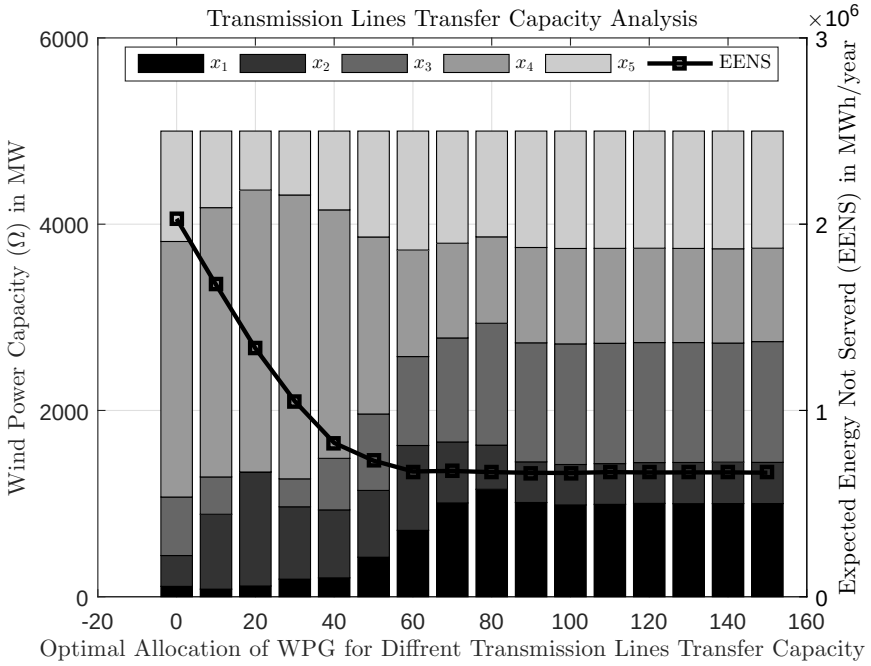

Figure 3.8: The optimal allocation of WPG with diffrent transmission lines transfer capacity

3.3.2.3 The Impact of the Conventional Power Generation Forced Outages Parameters

The following case studies are conducted to show how the reliability of generators affects the wind allocation decisions. It is assumed that the failure rates of generators in area 1 are changed from 50% to 150% of the original values, while the other parameters remain unchanged. The increase of failure rates can be effectively captured by parameters γ_{il} and δ_l in the ambiguity set, so the resultant DRO solutions can well adapt to various levels of system reliability. The figure shows that as generators in area 1 becomes less reliable, the wind capacity allocated in area 1 only increases slightly, while much more wind capacities are added to the neighboring area 3. This is probably because area 3 is connected to area 1 with sufficient transmission capac-

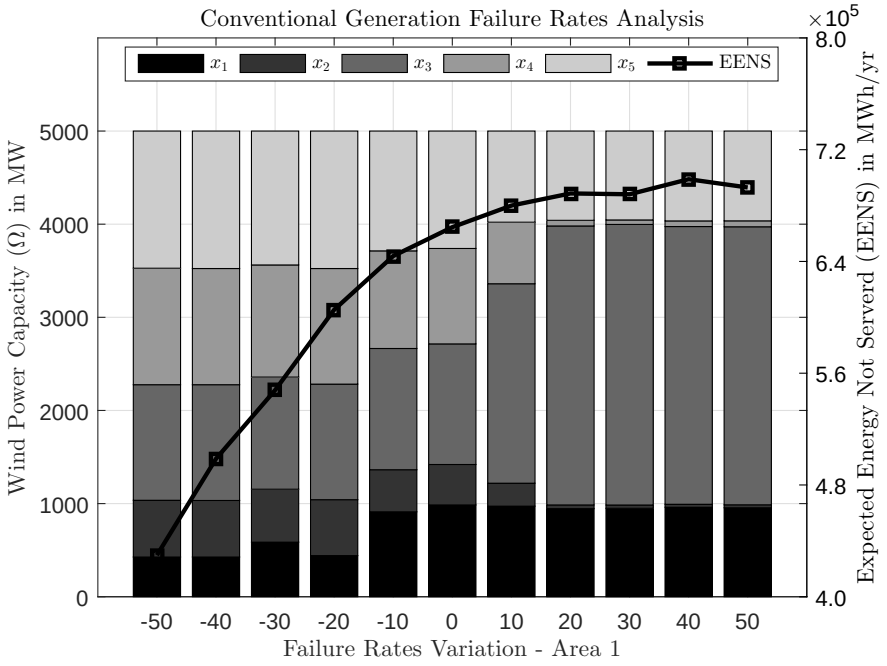

Figure 3.9: The effect of the generation failure rates on WPG

ity, and the wind power profile in area 3 has the highest mean value and a lower variation compared with area 1, as shown in Table 3.1. Therefore, wind power with higher efficiency and better availability can be delivered from area 3 to area 1 to prevent load loss caused by generator outages.

4. HYBRID WIND AND SOLAR POWER GENERATION ALLOCATION USING DISTRIBUTIONALLY ROBUST OPTIMIZATION

4.1 Introduction

Power grids are accepting higher integration of the large-scale renewable energy resources including wind and solar power generation plants. The variability and uncertainty issues that accompany the sustainable energy resources emphasize the research efforts on the hybrid systems where both wind and solar power resources are collaboratively employed for improving the system reliability by increasing the availability and reducing the variability.

Analyzing the hybrid system in the planning stage of the power generation expansion design needs more understanding of the correlation between the wind and solar energy. Such information is crucial to find a better approach to operating them once they are integrated, to maintain or improve the reliability and the security of the system while reducing the conventional generation by the renewable energy with assuring the power generation adequacy.

Studying the hybrid scheme in a multi-area system allows for more flexibility in distributing these resources in all around different areas, which depends on the particular characteristics of the resources specifications and patterns of each location. Such a system would provide as performance or better than the wind power or solar power alone as it creates more diversity in renewable energy deployment.

In [61], a decision support technique was developed to enable decision makers to study all factors (mainly political, social, technological and economic) influencing the design of hybrid wind solar power systems for the interconnected power grid. They used an analytic hierarchy process to identify robust and inferior plans, and

to identify riskier vs. less risky designs. They took into account previous work that had sought to minimize production cost while still meeting load requirements, choose the optimal size of generating units, and work that had integrated prediction of maximized reliability and minimized cost under uncertain future circumstances. Recognizing the potential advantages of combining two renewable energy sources to obtain more reliable and efficient energy, [62] presented a probabilistic planning system of integrating wind and solar power. They used probability density functions to model megawatt power output random variables. They were thus aiming to assess the sites with their potential available renewable energy resources in termos of wind or solar power generation. They used the probabilistic approach due to the stochastic nature of wind/solar power sources. They called their model for assessing sites the megawatt resource assessment model (MWRAM). In a related study, [63] analyzed the relationship between large-scale solar and wind power, including correlations between different units, aggregate production smoothing and combined output variability. Noting that unpredicted generation must be taken care of with system reserves, it is found that a generation which was more widely dispersed led to a more smooth output profile when the two power sources were combined. The intermittence of solar power is caused by clouds and the earth's movement and tilt, while wind power is dependent upon wind speed, which varies from time to time. A larger proportion of solar power led to greater hour-to-hour variability, largely due to the vast difference in production between days and nights, but that combining the two forms of sustainable power generation reduced the total variations in terms of standard deviation. Solar and wind power were found to be negatively correlated, but the smaller the time-scale, the less this correlation could be observed.

A generation expansion planning model of electric systems using renewable energy sources as well as conventional sources is developed in [64]. This model, called

MMGEP, (multiperiod multiobjective generation expansion planning) could simultaneously optimize several factors, including maximization of system reliability. They used mixed integer linear programming for optimization, and they used an efficient linearization technique for converting non-linear reliability metrics to a set of linear expressions. Fuzzy decision making was used to choose the best from among Pareto solutions, in order to meet the goals of decision makers. Major goals included minimizing costs and environmental impacts and maximizing reliability. A desired level of reliability must be obtained, which can be measured by loss of load probability (LOLP) and expected energy not served (EENS).

In [65], wind turbine, photovoltaic panel and battery were modeled to calculate the energy generated over one year. The objective function was selected using loss of power supply probability (LPSP) and total owning cost in order to meet the requirements of the power system economy and reliability. A particle swarm algorithm was used to find the optimal solution and obtain the capacity allocation of a wind/solar/battery hybrid system. The optimization is important because it enables a trade off between cost and reliability. Exploring the optimal sizing balance of components of these hybrid renewable energy power generation systems, [66] used different multicriteria decision analysis (MCDA) optimization approaches. Different weighting criteria techniques were considered with different wind and solar fluctuation scenarios; and so the pros and cons of different optimal sizing approaches were able to be analyzed. In their approach, different criteria were able to be applied without being converted into a single unit, and algorithm sensitivities were analyzed. Like many of the others studies listed here, the intent of the study was to give decision makers a tool to optimize their designs based on their goals.

A genetic algorithm-based optimization approach and a 2PEM to examine different scenarios to evaluate system efficiency considering different load shifting percent-

ages is explained in [67]. Maximum capacity and excess energy were calculated for each system, and these were considered to be the most important indices of efficiency. In [68] the benefits of placing solar power and wind power generating systems together in the same location and sharing transmission resources were explored. They found that doing so can improve the capacity factor of the power plant and can also improve the transmission investment, especially given the often remote location of the higher quality renewable resources. A model was developed to optimize the dispatch of the combined plants. Different deployment configurations connected to the grid by radial transmission lines were examined using historical market and weather data. A negative correlation between wind and solar power was demonstrated, and it was also shown that solar power with thermal energy storage increased the flexibility of the system, allowing excess transmission capacity to be filled in during times of less resource. It was found that adding transmission constraints reduced the performance as well as the ability of solar power to produce during periods of high demand and high wind.

A mathematical model to propose a probabilistic power flow (PPF) methodology called 2PEM (two point estimation method) is demonstrated in [69], so that it would apply to hybrid wind/solar power systems. This method considers correlation between uncertainty parameters. Looking at trends that could shape the future of the power grid, [70] noted that there will be the need to find new ways to manage voltage and loading of photovoltaic power distribution systems as they grow in usage. While solar has historically been used at a small scale, the authors stated that in recent years there is a shift to larger scale solar power systems. They also noted that more than 50 GW of wind power is operating in the United States. It is possible for solar integration into the grid to follow the model of wind power integration into the grid, in which the variability of the power source has been addressed. While high penetra-

tions at the local level are recognized as being potentially disruptive to operations, the power variability due to cloud shading is not mentioned to be of concern because at the transmission level, the energy balance is achieved at a wider basis.

Reference [71] proposes a methodology for applying smart metering technology to abate CO2 at the distribution level, in a system that uses wind, solar energy, and gas turbines. They developed a nodal based demand response to enable low-carbon planning that highlights the fading effect during load recovery of demand response activities. They were able to evaluate demand response benefits using a real-time pricing model, which takes into account the variation and uncertainty in wind and the behaviors of customers. This methodology is related to a central planning context, is aimed at minimizing both carbon emission and economic cost. An efficient hybrid algorithm is used for this purpose. In [72], an integration scheme of solar power and large capacity doubly excited induction generator-based wind energy system was presented. This system is able to introduce a large amount of solar power into the grid compared to conventional PV-grid systems. Prevention of circulating power during subsynchronous operation is accomplished with this scheme, enhancing system efficiency. Turbine inertia augments system stability, and this facilitates high solar power penetration into the grid. The complementary nature of wind and solar energy leads to increased utilization in this scheme. A PV power control algorithm is able to deal with any rare environmental glitches. Looking at the scheduling of a power system that incorporates traditional sources that can be dispatched and renewable sources that are based on environmental conditions, [73] inquired into a realistic optimum day-ahead schedule for such a hybrid system, with its uncertainties. This work provided a best-fit day ahead schedule, using an optimal scheduling strategy that takes into account the uncertainties in wind, solar, and load forecasts. A genetic algorithm-based scheduling is used, and genetic algorithm and

Monte Carlo simulations are chosen for testing the strategy.

Reference [74] presents a scheme for analyzing the statistical properties and sizing the storage for hybrid wind-photovoltaic-storage hybrid power systems, with concern for system optimization. A partial Fourier transform was obtained for spectrum analysis using solar data periodic sparse properties, and storage for stabilizing power variance due to fluctuation in wind and solar power was sized, using a system adviser model. Real wind speed, solar radiation and grid load data from South Eastern Australia were used to design and validate the scheme.

In [75], an algorithm for dispatching a utility-scale photovoltaic power plant with a hybrid energy storage system is presented. This algorithm regulated instantaneous power of the plant with the same level of dispatchability as traditional power plants. The algorithm is robust under large forecasting errors of solar irradiance, making it easily implemented in real-world scenarios; the algorithm only takes seconds to execute, even with worst-case scenarios of forecasting errors yielded good results.

More insight about the feasibility of incorporating wind and solar power penetration into a the power system is discussed in [76]. Several sensitivity analysis are carried out on interest and inflation rates, wind power law exponent, annual average daily energy demand, and fuel price in order to test system robustness.

In this chapter, the planning problem of allocating the renewable energy resources using DRO is extended to deal with a hybrid wind solar power generation (HWSPG) system to minimize the expected energy not served. The uncertainty of these two variable energy resources is investigated and represented by proper statistical parameters. The correlation between them is introduced to better allocate them under the interconnected multi-area environment to provide more flexibility between the areas and to reduce the global variability all over the system.

4.2 Formulation - Nonlinear Representation of Hybrid Wind and Solar Power Statistical Parameters

4.2.1 A Two-Stage Hybrid Wind and Solar Farms Allocation Model

Three types of uncertainties are introduced in the proposed hybrid wind and solar power generation (HWSPG) planning formulation: the random wind power generation $\tilde{\boldsymbol{w}}$, the random solar power generation $\tilde{\boldsymbol{e}}$ and the available conventional generation capacity $\tilde{\boldsymbol{p}}$. The model is mathematically expressed as a two-stage formulation where the wind and solar power allocation decisions are made in the first stage and the operational decisions are optimally decided as the $\tilde{\boldsymbol{w}}$, $\tilde{\boldsymbol{e}}$ and $\tilde{\boldsymbol{p}}$ are realized.The first-stage hybrid power planning problem is described as follows:

$$\min \ \sup_{\mathbb{P}\in\mathbb{F}} \mathbb{E}_{\mathbb{P}} \left\{ L(\boldsymbol{x}, \tilde{\boldsymbol{w}}, \tilde{\boldsymbol{e}}, \tilde{\boldsymbol{p}}) \right\} \tag{4.1}$$

$$\text{s.t. } 0 \leq x_i^w \leq \Pi_i^w \tag{4.2}$$

$$0 \leq x_i^e \leq \Pi_i^e \tag{4.3}$$

$$\sum_{i\in\mathcal{I}} x_i = \sum_{i\in\mathcal{I}^w} x_i^w + \sum_{i\in\mathcal{I}^e} x_i^e = \Omega \tag{4.4}$$

where $\boldsymbol{x}$ is the vector of first-stage decision variables and each x_i represents the summation of wind power capacity x_i^w and solar power capacity x_i^e of each area i. The constraint (4.2) indicates that the wind capacity x_i^w in area i belonging to the set $\mathcal{I}^w$ is subjected to an upper limitation Π_i^w and (4.3) represents the solar capacity x_i^e in each area i belonging to the set $\mathcal{I}^e$ is subjected to an upper limitation Π_i^e. The total capacity of installed renewable power for all areas in $\mathcal{I}$ is denoted by Ω in (4.4). The objective function (4.1) minimizes the expected energy not served (EENS) under the worst-case distribution of $\tilde{\boldsymbol{w}}$, $\tilde{\boldsymbol{e}}$ and $\tilde{\boldsymbol{p}}$, which is denoted by $\mathbb{P}$, over an *ambiguity set*

$\mathbb{F}$. The expression $L(\boldsymbol{x}, \boldsymbol{w}, \boldsymbol{e}, \boldsymbol{p})$ in (4.1) indicates the amount of energy not served for the hybrid wind and solar farm allocation decision $\boldsymbol{x}$ under the wind and solar power outcome $\boldsymbol{w}$ and $\boldsymbol{e}$ respectively, with the available conventional generation capacity realization $\boldsymbol{p}$. Similarly, the solar power is incorporated in the second stage model, which represents the optimal power flow equation and its constraints, as shown in (4.5)-(4.9).

$$L(\boldsymbol{x},\boldsymbol{w},\boldsymbol{e},\boldsymbol{p}) = \min \sum_{s\in\mathcal{S}}\sum_{t\in\mathcal{T}}\sum_{i\in\mathcal{I}} T_t^s l_{it}^s \tag{4.5}$$

$$\text{s.t.} \quad x_i^w w_i^s + x_i^e e_i^s + q_{it}^s - \sum_{j\in\mathcal{J}_i^f} f_{jit}^s + \sum_{j\in\mathcal{J}_i^t} f_{ijt}^s = D_{it}^s - l_{it}^s,$$

$$\forall i \in \mathcal{I}, \forall t \in \mathcal{T}, \forall s \in \mathcal{S} \tag{4.6}$$

$$-F_{ij} \le f_{ijt}^s \le F_{ij},$$

$$\forall j \in \mathcal{J}_i^f, \forall i \in \mathcal{I}, \forall t \in \mathcal{T}, \forall s \in \mathcal{S} \tag{4.7}$$

$$0 \le q_{it}^s \le p_i, \quad \forall i \in \mathcal{I}, \forall t \in \mathcal{T}, \forall s \in \mathcal{S} \tag{4.8}$$

$$l_{it}^s \ge 0 \quad \forall i \in \mathcal{I}, \forall t \in \mathcal{T}, \forall s \in \mathcal{S} \tag{4.9}$$

4.2.2 Ambiguity Set of the Hybrid System

The DRO model of the hybrid system addresses the system uncertainties by considering a family of probability distributions, that are defined by an ambiguity set $\mathbb{F}$. In this section, the renewable power distributions are represented using useful standard statistical parameters of data representation. The expressions (4.10)-(4.14)

are applied in the ambiguity set to define a family of wind power distributions.

$$\mathbb{P}\left\{\tilde{\boldsymbol{w}} \in \mathcal{W}\right\} = 1 \tag{4.10}$$

$$\mathbb{E}_{\mathbb{P}}\left\{\tilde{w}_i^s\right\} = \bar{w}_i^s, \forall i \in \mathcal{I}^w, \forall s \in \mathcal{S} \tag{4.11}$$

$$\mathbb{E}_{\mathbb{P}}\left\{|\tilde{w}_i^s - \bar{w}_i^s|\right\} \leq \phi_i^{ws}, \forall i \in \mathcal{I}^w, \forall s \in \mathcal{S} \tag{4.12}$$

$$\mathbb{E}_{\mathbb{P}}\left\{(\tilde{w}_i^s - \bar{w}_i^s)^2\right\} \leq \lambda_i^{ws}, \forall i \in \mathcal{I}^w, \forall s \in \mathcal{S} \tag{4.13}$$

$$\mathbb{E}_{\mathbb{P}}\left\{(\tilde{w}_i^s + \tilde{w}_j^s - \bar{w}_i^s - \bar{w}_j^s)^2\right\} \leq \lambda_i^{ws} + \lambda_j^{ws} + 2\zeta_{ij}^{ws},$$
$$\forall j < i \in \mathcal{I}^w, \forall s \in \mathcal{S} \tag{4.14}$$

Equation (4.10) suggests that the vector of random wind power generation is constrained within a support set $\mathcal{W}$. The support set $\mathcal{W}$ is defined by equation (4.15):

$$\mathcal{W} = \left\{\boldsymbol{w} \in \mathbb{R}^{|\mathcal{I}^w| \times |\mathcal{S}|} : \ 0 \leq w_i^s \leq 1, \ \forall i \in \mathcal{I}^w, \forall s \in \mathcal{S}\right\} \tag{4.15}$$

Equation (4.11) suggests that the expected value of random wind power $\tilde{w}_i^s$ is $\bar{w}_i^s$, and the next inequality (4.12) implies that the mean absolute deviation of $\tilde{w}_i^s$ is less than or equal to ϕ_i^{ws}. Similarly, constraints (4.13) suggest that the variance of $\tilde{w}_i^s$ does not exceed the constant λ_i^{ws}. The expression (4.14) denotes that the covariance between $\tilde{w}_i^s$ and $\tilde{w}_j^s$ is constrained below ζ_{ij}^{ws}. The constraints (4.10)-(4.14) in the ambiguity set try to capture the location, range, and dependence of random wind power generation regarding primary statistical measures, such as expectations, mean absolute deviations, variances and covariances. Such parameters should be more straightforward to measure than the exact probability distribution.

The expressions (4.16)-(4.20) are practiced in the ambiguity set to define a family of solar power distributions representations.

$$\mathbb{P}\left\{\tilde{\boldsymbol{e}} \in \mathcal{E}\right\} = 1 \tag{4.16}$$

$$\mathbb{E}_{\mathbb{P}}\left\{\tilde{e}_i^s\right\} = \bar{e}_i^s, \forall i \in \mathcal{I}^e, \forall s \in \mathcal{S} \tag{4.17}$$

$$\mathbb{E}_{\mathbb{P}}\left\{|\tilde{e}_i^s - \bar{e}_i^s|\right\} \leq \phi_i^{es}, \forall i \in \mathcal{I}^e, \forall s \in \mathcal{S} \tag{4.18}$$

$$\mathbb{E}_{\mathbb{P}}\left\{(\tilde{e}_i^s - \bar{e}_i^s)^2\right\} \leq \lambda_i^{es}, \forall i \in \mathcal{I}^e, \forall s \in \mathcal{S} \tag{4.19}$$

$$\mathbb{E}_{\mathbb{P}}\left\{(\tilde{e}_i^s + \tilde{e}_j^s - \bar{e}_i^s - \bar{e}_j^s)^2\right\} \leq \lambda_i^{es} + \lambda_j^{es} + 2\zeta_{ij}^{es},$$
$$\forall j < i \in \mathcal{I}^e, \forall s \in \mathcal{S} \tag{4.20}$$

Equation (4.16) suggests that the vector of random wind power generation is limited within a support set $\mathcal{E}$, which is expressed by equation (4.21):

$$\mathcal{E} = \left\{\boldsymbol{e} \in \mathbb{R}^{|\mathcal{I}^e| \times |\mathcal{S}|} : \ 0 \leq e_i^s \leq 1, \ \forall i \in \mathcal{I}^e, \forall s \in \mathcal{S}\right\} \tag{4.21}$$

Equation (4.17) indicates that the expected value of random solar power $\tilde{e}_i^s$ is $\bar{e}_i^s$, and the next inequality (4.18) implies that the mean absolute deviation of solar power $\tilde{e}_i^s$ is less than or equal to ϕ_i^{es}. Additionally, constraints (4.19) propose that the variance of $\tilde{e}_i^s$ does not exceed the constant λ_i^{es}. The expression (4.20) expresses that the covariance between $\tilde{e}_i^s$ and $\tilde{e}_j^s$ is reserved below ζ_{ij}^{es}. The constraints (4.16)-(4.20) in the ambiguity set attempt to obtain direct and useful information about probability distribution of the solar power generation.

To utilize the variety of the hybrid system, the covariance between the wind and solar power farms ζ_{ij}^{wes} is expressed in (4.22). Such expression is useful to determine the correlation between different renewable energy resources.

$$\mathbb{E}_{\mathbb{P}}\left\{(\tilde{w}_i^s + \tilde{e}_j^s - \bar{w}_i^s - \bar{e}_j^s)^2\right\} \leq \lambda_i^{ws} + \lambda_j^{es} + 2\zeta_{ij}^{wes},$$
$$\forall i \in \mathcal{I}^w, \forall j \in \mathcal{I}^e, \forall s \in \mathcal{S} \tag{4.22}$$

The covariance matrix of the entire included resources in the model is given in the (4.23),

$$Covariance = \begin{array}{c} \\ \tilde{w} \\ \\ \\ \\ \tilde{e} \\ \\ \\ \\ \end{array} \overbrace{\begin{array}{|ccc|ccc|} \multicolumn{3}{c}{} & \multicolumn{3}{c}{} \\ \multicolumn{3}{c}{\overbrace{\phantom{\zeta_{11}^{ws} \cdots \zeta_{1i}^{ws}}}^{\tilde{w}}} & \multicolumn{3}{c}{\overbrace{\phantom{\zeta_{11}^{wes} \cdots \zeta_{1j}^{wes}}}^{\tilde{e}}} \\ \hline \zeta_{11}^{ws} & \cdots & \zeta_{1i}^{ws} & \zeta_{11}^{wes} & \cdots & \zeta_{1j}^{wes} \\ \zeta_{21}^{ws} & \cdots & \zeta_{2i}^{ws} & \zeta_{21}^{wes} & \cdots & \zeta_{2j}^{wes} \\ \vdots & \ddots & \vdots & \vdots & \ddots & \vdots \\ \zeta_{i1}^{ws} & \cdots & \zeta_{ii}^{ws} & \zeta_{i1}^{wes} & \cdots & \zeta_{ij}^{wes} \\ \hline \zeta_{11}^{wes} & \cdots & \zeta_{j1}^{wes} & \zeta_{11}^{es} & \cdots & \zeta_{1j}^{es} \\ \zeta_{21}^{wes} & \cdots & \zeta_{j2}^{wes} & \zeta_{21}^{es} & \cdots & \zeta_{2j}^{es} \\ \vdots & \ddots & \vdots & \vdots & \ddots & \vdots \\ \zeta_{j1}^{wes} & \cdots & \zeta_{ji}^{wes} & \zeta_{j1}^{es} & \cdots & \zeta_{jj}^{es} \\ \hline \end{array}}^{(\mathcal{I}^w + \mathcal{I}^e) \times (\mathcal{I}^w + \mathcal{I}^e)} \tag{4.23}$$

The available conventional generation capacity $\tilde{\boldsymbol{p}}$ is modeled exactly as applied

in the previous chapter, by the equations (4.24)-(4.27):

$$\mathbb{P}\left\{\tilde{\boldsymbol{p}} \in \mathcal{P}\right\} = 1 \tag{4.24}$$

$$\mathbb{E}_{\mathbb{P}}\left\{\tilde{p}_i\right\} = \bar{p}_i, \qquad \forall i \in \mathcal{I} \tag{4.25}$$

$$\mathbb{E}_{\mathbb{P}}\left\{\max\{P_{il} - \tilde{p}_i, 0\}\right\} \leq \gamma_{il}, \quad \forall i \in \mathcal{I}, \forall l \in \mathcal{L}^{\gamma} \tag{4.26}$$

$$\mathbb{E}_{\mathbb{P}}\left\{\max\left\{Q_l - \sum_{i \in \mathcal{I}} \tilde{p}_i, 0\right\}\right\} \leq \delta_l, \qquad \forall l \in \mathcal{L}^{\delta} \tag{4.27}$$

The first expression (4.24) implies that the vector of uncertain generation capacity is constrained within a support set $\mathcal{P}$, which is defined as follows:

$$\mathcal{P} = \left\{\boldsymbol{p} \in \mathbb{R}^{|\mathcal{I}|} : \ p_i^{min} \leq p_i \leq p_i^{max}, \ \forall i \in \mathcal{I} \right\} \tag{4.28}$$

By combining the wind power uncertainty model (4.10)-(4.14) and the generation capacity expressions (4.24)-(4.27), the overall $\mathbb{F}$ can be formulated as (4.29). The proposed two-stage formulation is reformulated into a tractable second-order cone programming problem using linear decision rule approximations as applied in section 3.2. A case study which considers the hybrid system is discussed in the next section.

$$\mathbb{F} = \left\{ \mathbb{P} \in \mathcal{Q}_0\left(\mathbb{R}^{|\mathcal{I}|\times|\mathcal{S}|} \times \mathbb{R}^{|\mathcal{I}|}\right) : \begin{array}{l} \tilde{\boldsymbol{w}} \in \mathbb{R}^{|\mathcal{I}^w|\times|\mathcal{S}|} \\ \mathbb{P}\left\{\tilde{\boldsymbol{w}} \in \mathcal{W}\right\} = 1 \\ \mathbb{E}_{\mathbb{P}}\left\{\tilde{w}_i^s\right\} = \bar{w}_i^s, \forall i \in \mathcal{I}^w \\ \mathbb{E}_{\mathbb{P}}\left\{|\tilde{w}_i^s - \bar{w}_i^s|\right\} \leq \phi_i^{ws} \\ \mathbb{E}_{\mathbb{P}}\left\{(\tilde{w}_i^s - \bar{w}_i^s)^2\right\} \leq \lambda_i^{ws} \\ \mathbb{E}_{\mathbb{P}}\left\{(\tilde{w}_i^s + \tilde{w}_j^s - \bar{w}_i^s - \bar{w}_j^s)^2\right\} \leq \lambda_i^{ws} + \lambda_j^{ws} + 2\zeta_{ij}^{ws} \\ \tilde{\boldsymbol{e}} \in \mathbb{R}^{|\mathcal{I}^e|\times|\mathcal{S}|} \\ \mathbb{P}\left\{\tilde{\boldsymbol{e}} \in \mathcal{E}\right\} = 1 \\ \mathbb{E}_{\mathbb{P}}\left\{\tilde{e}_i^s\right\} = \bar{e}_i^s, \forall i \in \mathcal{I}^e \\ \mathbb{E}_{\mathbb{P}}\left\{|\tilde{e}_i^s - \bar{e}_i^s|\right\} \leq \phi_i^{es}, \forall i \in \mathcal{I}^e \\ \mathbb{E}_{\mathbb{P}}\left\{(\tilde{e}_i^s - \bar{e}_i^s)^2\right\} \leq \lambda_i^{es}, \forall i \in \mathcal{I}^e \\ \mathbb{E}_{\mathbb{P}}\left\{(\tilde{e}_i^s + \tilde{e}_j^s - \bar{e}_i^s - \bar{e}_j^s)^2\right\} \leq \lambda_i^{es} + \lambda_j^{es} + 2\zeta_{ij}^{es} \\ \tilde{\boldsymbol{p}} \in \mathbb{R}^{|\mathcal{I}|} \\ \mathbb{P}\left\{\tilde{\boldsymbol{p}} \in \mathcal{P}\right\} = 1 \\ \mathbb{E}_{\mathbb{P}}\left\{\tilde{p}_i\right\} = \bar{p}_i \\ \mathbb{E}_{\mathbb{P}}\left\{\max\{P_{il} - \tilde{p}_i, 0\}\right\} \leq \gamma_{il} \\ \mathbb{E}_{\mathbb{P}}\left\{\max\left\{Q_l - \sum\limits_{i\in\mathcal{I}} \tilde{p}_i, 0\right\}\right\} \leq \delta_l \end{array} \right\} \tag{4.29}$$

4.3 Case Study on Hybrid (Wind and Solar) Power Generation

In this case study, the DRO approach is employed to distribute 5000 MW of HWSPG in the five-area power system, so the worst cases expected energy not served is minimized. The power system considered in this test follows the same system specification as explained in section 2.3. The wind and solar power data for each area are collected and classified for several distribution types to obtain the fundamental statistical parameters such as the mean, absolute deviation, variance and covariance. The primary system data is shown in TABLE 4.1.

Table 4.1: The power system data

Five-Area Power System Data						
Area (i)	System Data		Wind Data		Solar Data	
	Peak Load (MW)	Installed Capacity (MW)	Mean $\tilde{w}_i$ (%)	Variance λ_i^w (%)	Mean $\tilde{e}_i$ (%)	Variance λ_i^e (%)
1	3,465	3,485	29.38	10.83	37.81	10.71
2	4,158	4,306	31.04	8.68	36.31	9.98
3	4,851	5,578	34.40	9.49	33.54	10.12
4	5,544	4,972	30.71	9.03	33.43	8.94
5	5,418	5,322	32.36	9.75	34.26	9.47

To adequately evaluate the hybrid system, the case study considers solving the allocation problem for WPG and SPG individually. Then, the HWSPG is examined and compared with the other two schemes. The DRO results of the three cases are given in TABLE 4.2. The worst case EENS of the wind is better than the solar by 6.22%, however, the hybrid system shows the best performance over the

other systems, which provides an improvement by 24.23% compared to solar power. Although, the designed DRO framework enables the renewable power generation budget to be allocated entirely to any single area, the decisions, on the other hand, are distributed all over the system to reduce the global variance, fulfill the load demand requirements and to provide the flexibility in supplying power.

Table 4.2: The DRO results

DRO Results							
Area (i)	WPG-DRO Results		SPG-DRO Results		HWSPG-DRO Results		
	WPG (MW)	EENS (GWh/yr)	SPG (MW)	EENS (GWh/yr)	WPG (MW)	SPG (MW)	EENS (GWh/yr)
1	800		1021		1190	766	
2	1015		522		175	0	
3	1005		1062		916	0	
4	950	542.04	1088	578.06	0	1188	438.60
5	1230		1307		765	0	

Fig. 4.1 demonstrates the wind and solar power generation decisions in MW which are allocated in the hybrid system for different installed generation capacities. The figure apparently indicates that area 3 is implemented with wind power and area 4 with solar power in all cases with a significant amount. This observation can be explained by looking at statistical data in TABLE 4.1, which shows that area 3 has the largest wind expectation and a relatively low variance comparing to the other areas which make this particular area is preferred to be engaged with wind power. Likewise, area 4 has the lowest solar power variance and fair mean value that

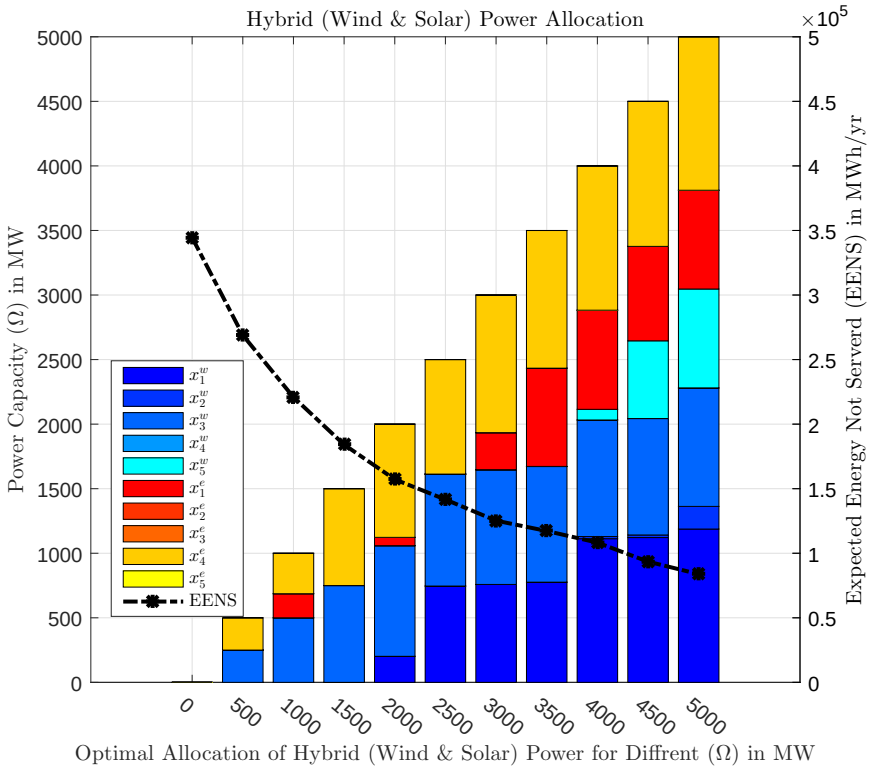

Figure 4.1: Optimal wind and solar power allocation for different capacities in the five-area system

makes it a favored candidate to be utilized with solar power. However, this general information is useful but not the only data that are used by the DRO to drive the decisions, since there are so many factors related to the system configuration and to the statistical information as explained in the modeling part.

Fig. 4.2 demonstrates the EENS of the three schemes under the isolated and interconnected system, to evaluate the effect of deploying different capacities of renewable power generation on the power system reliability.

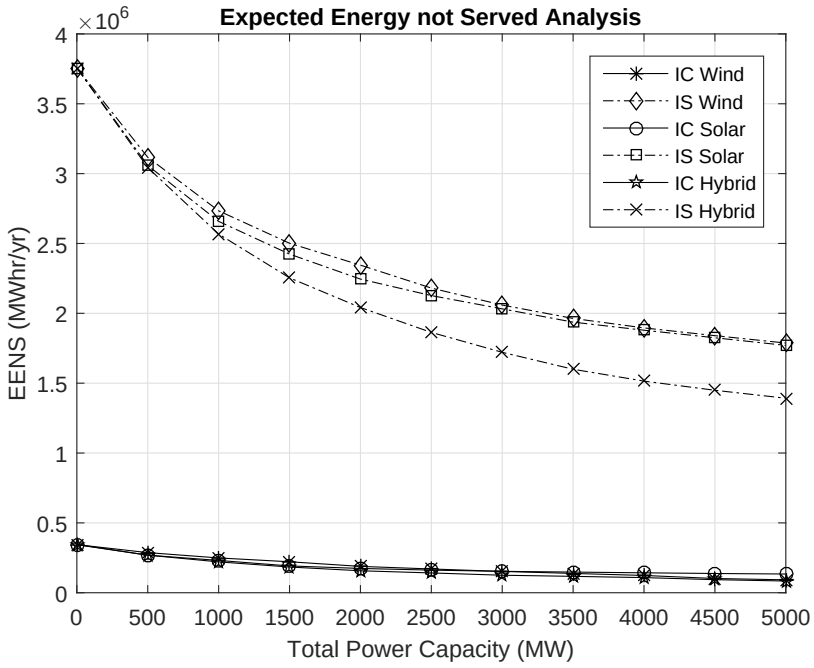

Figure 4.2: Overall EENS evaluation comparison

In general, the interconnected systems are more reliable in all cases. However, the impact of renewable power installation is captured in all cases with different influential level. The trend shows an improvement in the EENS as more renewable power generation is increased, and significantly with the hybrid system in the isolated system. As a result, the influence of incorporating renewable power generation is apparently captured in the isolated areas, and this is understandable since the isolated area has no assistance from neighboring areas in case of generation shortages or outages.

Furthermore, the advantage of combining both the wind and solar in a hybrid power system is because it allows for more availability and flexibility which is extremely crucial in such an intermittent source of power to ensure the reliability and the security.

5. CAPACITY CREDIT ANALYSIS OF RENEWABLE POWER GENERATION

5.1 Introduction

As renewable power generation is significantly variable and stochastic compared with other thermal energy sources, developing an appropriate means of calculating the capacity credit value of wind power or any variable electrical power generation resource is essential for assessing the effective load carrying capability during planning studies [77]. The unpredictability of wind makes it challenging to determine the capacity credit of wind energy systems, and so utility companies tend to assign wind power a discounted economic value in regards to its actual load carrying capacity. The capacity credit provides essential information to the independent system operator (ISO) about the amount of additional load that can be served while not violating the system reliability. Such information is useful for developing efficient long-term planning strategies to undertake the increase in load demand [78, 79].

As there are different definitions of capacity credit, the chosen definition can influence the value obtained. From the electric power market point of view, the capacity credit is the amount of resources contributed by the market-oriented sector that could replace the most conventional energy in a dependable manner. Therefore, defining an accurate capacity credit value of renewable power generation is an important planning factor for the feasibility determination of renewable energy integration and for understanding the exact load carrying capacity of the added generation units [80]. So from the generation expansion planning point of view, the capacity credit of generators is how much the generator (or group of generators) contributes to a power system's generation adequacy, which determines the difference between the installed

peak capacity and the equivalent load carrying capacity yield from the installed wind power generation. [81]. Accordingly, to determine the adequacy of wind power systems, the loss of load expectation (LOLE), which is the amount of time that the load won't be met over a given period of time (in hours per year or days per year), and the loss of load probability (LOLP), which is defined as the probability that the load will exceed available generation, can be utilized to calculate the capacity credit. Wind farms do not contribute as much to generation adequacy as conventional power plants with equivalent energy output; this necessitates backup power alternatives as wind farms replace power plants.

While wind power capacity credit has gained much attention for the past several decades, no standard definition of capacity credit exists [81]. As a result, so many different computing methods have been used, causing results to vary widely. In [82], a probabilistic method to evaluate the loss of load expectation of the combined total generating system is used by taking into account maintenance scheduling, uncertainty of load forecast, and interconnection with other utility systems. Outages were defined as either outage that was forced or outage from scheduled maintenance. A distribution function was introduced for the load since it cannot be accurately predicted to enable a realistic LOLE calculation. In this work, the wind power capacity factor means the average amount of electricity produced by wind energy, and it is calculated by subtracting it from the hourly utility load before calculating the loss of load expectation. This method is appropriate when the capacity of wind generators is small compared to the conventional means of generating power. With this concept, loss of load expectation is first calculated for a baseline scenario without wind power generation.

Probabilistic methods using nonsequential Monte Carlo simulation are widely used to calculate the capacity credit in planning studies; they are computationally

straightforward and rather fast and accurate. In [83], chronological and probabilistic methods of estimating capacity credit of wind power are compared. The chronological or sequential approach is based on the ratio between average and total output computation, which is identified as the wind energy capacity factor. Under the chronological approach, it is necessary to understand the proper time-scale relationship between load and wind power output generated. They found that chronological methods were best for use by system operators, and system planners best use probabilistic methods.

In [84], a probabilistic method to determine capacity credit of the wind power generators is used. Their probabilistic approach used reliability aspects of electrical power systems, and Monte Carlo simulations were used due to the stochastic nature of the simulations. They acknowledged that amount of wind energy depends on aspects including wind nature, landscape, and wind obstacles. Also, they acknowledged the importance of benchmarking a base case reliability of the network, voltage levels at which wind turbines are connected, and distance from load centers. The authors used a wind power series model to simulate the wind and a Monte Carlo reliability model to simulate the larger amount of potential interactions.

Determining wind capacity credit using a reliability index is particularly useful for system strategical planning, to dependably increase efficiency. Reliability indices, which are used to calculate capacity credit, can be obtained from either the analytical approach or the simulation approach. While analytical methods have been used effectively in the past, the need for more information on system reliability indices necessitates Monte Carlo simulations [85]. Though Monte Carlo is more flexible, it also needs longer simulation time than the analytical methods, and thousands of simulations for each year to get accurate results.

A rigorous model for obtaining wind power capacity credit that is based on the

definition of reliability functions is proposed in [86]. The model doesn't require strong hypotheses and can be used when the standard evaluation techniques are likely to err, such as when wind power and load profile are not statistically independent. This model explains how statistical characteristics of load and wind power relate to capacity credit, from statistical and chronological perspectives. The authors state that capacity credit was first used to estimate load carrying capability of conventional power generation. They divide the methods of evaluating capacity credit into four realms: Monte Carlo, peak-period capacity factors, convolution, and analytical.

Extending to the previous literature, the evaluation of capacity credit from just looking at power generation is developed to consider the electrical energy storage and demand response is introduced in [87]. Using electrical energy storage supplies additional load and improves the demand response while maintaining or improving the reliability. Taking these factors into account enables more accurate understanding of capacity credit.

Capacity credit of wind power is a function of many different parameters; it is proportional to the availability of renewable energy wind power generation and the increase in load demand. Other parameters include thermal generation schedules and import-export schedules, as adding any generator increases the capacity value and the adequacy of a system. If maintenance is needed at a time when it would have a significant impact on LOLP and at periods of significant wind, then this is a factor as well. Penetration factor is also important for the capacity credit of wind power, which is defined as the ratio of the capacity of the single unit added to the capacity of all existing units plus the new unit [81]. Transmission line transfer capacities between the areas are also an important factor that affects the wind power penetration factor and, as a result, the wind power capacity credit.

A target reliability level can be selected, which will have a significant impact

on the capacity value. To find the capacity credit, chronological or probabilistic methods can be employed. An auto-regressive moving average model of wind power has been applied, along with sequential Monte Carlo simulation to obtain capacity credit value. This capacity credit is influenced by the overall adequacy of generation and power plant generation factor. It is of interest to determine how adding another generator unit affects generation adequacy. Loss of load probability is also changed by adding a new generator. Each new generating unit in a system allows for the greater load while maintaining generation adequacy.

5.2 Analytical Approach for Capacity Credit Evaluation

The capacity credit evaluation of the renewable power generation planning decisions is assessed in this section using the analytical approach. The assessment discusses the actual load carrying capacities while adding WPG, SPG and HWSPG for both isolated and interconnected power systems. Fig. 5.1 explains the procedure of capacity credit estimation criteria, which measure the improvement in the generation adequacy by investigating the system reliability at a particular reliability index due to the integration of the new renewable power generation. Such test indicates the secured allowable increase in load demand while maintaining the targeted reliability level.

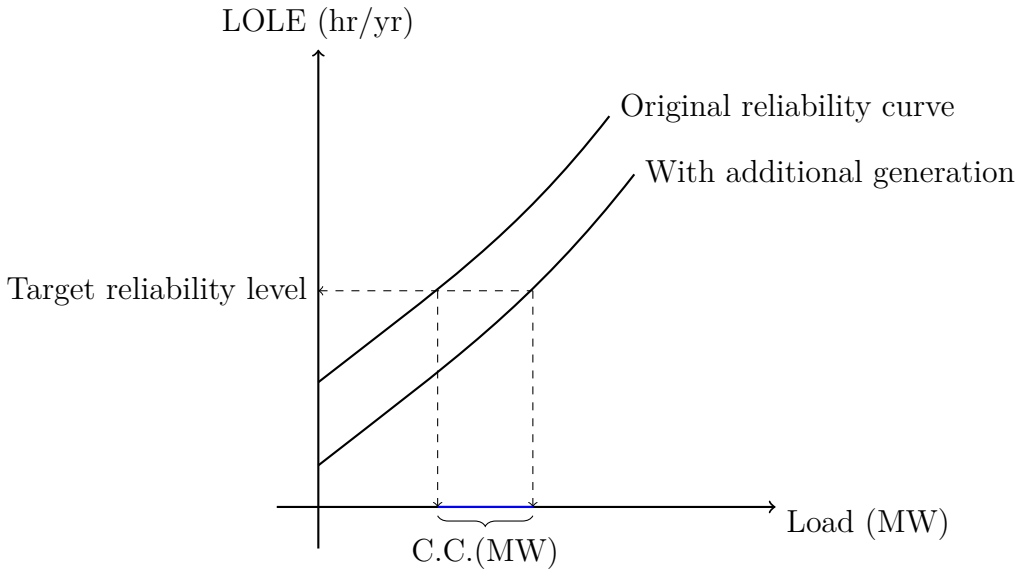

Figure 5.1: Graphical example of capacity credit evaluation

The random sampling Monte Carlo simulation (MCS) is used to estimate the LOLE for different load levels to construct the curves with and without additional

renewable power generation units. A sufficient number of sample years has to be simulated to reach an acceptable level of coefficient of variation (COV), which is 5% or lower for this kind of planning study. In this test, after conducting one thousand sample years of simulation, the resultant COV is 4.8983 %, which provides confidence about the estimated reliability index.

5.2.1 Capacity Credit Evaluation of Wind Power Generation

The MCS is performed to estimate the LOLE for several load levels at different WPG capacities. Fig. shows 11 overall LOLE curves of the five area system example, each curve is calculated at a particular total wind power capacities Ω that varies between 0 MW and 5000 MW. It shows the improvement of LOLE as more generation is added. Equation (5.1) explains how to analytically extract the capacity credit of 500 MW of wind power at chosen LOLE of 100 hr/yr.

$$CC(\Omega = 500) = D(LOLE_{\Omega=500} = 100) - D(LOLE_{\Omega=0} = 100) \tag{5.1}$$

Where $CC(\Omega)$ is the capacity credit at a total wind power capacity Ω. $D(LOLE_{\Omega})$ is the load in MW at a targeted LOLE in hr/yr with installed wind power capacity Ω. In the next section 5.2.1.1, the LOLE vs. Load curves are estimated for different wind power capacities, in order to calculate the capacity credit and capture its trend as the wind power generation increases. The same procedure is carried out for SPG and HWSPG as well.

5.2.1.1 Capacity Credit Analysis of Wind Power Generation

The purpose of this evaluation is to find the effective load caring capacity of the suggested DRO planning decisions of wind power generation in isolated and interconnected power systems. Fig. 5.2 shows the LOLE results for the isolated system with a base case that has no wind power and the other cases are produced with installed wind power generation from 500 MW up to 5000 MW in 500 MW steps. The plot clearly indicates that LOLE increases as the load demand increases. Also there is improvement in reliability as more wind power is installed, as the expected time period of not supplying the load is reduced as more power generation units are added to the grid.

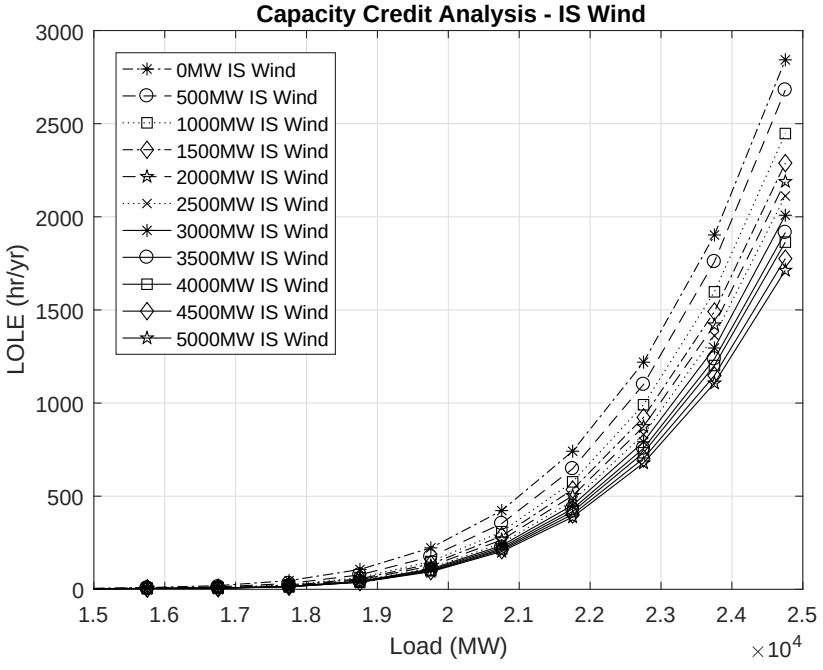

Figure 5.2: Capacity credit analysis of WPG in isolated system

Similarly, the LOLE study is conducted on the interconnected system as explained in Fig. 5.3, which definitely has better reliability level since the transmission lines allow for feeding the neighboring areas with the excess power, whether it is from conventional or renewable generation units, which contribute positively in the system generation adequacy.

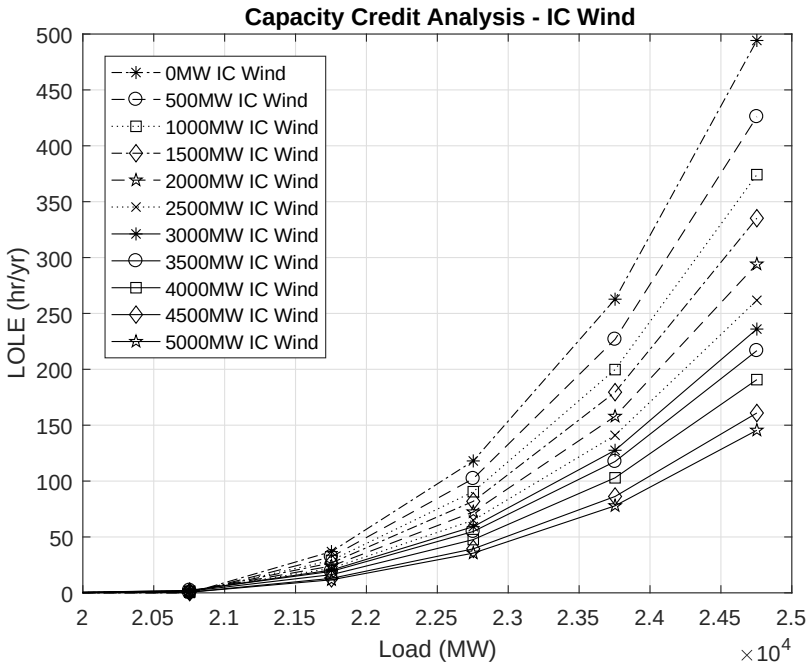

Figure 5.3: Capacity credit analysis of WPG in interconnected system

The capacity credited is calculated using the equation (5.1) and the results of this case study are listed in TABLE 5.1. The TABLE includes the percentage penetration factor of the WPG compared to the peak load in isolated and interconnected system for each installed wind power capacity. The capacity credit is introduced as its effective load carrying capacity in MW and also as a percentage of Nominal WPG installed in each case.

Table 5.1: Capacity credit relation to the WPG penetration factor

Capacity Credit Analysis of WPG							
		Isolated System			Interconnected System		
Installed Capacity WPG (MW)	Installed Penet. Factor WPG (%)	Effective Penet. Factor WPG (%)	Capacity Credit		Effective Penet. Factor WPG (%)	Capacity Credit	
			(MW)	% of Nominal WPG		(MW)	% of Nominal WPG
500	2.11	0.72	379	75.79	0.50	149	29.95
1000	4.22	1.16	595	59.57	0.75	284	28.48
1500	6.33	1.42	708	47.20	0.90	402	26.85
2000	8.45	1.60	815	40.74	1.48	556	27.80
2500	10.56	1.80	918	36.73	1.88	697	27.90
3000	12.67	1.95	979	32.64	2.19	828	27.60
3500	14.79	2.08	1029	29.41	2.41	940	26.86
4000	16.90	2.16	1083	27.09	2.71	1131	28.28
4500	19.02	2.24	1111	24.69	3.17	1393	30.97
5000	21.13	2.32	1151	23.03	3.58	1550	31.00

The capacity credit is mainly affected by two important factors which are the penetration factor of the new generation units and the generation adequacy represented in this case study by the LOLE. The capacity credit of the wind power is smaller compared to the total installed capacity. This is understandable since the wind power is a variable source of power generation. Moreover, the ratio of the capacity credit to the installed WPG is generally reduced as the installed wind power capacity increases. This observation is quite clear in the isolated system, however, in the interconnected system the ratio is relatively constant and it is higher than the isolated system in case of large wind power penetration, which is accounted as an advantage for the interconnected power system with a high wind power deployment.

5.2.1.2 Capacity Credit Analysis of Solar Power Generation

The capacity credit evaluation procedure of the Solar power generation follows the same steps as the wind power. This assessment enables the system planners to distinguish the differences between these two sustainable energy resources, and decide which one fulfills their requirements. Fig 5.4 shows the LOLE estimation for different peak load levels using Monte Carlo simulation at each solar power capacity for the isolated system.

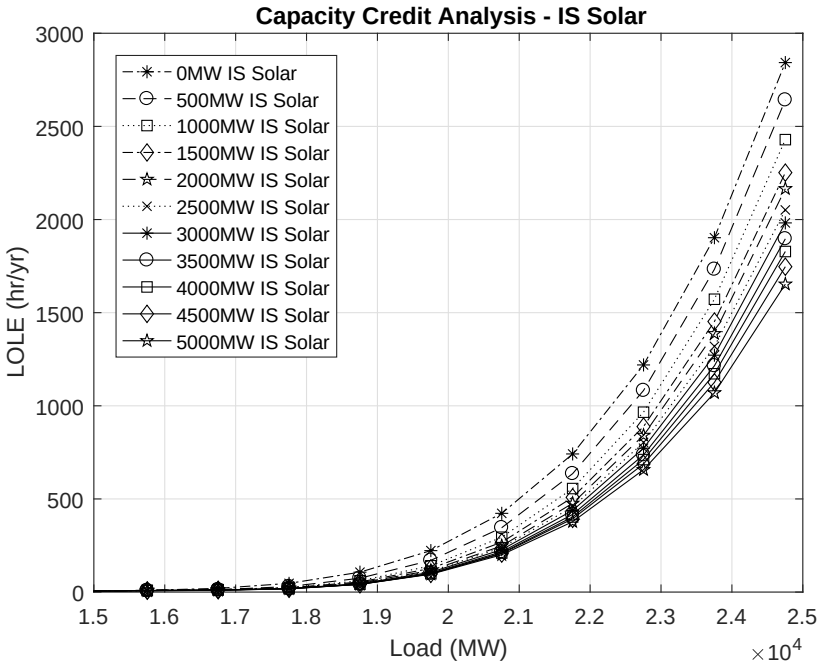

Figure 5.4: Capacity credit analysis of SPG in isolated system

The interconnected system LOLE evaluation is demonstrated in Fig. 5.5. It clearly shows how the tie-lines between areas improve tremendously the reliability of the system. The LOLE is dropped around 85% just for using the transmission lines.

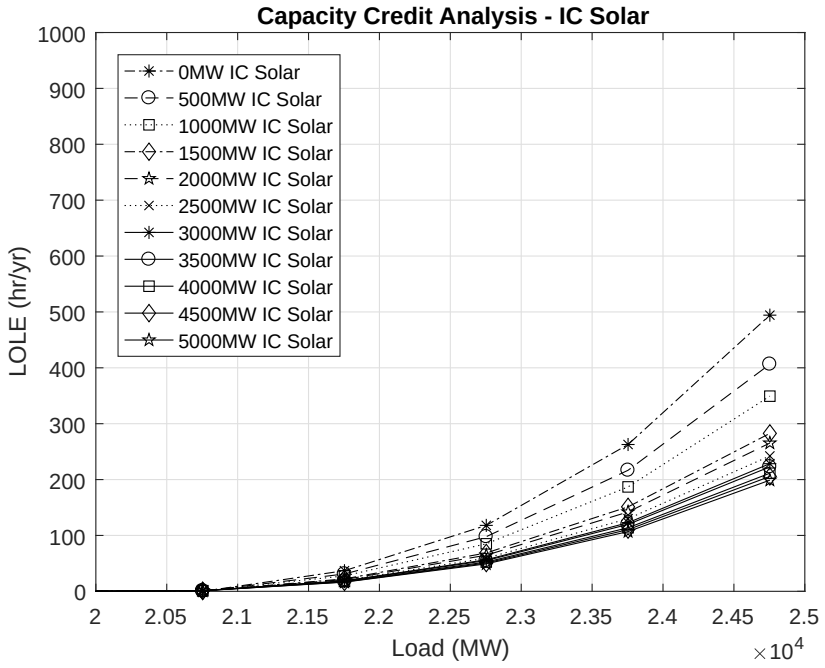

Figure 5.5: Capacity credit analysis of SPG in interconnected system

On the other hand, the effect of transmission lines has different aspect when it comes to capacity credit, that can be seen in TABLE 5.2, where the capacity credit values of different installed capacity of solar power generation are listed. The capacity credit of 500 MW of solar power is 422 MW in isolated system whereas it is only 197 MW in interconnected, this is because the areas have other reliable and less uncertain source of power, which is the conventional power generation, which is delivered from other neighboring ares in case of excess power are available. The conventional power generation in this case reduces the penetration factor of solar

power in the interconnected power system. With higher penetration of solar power, the capacity credit in term of MW increases but the ratio of the capacity credit to the installed capacity reduces and this is mentioned in many literature [88, 89], as it is inversely proportional to the solar power penetration factor. The capacity credit ratio drops sharply in the isolated system from 84.53% to 22.74%, also in the interconnected system the ratio is only 21.52%, such percentage is preferred to be increased and such observation motivates the investigation in the effect of renewable resources diversity in this kind of assessment.

Table 5.2: Capacity credit relation to the SPG penetration factor

Capacity Credit Analysis of SPG							
		Isolated System			Interconnected System		
Installed Capacity SPG (MW)	Installed Penet. Factor SPG (%)	Effective Penet. Factor SPG (%)	Capacity Credit		Effective Penet. Factor SPG (%)	Capacity Credit	
			(MW)	% of Nominal SPG		(MW)	% of Nominal SPG
500	2.11	0.81	422	84.53	0.55	197	39.49
1000	4.22	1.28	662	66.22	0.61	357	35.76
1500	6.33	1.57	789	52.62	1.33	615	41.04
2000	8.45	1.79	900	45.03	1.88	694	34.70
2500	10.56	1.93	947	37.89	2.19	808	32.35
3000	12.67	2.05	1007	33.58	2.47	883	29.43
3500	14.79	2.18	1069	30.55	2.54	917	26.21
4000	16.90	2.26	1104	27.61	2.89	988	24.71
4500	19.02	2.35	1111	24.69	3.25	1031	22.91
5000	21.13	2.46	1137	22.74	3.58	1076	21.52

5.2.1.3 Capacity Credit Analysis of Hybrid Power Generation

The results of the hybrid power generation allocation problem using DRO technique are applied in the five-area power system. The performance of this approach can be evaluated by finding the capacity credit of the new added HWSPG units which are compared with the cases of WPG and SPG alone systems.

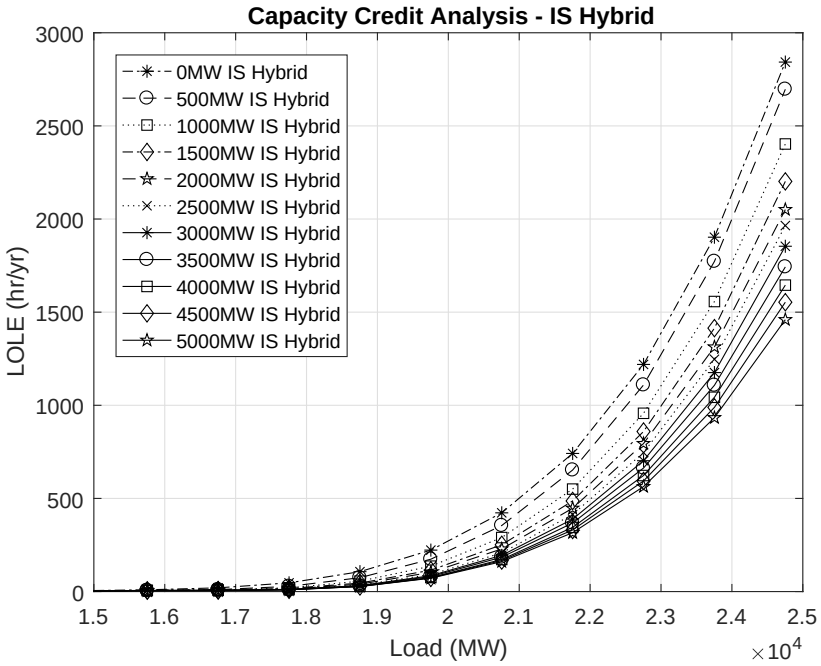

Figure 5.6: Capacity credit analysis of HWSPG in isolated system

The Monte Carlo simulation is used to find the LOLE for several peak load values for isolated and interconnected systems as explained in Fig. 5.6 and Fig. 5.7 respectively.

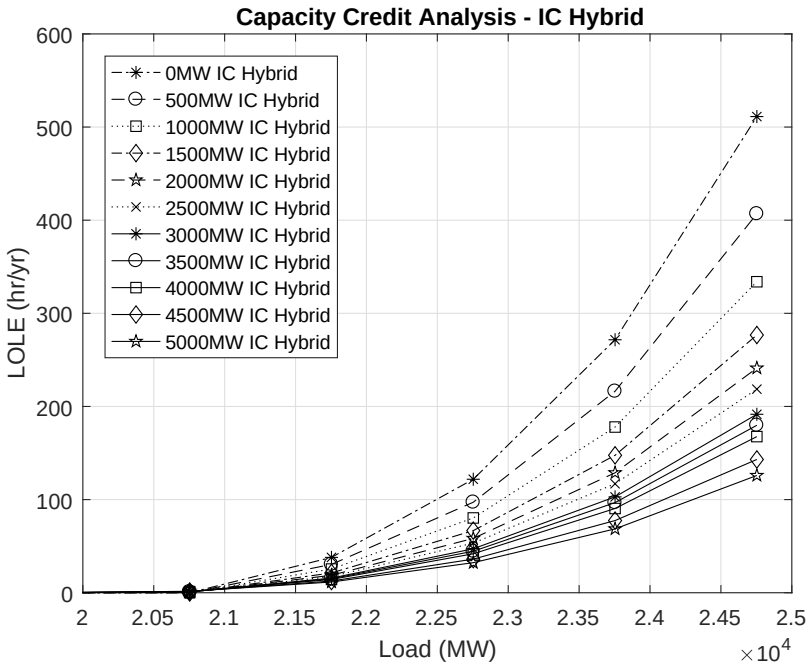

Figure 5.7: Capacity credit analysis of HWSPG in interconnected system

The capacity credit values which reflect the effective load carrying capacities are calculated with their associated penetration factors of WPG, SPG and HWSPG for both Isolated and interconnected system as explained in TABLE 5.3. The capacity credit results show better performance compared to the wind or solar power generation alone, since the hybrid system provides more diversity which increases the availability and as a result reduces the uncertainty of renewable power generation. For instance, at 5000 MW of HWSPG, the capacity credit is 1804 MW whereas it is 1550 MW in WPG and 1076 MW in SPG. For more insight on the differences between the three proposed schemes, a comparisons are carried out in the the next subsection 5.8.

Table 5.3: Capacity credit relation to the HWSPG penetration factor

Capacity Credit Analysis of HWSPG										
	Isolated System					Interconnected System				
Installed Capacity HWSPG (MW)	Penetration Factor WPG (%)	Penetration Factor SPG (%)	Penetration Factor HWSPG (%)	Capacity Credit		Penetration Factor WPG (%)	Penetration Factor SPG (%)	Penetration Factor HWSPG (%)	Capacity Credit	
				(MW)	% of Nominal HWSPG				(MW)	% of Nominal HWSPG
500	0.40	0.41	0.81	411	82.23	0.27	0.41	0.68	235	47.16
1000	0.72	0.63	1.35	717	71.71	0.50	0.52	1.02	453	45.37
1500	0.96	0.75	1.71	922	61.47	0.67	1.11	1.78	680	45.38
2000	1.15	0.81	1.96	1048	52.44	0.76	1.28	2.04	855	42.78
2500	1.29	0.89	2.18	1184	47.38	0.83	1.27	2.10	983	39.33
3000	1.41	0.94	2.35	1264	42.15	0.84	1.50	2.35	1163	38.78
3500	1.52	0.97	2.50	1324	37.83	0.85	1.52	2.37	1253	35.81
4000	1.66	0.97	2.64	1406	35.15	0.98	1.55	2.53	1355	33.87
4500	1.72	1.028	2.75	1439	31.99	1.56	1.50	3.06	1598	35.51
5000	1.77	1.066	2.84	1473	29.47	1.79	1.53	3.32	1804	36.08

5.2.1.4 Capacity Credit Analysis Comparison

The factors which influence the capacity credit value of different renewable energy resources are introduced. These factors are mainly related to the penetration factors, the availability of the renewable energy resources and the existence of the transmission lines connecting the areas with each other. The optimal power flow, which is impeded inside the Monte Carlo simulation, optimally find the operational decisions and commit the generation unites to feed the load so the EENS is minimized. Fig. 5.8 shows the LOLE curves of the system with 5000 MW of WPG, SPG and HWSPG for isolated and interconnected systems.

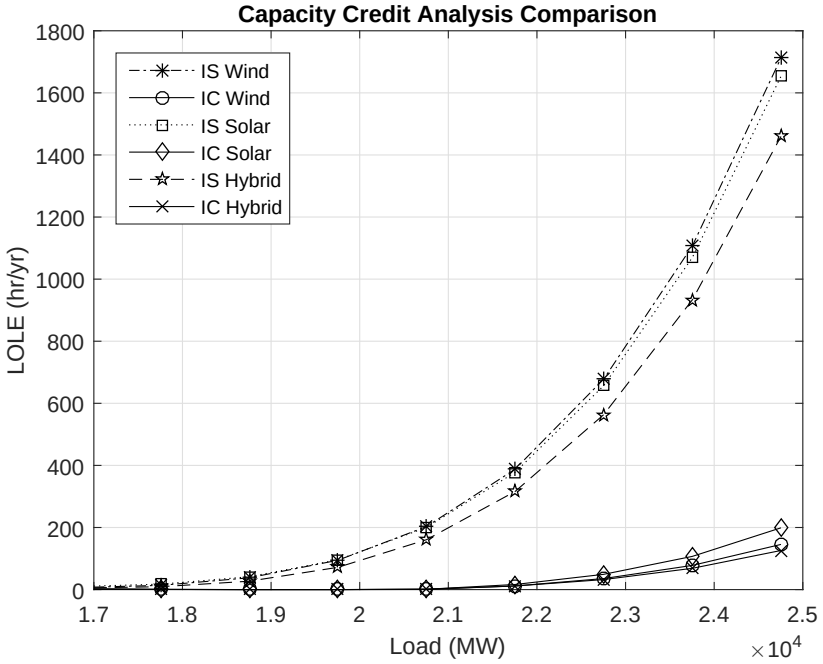

Figure 5.8: Capacity credit analysis comparison

The general trend indicates that the interconnected systems are more reliable since the generation adequacy is improved by utilizing the tie-lines to support the shortage in electric power from the excess power of neighboring areas. The hybrid systems in both isolated and interconnected schemes preform better compared to the single renewable source systems. The capacity credit for the proposed systems are calculated for the installed capacities upto 5000 MW in 500 MW steps as explained in Fig. 5.9.

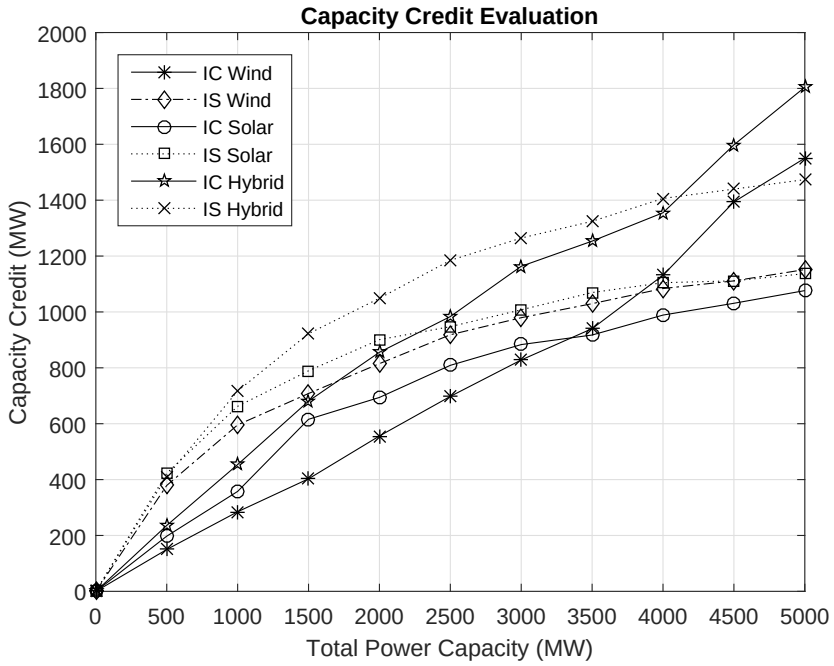

Figure 5.9: Capacity credit analysis evaluation

The results show that at low renewable installed capacities the capacity credit has higher value in isolated systems compared to the interconnected systems, however, it is the opposite when the installed capacity is high. for example, at 500 MW of renewable power generation, the capacity credit value is approximately 200 MW in

the interconnected system whereas it is around 400 MW in the isolated systems. In contrast, for high renewable power installed capacity the interconnected system perform better than isolated system with around 1800 MW capacity credit when the hybrid system is considered in the interconnected environment while it is 1473 MW in isolated power system. A likewise trend can be observed in Fig. 5.10, which proves that the percentage of the effective penetration factor has a direct impact and it is proportional related to the capacity credit values.

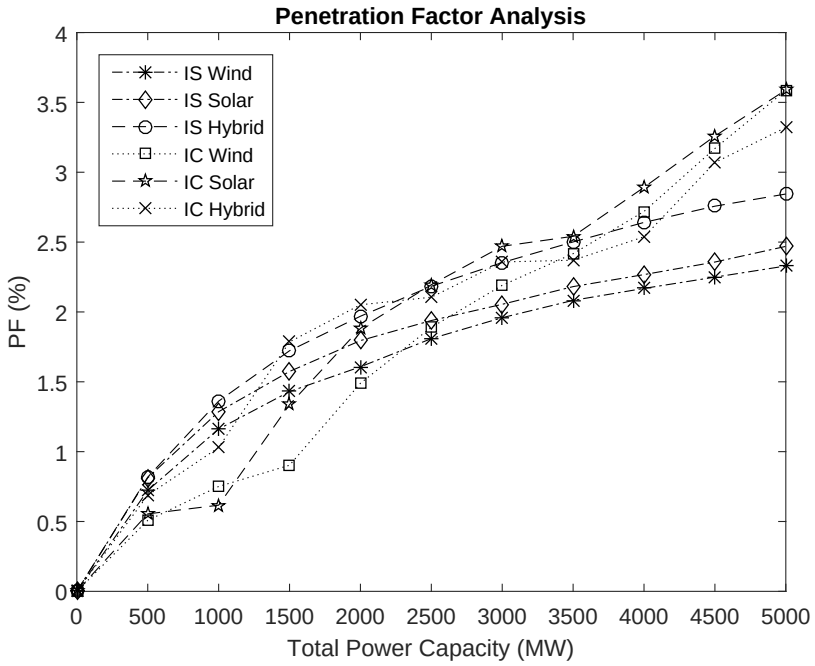

Figure 5.10: Penetration factor analysis Comparison

There are several factors governing the behavior of the capacity credit. The most influential factor is the renewable power availability since the low availability leads to a limited renewable power generation which is more likely consumed within the area, and that is why it has a high capacity credit in the isolated system for only small

installed capacity. Whereas, at the interconnected system, the low renewable power generation has no significant effect compared to the conventional electricity that is generated within the area or transmitted from the neighboring areas, which gives low credit to the low generated renewable power. Therefore, the issue of renewable power uncertainty is degraded by the hybrid system which improves the availability and increases the capacity credit of installing renewable power generation which ultimately assists to enhances the reliability of the electrical power system.

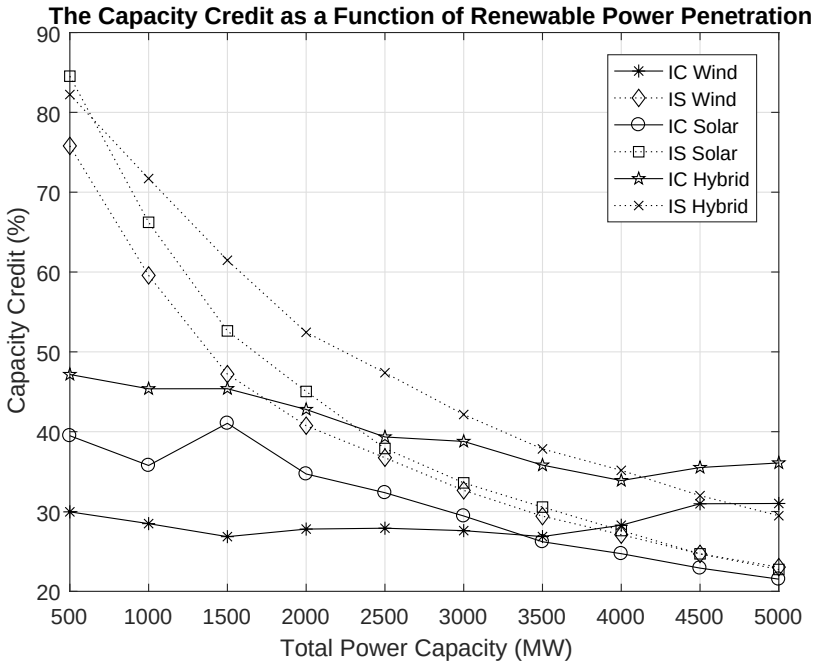

Figure 5.11: Capacity credit relation to the renewable power penetration

Fig. 5.11 demonstrates the ratio of the capacity credit to the installed capacity, which reflects the effective usage of the installed renewable energy capacity. The ratio shows a high rate in the isolated system for low penetration of renewable generation and it decreases at the high penetration, while the interconnected system

shows a relatively stable performance on the ratio due to the increase in the renewable installed capacities. The hybrid system shows the best performance for both interconnected and isolated systems by generally securing the highest rate compared to the WPG and SPG alone.

6. CONCLUSION

6.1 The Contributions of the Dissertation

This dissertation proposes a DRO based wind power allocation model for multi-area power systems. The objective of the proposed method is to pursue the highest power system reliability and the generation adequacy, indicating the lowest EENS for the overall system, considering wind power uncertainties and the forced outages of generators. The stochastic nature of the uncertainty factors is represented by an ambiguity set model, without assuming the knowledge of the exact underlying distributions. The statistical information about the uncertain variables is expressed in the ambiguity set to enable data-driven approach decision-making.

The generalized linear decision rules approach is used to represent the second stage recourse decisions as affinely related to the uncertain parameters to introduce distributional statistical information of uncertain variables in a tractable optimization system model. The mathematical representation of the statistical data parameters are described linearly using piece wise representation which is linear and incorporated in the model using linear programming. The approximation in the linear model is mitigated using the standard statistical representation of the wind power data using expectation, mean absolute deviation, variance and covariance. The nonlinearity presented in the variance and covariance requires the development of the DRO model to handle the nonlinear constraints by utilizing the second order-cone programming.

The decision-making procedure is improved by providing more statistical data about the wind power availability which enables the DRO technique to better optimize the decisions that provide more wind power diversity and reduces the global

wind power variance. Extensive case studies have been conducted on a five-area system, demonstrating the effectiveness of this method in capturing various ambiguous distribution data of wind power outputs, as well as the failure probabilities of generators.

To investigate the benefits of the renewable energy diversification on the renewable power generation allocation problem, the hybrid system is introduced to include both wind and solar power in the generation distribution problem to obtain the minimum EENS. The covariance between the wind and solar power is introduced to capture the correlation and to better allocate the resources. The results show better performance in the hybrid system compared to the other two schemes due to the availability of the different sources at different times and locations which is represented by the negatively correlated relation between the renewable energy resources.

The capacity credit analysis is applied to indicate the effective load carrying capacity of the installed wind and solar power generation units at designated reliability level. Calculating the capacity credit values assists the decision makers to better manage the operation and planning of the electrical power system. The probabilistic method including Monte Carlo simulation is employed to calculate the LOLE at different peak loads and then the capacity credit of wind power generation is analytically determined for several installed power capacities. The results demonstrate that the penetration factor of the renewable power generation units and its availability are the two main factors effecting the capacity credit value.

6.2 Future work

The DRO renewable generation planning framework could be improved by including the cost minimization beside the reliability improvement in the objective function. The energy storage could be further allocated along with the renewable power generation to accomplish the objective of planning and operation perspective. As a next step after the renewable power generation allocation, the operational studies like unit commitment and economic dispatch could be carried out after modifying the load model to be chronological. The capacity credit can be considered in the objective by distributing the renewable generation that achieves the higher capacity credit value.

REFERENCES

[1] Z. Dong, K. P. Wong, K. Meng, F. Luo, F. Yao, and J. Zhao, "Wind power impact on system operations and planning," in *Power and Energy Society General Meeting, 2010 IEEE*, pp. 1–5, July 2010.

[2] F. Luo, K. Meng, Z. Y. Dong, Y. Zheng, Y. Chen, and K. P. Wong, "Coordinated operational planning for wind farm with battery energy storage system," *Sustainable Energy, IEEE Transactions on*, vol. 6, pp. 253–262, Jan 2015.

[3] M. Javadi, M. Saniei, H. Mashhadi, and G. GutieÌĄrrez-Alcaraz, "Multi-objective expansion planning approach: distant wind farms and limited energy resources integration," *Renewable Power Generation, IET*, vol. 7, pp. 652–668, Nov 2013.

[4] P. Xiong and C. Singh, "Optimal planning of storage in power systems integrated with wind power generation," *IEEE Transactions on Sustainable Energy*, vol. 7, pp. 232–240, Jan 2016.

[5] A. Leite, C. Borges, and D. Falcao, "Probabilistic wind farms generation model for reliability studies applied to brazilian sites," *Power Systems, IEEE Transactions on*, vol. 21, pp. 1493–1501, Nov 2006.

[6] R. Dominguez, A. Conejo, and M. Carrion, "Toward fully renewable electric energy systems," *Power Systems, IEEE Transactions on*, vol. 30, pp. 316–326, Jan 2015.

[7] P. Siano and G. Mokryani, "Evaluating the benefits of optimal allocation of wind turbines for distribution network operators," *Systems Journal, IEEE*, vol. 9, pp. 629–638, June 2015.

[8] M. Lubin, Y. Dvorkin, and S. Backhaus, "A robust approach to chance constrained optimal power flow with renewable generation," *Power Systems, IEEE Transactions on*, vol. PP, no. 99, pp. 1–10, 2015.

[9] Z. Qin, W. Li, and X. Xiong, "Generation system reliability evaluation incorporating correlations of wind speeds with different distributions," *Power Systems, IEEE Transactions on*, vol. 28, pp. 551–558, Feb 2013.

[10] W. Wei, F. Liu, and S. Mei, "Distributionally robust co-optimization of energy and reserve dispatch," *Sustainable Energy, IEEE Transactions on*, vol. 7, pp. 289–300, Jan 2016.

[11] E. Hajipour, M. Bozorg, and M. Fotuhi-Firuzabad, "Stochastic capacity expansion planning of remote microgrids with wind farms and energy storage," *Sustainable Energy, IEEE Transactions on*, vol. 6, pp. 491–498, April 2015.

[12] S. Dehghan, N. Amjady, and A. Conejo, "Reliability-constrained robust power system expansion planning," *Power Systems, IEEE Transactions on*, vol. PP, no. 99, pp. 1–10, 2015.

[13] A. Papavasiliou, S. Oren, and I. Aravena, "Stochastic modeling of multi-area wind power production," in *System Sciences (HICSS), 2015 48th Hawaii International Conference on*, pp. 2616–2626, Jan 2015.

[14] E. Ela and M. O'Malley, "Studying the variability and uncertainty impacts of variable generation at multiple timescales," *Power Systems, IEEE Transactions on*, vol. 27, pp. 1324–1333, Aug 2012.

[15] J. Ma, V. Silva, R. Belhomme, D. Kirschen, and L. Ochoa, "Evaluating and planning flexibility in sustainable power systems," in *Power and Energy Society General Meeting (PES), 2013 IEEE*, pp. 1–11, July 2013.

[16] K. Hasan, T. Saha, and M. Eghbal, "Modelling uncertainty in renewable generation entry to deregulated electricity market," in *Universities Power Engineering Conference (AUPEC), 2011 21st Australasian*, pp. 1–6, Sept 2011.

[17] J. Birge and F. Louveaux, *Introduction to stochastic programming*. Springer Verlag, 1997.

[18] Q. Bian, H. Xin, Z. Wang, D. Gan, and K. P. Wong, "Distributionally robust solution to the reserve scheduling problem with partial information of wind power," *Power Systems, IEEE Transactions on*, vol. 30, pp. 2822–2823, Sept 2015.

[19] A. Ben-Tal and A. Nemirovski, "Robust Convex Optimization," *Mathematics of Operations Research*, vol. 23, no. 4, pp. 769–805, 1998.

[20] A. Ben-Tal, L. El Ghaoui, and A. Nemirovski, *Robust Optimization*. Princeton Series in Applied Mathematics, Princeton University Press, October 2009.

[21] D. Bertsimas and A. Thiele, "Robust and data-driven optimization: Modern decision-making under uncertainty," *Tutorials on Operations Research*, 2006.

[22] C. Liu, C. Lee, H. Chen, and S. Mehrotra, "Stochastic robust mathematical programming model for power system optimization," *Power Systems, IEEE Transactions on*, vol. PP, no. 99, pp. 1–2, 2015.

[23] W. Wiesemann, D. Kuhn, and M. Sim, "Distributionally robust convex optimization," *Operations Research*, vol. 62, no. 6, pp. 1358–1376, 2014.

[24] J. Goh and M. Sim, "Distributionally robust optimization and its tractable approximations," *Operations Research*, vol. 58, pp. 902–917, Apr. 2010.

[25] E. Delage and Y. Ye, "Distributionally robust optimization under moment uncertainty with application to data-driven problems," *Operations Research*, vol. 58, no. 3, pp. 595–612, 2010.

[26] S. Agrawal, Y. Ding, A. Saberi, and Y. Ye, "Price of correlations in stochastic optimization," *Operations Research*, vol. 60, pp. 150–162, Jan. 2012.

[27] P. Xiong, P. Jirutitijaroen, and C. Singh, "A distributionally robust optimization model for unit commitment considering uncertain wind power generation," *IEEE Transactions on Power Systems*, vol. PP, no. 99, pp. 1–11, 2016.

[28] H. Xu, C. Caramanis, and S. Mannor, "A distributional interpretation of robust optimization," in *Communication, Control, and Computing (Allerton), 2010 48th Annual Allerton Conference on*, pp. 552–556, Sept 2010.

[29] P. Yu and H. Xu, "Distributionally robust counterpart in markov decision processes," *Automatic Control, IEEE Transactions on*, vol. PP, no. 99, pp. 1–1, 2015.

[30] H. Heitsch and W. RÃűmisch, "Scenario reduction algorithms in stochastic programming," *Computational Optimization and Applications*, vol. 24, pp. 187–206, 2003.

[31] A. Georghiou, W. Wiesemann, and D. Kuhn, "Generalized decision rule approximations for stochastic programming via liftings," *Mathematical Programming*, vol. 152, no. 1-2, pp. 301–338, 2015.

[32] D. Bertsimas, M. Sim, and M. Zhang, "A practicable framework for distributionally robust linear optimization," July 2013.

[33] A. Ben-Tal, A. Goryashko, E. Guslitzer, and A. Nemirovski, "Adjustable robust solutions of uncertain linear programs," *Mathematical Programming*, vol. 99,

no. 2, pp. 351–376, 2004.

[34] N. Rau and F. Zeng, "Adequacy and responsibility of locational generation and transmission-optimization procedures," *Power Systems, IEEE Transactions on*, vol. 19, pp. 2093–2101, Nov 2004.

[35] P. Jirutitijaroen and C. Singh, "Reliability and cost tradeoff in multiarea power system generation expansion using dynamic programming and global decomposition," *Power Systems, IEEE Transactions on*, vol. 21, pp. 1432–1441, Aug 2006.

[36] P. Jirutitijaroen and C. Singh, "Reliability and cost tradeoff in multiarea power system generation expansion using dynamic programming and global decomposition," *Power Systems, IEEE Transactions on*, vol. 21, pp. 1432–1441, Aug 2006.

[37] P. Jirutitijaroen and C. Singh, "Multi-area generation adequacy planning using stochastic programming," in *Power Systems Conference and Exposition, 2006. PSCE '06. 2006 IEEE PES*, pp. 1327–1332, Oct 2006.

[38] P. Jirutitijaroen and C. Singh, "Stochastic programming approach for unit availability consideration in multi-area generation expansion planning," in *Power Engineering Society General Meeting, 2007. IEEE*, pp. 1–5, June 2007.

[39] P. Jirutitijaroen and C. Singh, "Unit availability considerations in composite system generation planning," in *Probabilistic Methods Applied to Power Systems, 2008. PMAPS '08. Proceedings of the 10th International Conference on*, pp. 1–5, May 2008.

[40] P. Jirutitijaroen and C. Singh, "Reliability constrained multi-area adequacy planning using stochastic programming with sample-average approximations,"

Power Systems, IEEE Transactions on, vol. 23, pp. 504–513, May 2008.

[41] G. Orfanos, P. Georgilakis, and N. Hatziargyriou, "Transmission expansion planning of systems with increasing wind power integration," *Power Systems, IEEE Transactions on*, vol. 28, pp. 1355–1362, May 2013.

[42] L. Wang and C. Singh, "Multicriteria design of hybrid power generation systems based on a modified particle swarm optimization algorithm," *IEEE Transactions on Energy Conversion*, vol. 24, pp. 163–172, March 2009.

[43] P. Jirutitijaroen and C. Singh, "Comparison of simulation methods for power system reliability indexes and their distributions," *Power Systems, IEEE Transactions on*, vol. 23, pp. 486–493, May 2008.

[44] R. Billinton, R. Karki, Y. Gao, D. Huang, P. Hu, and W. Wangdee, "Adequacy assessment considerations in wind integrated power systems," *Power Systems, IEEE Transactions on*, vol. 27, pp. 2297–2305, Nov 2012.

[45] A. Khodaei, M. Shahidehpour, L. Wu, and Z. Li, "Coordination of short-term operation constraints in multi-area expansion planning," *Power Systems, IEEE Transactions on*, vol. 27, pp. 2242–2250, Nov 2012.

[46] R. Billinton and W. Li, *Reliability assessment of electric power systems using Monte Carlo methods*. The language of science, Springer, 1994.

[47] R. Billinton and A. Sankarakrishnan, "A comparison of monte carlo simulation techniques for composite power system reliability assessment," in *WESCANEX 95. Communications, Power, and Computing. Conference Proceedings., IEEE*, vol. 1, pp. 145–150 vol.1, May 1995.

[48] J. Choi, T. Tran, J. Kwon, R. Thomas, T. Mount, and R. Billinton, "Nodal probabilistic production cost simulation considering transmission system un-

availabilty," *IET Generation, Transmission Distribution*, vol. 2, pp. 32–42, January 2008.

[49] A. Sankarakrishnan and R. Billinton, "Sequential monte carlo simulation for composite power system reliability analysis with time varying loads," *IEEE Transactions on Power Systems*, vol. 10, pp. 1540–1545, Aug 1995.

[50] Y. Dvorkin, M. Lubin, S. Backhaus, and M. Chertkov, "Uncertainty sets for wind power generation," *Power Systems, IEEE Transactions on*, vol. PP, no. 99, pp. 1–2, 2015.

[51] W. Tong, *Wind power generation and wind turbine design.* WIT Press, 2010.

[52] U. B. Gunturu and C. A. Schlosser, "Characterization of wind power resource in the united states," *Atmospheric Chemistry and Physics*, vol. 12, no. 20, pp. 9687–9702, 2012.

[53] O. Jaramillo and M. Borja, "Wind speed analysis in la ventosa, mexico: a bimodal probability distribution case," *Renewable Energy*, vol. 29, no. 10, pp. 1613–1630, 2004.

[54] R. Kollu, S. R. Rayapudi, S. Narasimham, and K. M. Pakkurthi, "Mixture probability distribution functions to model wind speed distributions," *International Journal of Energy and Environmental Engineering*, vol. 3, no. 1, p. 27, 2012.

[55] H. Bludszuweit, J. A. Dominguez-Navarro, and A. Llombart, "Statistical analysis of wind power forecast error," *IEEE Transactions on Power Systems*, vol. 23, pp. 983–991, Aug 2008.

[56] L. Wang, C. Singh, and A. Kusiak, *Wind power systems : applications of computational intelligence.* Green energy and technology, Springer, 2010.

[57] X. Chen and Y. Zhang, "Uncertain linear programs: Extended affinely adjustable robust counterparts," *Operations Research*, vol. 57, no. 6, pp. 1469–1482, 2009.

[58] P. Wong, P. Albrecht, R. Allan, R. Billinton, Q. Chen, C. Fong, S. Haddad, W. Li, R. Mukerji, D. Patton, A. Schneider, M. Shahidehpour, and C. Singh, "The ieee reliability test system-1996. a report prepared by the reliability test system task force of the application of probability methods subcommittee," *Power Systems, IEEE Transactions on*, vol. 14, pp. 1010–1020, Aug 1999.

[59] F. Alizadeh and D. Goldfarb, "Second-order cone programming," *Mathematical programming*, vol. 95, no. 1, pp. 3–51, 2003.

[60] P. CW., L. D., M. J., C. S., E. S., and G. E., "Creating the dataset for the western wind and solar integration study," in *7th international workshop on large scale integration of wind power and on transmission networks for offshore wind farms, Madrid, Spain*, May 2008.

[61] R. Chedid, H. Akiki, and S. Rahman, "A decision support technique for the design of hybrid solar-wind power systems," *IEEE Transactions on Energy Conversion*, vol. 13, pp. 76–83, Mar 1998.

[62] S. Sarkar and V. Ajjarapu, "Mw resource assessment model for a hybrid energy conversion system with wind and solar resources," *IEEE Transactions on Sustainable Energy*, vol. 2, pp. 383–391, Oct 2011.

[63] J. Widen, "Correlations between large-scale solar and wind power in a future scenario for sweden," *IEEE Transactions on Sustainable Energy*, vol. 2, pp. 177–184, April 2011.

[64] J. Aghaei, M. A. Akbari, A. Roosta, M. Gitizadeh, and T. Niknam, "Integrated renewable-conventional generation expansion planning using multiobjective framework," *IET Generation, Transmission Distribution*, vol. 6, pp. 773–784, August 2012.

[65] J. Wang and F. Yang, "Optimal capacity allocation of standalone wind/solar/battery hybrid power system based on improved particle swarm optimisation algorithm," *IET Renewable Power Generation*, vol. 7, pp. 443–448, Sept 2013.

[66] M. Alsayed, M. Cacciato, G. Scarcella, and G. Scelba, "Multicriteria optimal sizing of photovoltaic-wind turbine grid connected systems," *IEEE Transactions on Energy Conversion*, vol. 28, pp. 370–379, June 2013.

[67] A. Arabali, M. Ghofrani, M. Etezadi-Amoli, M. S. Fadali, and Y. Baghzouz, "Genetic-algorithm-based optimization approach for energy management," *IEEE Transactions on Power Delivery*, vol. 28, pp. 162–170, Jan 2013.

[68] R. Sioshansi and P. Denholm, "Benefits of colocating concentrating solar power and wind," *IEEE Transactions on Sustainable Energy*, vol. 4, pp. 877–885, Oct 2013.

[69] M. Aien, M. G. Khajeh, M. Rashidinejad, and M. Fotuhi-Firuzabad, "Probabilistic power flow of correlated hybrid wind-photovoltaic power systems," *IET Renewable Power Generation*, vol. 8, pp. 649–658, August 2014.

[70] D. Manz, R. Walling, N. Miller, B. LaRose, R. D'Aquila, and B. Daryanian, "The grid of the future: Ten trends that will shape the grid over the next decade," *IEEE Power and Energy Magazine*, vol. 12, pp. 26–36, May 2014.

[71] B. Zeng, J. Zhang, X. Yang, J. Wang, J. Dong, and Y. Zhang, "Integrated planning for transition to low-carbon distribution system with renewable energy generation and demand response," *IEEE Transactions on Power Systems*, vol. 29, pp. 1153–1165, May 2014.

[72] R. G. Wandhare and V. Agarwal, "Novel integration of a pv-wind energy system with enhanced efficiency," *IEEE Transactions on Power Electronics*, vol. 30, pp. 3638–3649, July 2015.

[73] S. S. Reddy and J. A. Momoh, "Realistic and transparent optimum scheduling strategy for hybrid power system," *IEEE Transactions on Smart Grid*, vol. 6, pp. 3114–3125, Nov 2015.

[74] P. Li, R. Dargaville, F. Liu, J. Xia, and Y. D. Song, "Data-based statistical property analyzing and storage sizing for hybrid renewable energy systems," *IEEE Transactions on Industrial Electronics*, vol. 62, pp. 6996–7008, Nov 2015.

[75] G. Wang, M. Ciobotaru, and V. G. Agelidis, "Power management for improved dispatch of utility-scale pv plants," *IEEE Transactions on Power Systems*, vol. 31, pp. 2297–2306, May 2016.

[76] H. M. Al-Masri and M. Ehsani, "Feasibility investigation of a hybrid on-grid wind photovoltaic retrofitting system," *IEEE Transactions on Industry Applications*, vol. 52, pp. 1979–1988, May 2016.

[77] A. Keane, M. Milligan, C. J. Dent, B. Hasche, C. D'Annunzio, K. Dragoon, H. Holttinen, N. Samaan, L. Soder, and M. O'Malley, "Capacity value of wind power," *IEEE Transactions on Power Systems*, vol. 26, pp. 564–572, May 2011.

[78] Z. Chen, L. Wu, and M. Shahidehpour, "Effective load carrying capability evaluation of renewable energy via stochastic long-term hourly based scuc," *IEEE*

Transactions on Sustainable Energy, vol. 6, pp. 188–197, Jan 2015.

[79] L. Wang and C. Singh, "A new method for capacity credit estimation of wind power," in *Fifteenth National Power Systems Conference (NPSC), IIT Bombay*, December 2008.

[80] S. Zhu, Y. Zhang, and A. A. Chowdhury, "Capacity credit of wind generation based on minimum resource adequacy procurement," *IEEE Transactions on Industry Applications*, vol. 48, pp. 730–735, March 2012.

[81] M. Amelin, "Comparison of capacity credit calculation methods for conventional power plants and wind power," *IEEE Transactions on Power Systems*, vol. 24, pp. 685–691, May 2009.

[82] A. van Wijk, N. Halberg, and W. Turkenburg, "Capacity credit of wind power in the netherlands," *Electric Power Systems Research*, vol. 23, no. 3, pp. 189 – 200, 1992.

[83] R. M. G. Castro and L. A. F. M. Ferreira, "A comparison between chronological and probabilistic methods to estimate wind power capacity credit," *IEEE Transactions on Power Systems*, vol. 16, pp. 904–909, Nov 2001.

[84] G. R. Pudaruth and F. Li, "Locational capacity credit evaluation," *IEEE Transactions on Power Systems*, vol. 24, pp. 1072–1079, May 2009.

[85] J. Usaola, "Capacity credit of concentrating solar power," *IET Renewable Power Generation*, vol. 7, pp. 680–688, Nov 2013.

[86] N. Zhang, C. Kang, D. S. Kirschen, and Q. Xia, "Rigorous model for evaluating wind power capacity credit," *IET Renewable Power Generation*, vol. 7, pp. 504–513, Sept 2013.

[87] Y. Zhou, P. Mancarella, and J. Mutale, "Framework for capacity credit assessment of electrical energy storage and demand response," *IET Generation, Transmission Distribution*, vol. 10, no. 9, pp. 2267–2276, 2016.

[88] S. Samadi and C. Singh, "Capacity credit evaluation of solar power plants," in *2014 IEEE PES General Meeting | Conference Exposition*, pp. 1–5, July 2014.

[89] A. Gusmao and M. GroissbÃűck, "Capacity value of photovoltaic and wind power plants in an isolated mini-grid in the kingdom of saudi arabia," in *2015 Saudi Arabia Smart Grid (SASG)*, pp. 1–8, Dec 2015.

APPENDIX A

POWER SYSTEM RELIABILITY INDICES

A.1 Loss of Load Probability ($LOLP_i$)

$$LOLP_i = \frac{LOEE_i}{8736} \tag{A.1}$$

A.2 Loss of Load Expectation ($LOLE_i$)

$$LOLE_i = \frac{\sum_{y=1}^{N} LLD_{iy}}{N}; \quad (hr/yr) \tag{A.2}$$

where LLD_i is the loss of load duration in (h) for each area i and N is the number of sample years.

A.3 Loss of Energy Expectation ($LOEE_i$)

$$LOEE_i = \frac{\sum_{y=1}^{N} ENS_{iy}}{N}; \quad (MWh/yr) \tag{A.3}$$

where ENS_i is the energy not served in (MWh) for each area i.

APPENDIX B

DATA FORMAT

The data on random wind power $\tilde{\boldsymbol{w}}$ and uncertain generation capacities $\tilde{\boldsymbol{p}}$ is organized as structures shown in Table B.1 and Table B.2, respectively. Table B.3 provides the data structure of the load segment model, and the other system parameters are organized as the format in Table B.4.

B.1 Wind Data

Table B.1: Wind data structure

Structure	Fields	Data	Dimension
Wind(s), $\forall s \in \mathcal{S}$	Mean	$\bar{w}_i^s$	$\lvert\mathcal{I}\rvert \times 1$
	Level	W_{il}^s	$\lvert\mathcal{I}\rvert \times \lvert\mathcal{L}^\alpha\rvert$
	Alpha	α_{il}^s	$\lvert\mathcal{I}\rvert \times \lvert\mathcal{L}^\alpha\rvert$
	Beta	β_{ij}^s	$((\lvert\mathcal{I}\rvert \times (\lvert\mathcal{I}-1\rvert)/2)) \times 3$

B.2 Generation Data

Table B.2: Generation capacity data structure

Structure	Fields	Data	Dimension
Gen	Mean	$\bar{p}_i$	$\lvert\mathcal{I} \times 1\rvert$
	Bounds	$[p_i^{min}, p_i^{max}]$	$\lvert\mathcal{I} \times 1\rvert \times 2$
	Level	P_{il}	$\lvert\mathcal{I}\rvert \times \lvert\mathcal{L}^{\gamma}\rvert$
	SumLevel	Q_l	$1 \times \lvert\mathcal{L}^{\delta}\rvert$
	Gamma	γ_{il}	$\lvert\mathcal{I}\rvert \times \lvert\mathcal{L}^{\gamma}\rvert$
	Delta	δ_l^s	$1 \times \lvert\mathcal{L}^{\delta}\rvert$

B.3 Load Data

Table B.3: Load data structure

Structure	Fields	Data	Dimension
Load(s), $\forall s \in \mathcal{S}$	Segment	D_{it}^s	$\lvert\mathcal{I}\rvert \times \lvert\mathcal{T}\rvert$
	Duration	T_t^s	$1 \times \lvert\mathcal{T}\rvert$

B.4 System Data

Table B.4: System data structure

Structure	Fields	Data	Dimension
System	Line	[area i, area j, F_{ij}]	$\lvert\mathcal{F}\rvert \times 3$
	MaxCap	Π_i	$\lvert\mathcal{I}\rvert \times 1$
	TotalCap	Ω	1×1

APPENDIX C

DERIVING THE UNCERTAIN WIND POWER GENERATION STATISTICAL EXPRESSIONS

C.1 Deriving the Covariance and the Correlation Coefficient Expression

$$
\begin{aligned}
\mathbb{E}_{\mathbb{P}}\left\{[(\tilde{w}_i^s - \bar{w}_i^s) + (\tilde{w}_j^s - \bar{w}_j^s)]^2\right\} &\leq \mathbb{E}_{\mathbb{P}}\left\{(\tilde{w}_i^s - \bar{w}_i^s)^2 + (\tilde{w}_j^s - \bar{w}_j^s)^2 + 2(\tilde{w}_i^s - \bar{w}_i^s)(\tilde{w}_j^s - \bar{w}_j^s)\right\} \\
&\leq \mathbb{E}_{\mathbb{P}}\left\{(\tilde{w}_i^s - \bar{w}_i^s)^2\right\} + \mathbb{E}_{\mathbb{P}}\left\{(\tilde{w}_j^s - \bar{w}_j^s)^2\right\} + \mathbb{E}_{\mathbb{P}}\left\{2(\tilde{w}_i^s - \bar{w}_i^s)(\tilde{w}_j^s - \bar{w}_j^s)\right\} \\
&\leq \mathbb{E}_{\mathbb{P}}\left\{(\tilde{w}_i^s - \bar{w}_i^s)^2\right\} + \mathbb{E}_{\mathbb{P}}\left\{(\tilde{w}_j^s - \bar{w}_j^s)^2\right\} + 2\mathbb{E}_{\mathbb{P}}\left\{(\tilde{w}_i^s - \bar{w}_i^s)(\tilde{w}_j^s - \bar{w}_j^s)\right\} \\
&\leq \lambda_i^s + \lambda_j^s + 2\zeta_{ij}^s, \forall j < i \in \mathcal{I}, \forall s \in \mathcal{S} \\
&\leq \lambda_i^s + \lambda_j^s + 2\left\{\sqrt{\lambda_i^s}\sqrt{\lambda_j^s}\xi_{ij}^s\right\}, \forall j < i \in \mathcal{I}, \forall s \in \mathcal{S}
\end{aligned}
$$